MOLECULAR CLONING AND CHARACTERIZATION OF A cDNA ENCODING ARGONAUTE PROTEIN FROM *PENAEUS MONODON*

MANASAVE DECHKLAR

A THESIS SUBMITTED IN PARTIAL FULFILLMENT
OF THE REQUIREMENTS FOR
THE DEGREE OF MASTER OF SCIENCE
(MOLECULAR GENETICS AND GENETIC ENGINEERING)
FACULTY OF GRADUATE STUDIES
MAHIDOL UNIVERSITY
2006

ISBN 974-04-6899-3

Thesis
Entitled

MOLECULAR CLONING AND CHARACTERIZATION OF A cDNA ENCODING ARGONAUTE PROTEIN FROM *PENAEUS MONODON*

Manasave Dechklar
.....
Miss Manasave Dechklar
Candidate

Apinunt Udomkit
.....
Asst. Prof. Apinunt Udomkit, Ph.D.
Major-Advisor

Chalermporn Ongvarrasopone
.....
Lect. Chalermporn Ongvarrasopone, Ph.D.
Co-Advisor

Witoon Tirasophon
.....
Asst. Prof. Witoon Tirasophon, Ph.D.
Co-Advisor

Salee Kiewkarnka
.....
Asst. Prof. Salee Kiewkarnka, Ph.D
Acting Dean
Faculty of Graduate Studies

V. Akkarapatumwong
.....
Asst. Prof. Varaporn Akkarapatumwong, Ph.D.
Chair
Master of Science Programme in Molecular Genetics and Genetic Engineering
Institute of Molecular Biology and Genetics

Thesis
Entitled

MOLECULAR CLONING AND CHARACTERIZATION OF A cDNA ENCODING ARGONAUTE PROTEIN FROM *PENAEUS MONODON*

was submitted to the Faculty of Graduate Studies, Mahidol University
for the degree of Master of Science (Molecular Genetics and Genetic Engineering)
on
February 16, 2006

Miss Manasave Dechklar
Candidate

Asst. Prof. Apinunt Udomkit, Ph.D.
Chair

Prof. Emeritus Sakol Panyim, Ph.D.
Member

Lect. Chalermporn Ongvarrasopone, Ph.D.
Member

Miss Plernpis Luxananil, Ph.D.
Member

Asst. Prof. Witoon Tirasophon, Ph.D.
Member

Asst. Prof. Salee Kiewkarnka, Ph.D
Acting Dean
Faculty of Graduate Studies
Mahidol University

Asst. Prof. Chartchai Krittanai, Ph.D.
Acting Director
Institute of Molecular Biology and Genetics
Mahidol University

ACKNOWLEDGEMENTS

I would like to express my sincere appreciation to my advisor, Asst. Prof. Apinunt Udomkit, for his valuable advice, helpfulness and encouragement. Prof. Emeritus Sakol Panyim, for financial support throughout this thesis work. I am also grateful to Dr. Chalermporn Ongvarrasopone, Asst. Prof. Witoon Tirasophon and Dr. Plernpis Luxananil for their helpful discussions and recommendations.

I am especially grateful to Miss Supattra Treerattrakool for her kindness, suggestion, encouragement, and effort to teach me all about the scientific knowledge and laboratory techniques.

My appreciation is also expressed to Miss Supansa Yodmuang for her advice and kindness to provide pET3a vector and for YHV and GFP colony. I would like to thank Dr. Pongsopee Attasart for giving special advice recommendations in all techniques.

Special thanks are also expressed to Mr. Wanlop Chinnirunvong for his help in the part of primary shrimp cell culture. I would like to thank Dr. Wanchai Assavalapsakul and Miss Yaowaluck Roshorm for their useful suggestions about shrimp cell preparation.

Finally, I would like to express my special appreciation to all my friends, staff, and technicians of the Institute of Molecular Biology and Genetics for their friendships, generosity, and sharing the happy time throughout my studying. Special thanks are also extended to my best friends for their encouragement and friendships.

Manasave Dechklar

MOLECULAR CLONING AND CHARACTERIZATION OF A cDNA ENCODING ARGONAUTE PROTEIN FROM *PENAEUS MONODON*

MANASAVE DECHKLAR 4636878 MBMG/M

M.Sc. (MOLECULAR GENETICS AND GENETIC ENGINEERING)

THESIS ADVISORS : APINUNT UDOMKIT, Ph.D.,
CHALERMPORN ONGVARRASOPONE, Ph.D., WITOON TIRASOPHON, Ph.D.

ABSTRACT

Argonaute proteins are present in diverse organisms ranging from yeast to humans. In addition to their role in developmental control, some Argonautes have been shown to play essential roles in a variety of post-transcriptional RNA-mediated gene silencing pathways, including RNA interference or RNAi mediated by sequence-specific double-stranded RNA. This work is aimed at the characterization of an Argonaute that associates with RNAi in the shrimp *Penaeus monodon* in order to provide an in-depth understanding of the RNA-mediated gene silencing mechanism in the shrimp. A total of 2,829 bp of the cDNA encoding Argonaute of *P. monodon* (Pem-AGO) was obtained from RT-PCR and RACE methods, using mRNA from the lymphoid (Oka) organ as a template. The deduced amino acid sequence of Pem-AGO contained the two conserved domains, PAZ and PIWI, which are the signature of the Argonaute family. The requirement for Pem-AGO in RNAi was explored in the primary Oka cell culture of *P. monodon*. Transfection with three dsRNAs corresponding to different regions in the Pem-AGO sequence resulted in approximately 30% reduction of Pem-AGO expression in the Oka cells. The subsequent effect of the depletion in Pem-AGO mRNA level on the efficacy of RNAi was determined by the amount of silencing in the endogenous 5-HT receptor gene by its specific dsRNA. Pem-AGO depletion led to impaired RNAi as demonstrated by partial restoration of 5-HT receptor gene expression in the cells that acquired dsRNAs, which target both the Pem-AGO and 5-HT receptor genes. By contrast, only slight or no impairment of RNAi was seen when the exogenous gene, the protease gene of yellow head virus, was targeted for silencing in Pem-AGO depleted cells. In summary, the results from this study suggest the involvement of Pem-AGO in RNA-mediated gene silencing by RNAi mechanism in *P. monodon*.

KEY WORDS: *PENAEUS MONODON*/ ARGONAUTE PROTEIN/ RNAi PATHWAY/ dsRNA/POST-TRANSCRIPTIONAL GENE SILENCING

117 P. ISBN 974-04-6899-3

การโคลนและการศึกษาหน้าที่ของ cDNA ที่สร้างโปรตีน Argonaute ในกุ้งกุลาดำ
(MOLECULAR CLONING AND CHARACTERIZATION OF A cDNA ENCODING ARGONAUTE PROTEIN FROM *PENAEUS MONODON*)

มนัสวี เดชกล้า 4636878 MBMG/M

วท.ม. (อณูพันธุศาสตร์และพันธุวิศวกรรมศาสตร์)

คณะกรรมการควบคุมวิทยานิพนธ์ : อภินันท์ อุดมกิจ, Ph.D., เฉลิมพร องศ์วรโสภณ, Ph.D., วิฑูรย์ ถิระโสภณ, Ph.D.

บทคัดย่อ

Argonaute เป็นโปรตีนที่พบในสิ่งมีชีวิตหลายชนิด โปรตีนชนิดนี้ทำหน้าที่หลากหลายทั้งในกระบวนการเจริญเติบโตและในกระบวนการยับยั้งการแสดงออกของยีนด้วยอาร์เอ็นเอสายคู่ ที่เรียกว่า RNA interference (RNAi) การศึกษาวิจัยนี้เป็นการโคลนยีน Argonaute ของกุ้งกุลาดำ โดยใช้อาร์เอ็นเอซึ่งสกัดจากต่อมน้ำเหลืองของกุ้งกุลาดำในการสังเคราะห์ชิ้น cDNA ด้วยปฏิกิริยา RT-PCR ซึ่งใช้ไพร์เมอร์ที่ถูกออกแบบจากลำดับของกรดอะมิโนของโปรตีนชนิดนี้ซึ่งมีความคล้ายคลึงกันในสิ่งมีชีวิตชนิดอื่นๆ ชิ้นของ cDNA ที่สร้างโปรตีน Argonaute ของกุ้งกุลาดำ (Pem-AGO) มีขนาด 2,829 นิวคลีโอไทด์ และลำดับของกรดอะมิโนที่ถอดรหัสจากลำดับนิวคลีโอไทด์ประกอบด้วยลักษณะสำคัญของโปรตีน Argonaute ได้แก่ส่วนอนุรักษ์ที่เรียกว่า PAZ และ PIWI domain การศึกษาหน้าที่ของโปรตีนชนิดนี้ในกระบวนการ RNAi ได้ใช้วิธีการนำอาร์เอ็นเอสายคู่ที่สังเคราะห์จากลำดับนิวคลีโอไทด์ของ Argonaute เข้าสู่เซลล์ปฐมภูมิจากต่อมน้ำเหลืองของกุ้งกุลาดำ จากการทดลองพบว่าอาร์เอ็นเอสายคู่ที่จำเพาะต่อ Argonaute มีผลทำให้มีการแสดงออกของ Argonaute ในเซลล์ลดลงประมาณ 30% การศึกษาผลกระทบของระดับ Argonaute ในเซลล์ ต่อกระบวนการ RNAi ในการยับยั้งการแสดงออกของยีนในกุ้งกุลาดำ พบว่าอาร์เอ็นเอสายคู่ที่จำเพาะต่อตัวตอบรับซีโรโตนินสามารถยับยั้งการแสดงออกของยีนสร้างตัวตอบรับซีโรโตนินได้ในเซลล์ที่มี Argonaute ในระดับปรกติ ในทางตรงกันข้ามอาร์เอ็นเอสายคู่ของตัวตอบรับซีโรโตนินไม่สามารถยับยั้งการแสดงออกของยีนเป้าหมายได้เมื่อระดับของArgonaute ลดลง อย่างไรก็ตาม การศึกษาทำนองเดียวกันนี้กับยีนที่สร้างโปรตีนของไวรัสหัวเหลือง ไม่เห็นผลที่ชัดเจนของระดับของ Argonaute ในเซลล์ต่อการยับยั้งการแสดงออกของยีนไวรัสหัวเหลืองด้วยอาร์เอ็นเอสายคู่ที่จำเพาะ กล่าวโดยสรุปยีนที่สร้าง Argonaute ที่ศึกษาในงานวิจัยนี้ มีความสำคัญต่อกระบวนการยับยั้งการแสดงออกของยีนด้วยอาร์เอ็นเอสายคู่หรือ RNAi ในเซลล์ของกุ้งกุลาดำ

117 หน้า ISBN 974-04-6899-3

CONTENTS

CONTENTS (Continued)

Page

CONTENTS (Continued)

Page

CONTENTS (Continued)

Page

CONTENTS (Continued)

Page

LIST OF TABLES

LIST OF FIGURES

Figure **Page**

LIST OF FIGURES (Continued)

Figure **Page**

LIST OF FIGURES (Continued)

Figure **Page**

LIST OF ABBREVIATIONS

ATP	Adenosine triphosphate
bp	Base pair (s)
BSA	Bovine serum albumin
^{o}C	Degree Celsius
cDNA	Complementary deoxyribonucleic acid
CTAB	Cetyl trimethyl ammonium bromide
DEPC	Diethyl pyrocarbonate
DNA	Deoxyribonucleic acid
DNase	Deoxyribonuclease
dNTPs	dATP, dCTP, dGTP, and dTTP
dsRNA	double-stranded RNA
DTT	Dithiothreitol
EDTA	Ethylenediamine tetraamino acid
FBS	Fetal bovine serum
g	Gravity or centrifugal force
h	Hour
IPTG	Isopropyl-β-D-thiogalactopyranoside
Kb	Kilobase pair (s)
kDa	Kilodalton (s)
lacZ	β-galactosidase gene
LB	Luria-Bertani medium
M	Molar
min	Minute (s)
mg	Milligram (s)
ml	Millilitre (s)
mM	Millimolar
MOPS	4-morpholinepropanesulfonic acid
nt	Nucleotide (s)

LIST OF ABBREVIATIONS (Continued)

O.D.	Optical density
PBS	Phosphate buffer saline
PCR	Polymerase chain reaction
RNA	Ribonucleic acid
RNase	Ribonuclease
RT	Reverse transcriptase
RT-PCR	Reverse transcription-polymerase chain Reaction
rpm	Revolutions per minute
sec	Second (s)
SME	Shrimp meat extract
T_m	Melting temperature
Tris	Tris-(hydroxylmethyl)-aminomethane
µF	Microfarad (s)
µg	Microgram (s)
µl	Microlitre (s)
µM	Micromolar
V	Volt (s)
v/v	volume/volume
WSSV	White spot syndrome virus
w/v	weight/volume
X-gal	5-bromo-4-chloro-3-indolyl-beta-D-galactopyranoside
YEPD	Yeast extract peptone dextrose
YHV	Yellow head virus

CHAPTER I
INTRODUCTION

Black tiger shrimp (*Penaues monodon*, Fabricius) is widely distributed throughout tropical and subtropical areas, along the coastlines of the Indo-west Pacific region including both the Andaman Sea and the Gulf of Thailand (1). The black tiger shrimp has become one of the most important agricultural species because of their high survival rate and fast growth in a wide range of salinity (15-20 ppt) (2). The maximum growth rates are achieved in a wide range of water temperature ranging from 25 to 35 ºC. Thailand is the largest frozen shrimp producer and exporter in the world. Shrimp export generated approximately 1.7 billion USD annual export value in 2003 (3). Despite its high commercial impact, shrimp farming industry in Thailand has encountered several problems with pathogen diseases caused by bacterial, fungal and viral infection. These lead to a destructive effect on both shrimp production and economy of the country.

1.1 General crustacean anatomy (4)

All crustaceans have bilaterally symmetrical bodies covered with a chitinous exoskeleton, which may be thick and calcareous (as in the crayfish) or delicate and transparent (as in the water fleas). Crustaceans are the only arthropods that are mainly aquatic, and most of them are marine. They use gills for respiration. Their thoracic region typically bears walking legs (pereopods), which are also used for capturing preys. The abdominal region oftenly is equipped with swimmeretes (pleopods) and a tails fan made up a pair of appendages (uropods) and the telson.

1.1.1 The Decapods crustaceans

The order Decapoda contains those animals most people recognize as crustaceans: shrimps, lobsters, and crabs. Decapods (meaning ten feet) have the last five pairs of thoracic appendages modified as walking leg while the first three pairs,

the maxillipeds, function as mouthparts. If one pair of walking legs has enlarged pincers (chelae) they are referred to as chelipeds (5).

1.1.2 *Penaeus monodon* (Black tiger shrimp)

The taxonomy definition of the black tiger shrimp is as follows: (6)

Phylum	:	Arthropoda
Class	:	Crustacea
Subclass	:	Malacostraca
Order	:	Decapoda
Suborder	:	Natantia
Superfamily	:	Penaeoidea
Family	:	Penaeidae Rafinesque
Genus	:	***Penaeus Fabricius***
Subgenus	:	***Penaeus***
Species	:	***Penaeus monodon***

1.1.3 Morphology of *Penaeus monodon*

The exterior morphology of Penaeid shrimp is distinguished by a cephalothorax with a characteristic hard rostrum, and by a segmented abdomen (Figure 1) (7). Most organ, such as gills, digestive system and heart, are located in the cephalothorax, while the muscles concentrated in the abdomen. Appendages of the cephalothorax vary in appearance and function. In the head region, antennules and antennae performed sensory functions. The mandibles and the two pairs of maxillae form the jaw-like structures that are involved in food uptake (8). In the thorax region, the millipedes are the first three pairs of appendages, modified for food handling, and the remaining five pairs are the walking legs (pereiopods). Five pairs of swimming legs (pleopods) are found on the abdomen (6).

Penaeids have an open circulartory system and a dorsal muscular heart located in the cephalothorax (Figure 2) (9). The valved hemolymph vessels leave the heart and branch several times before the hemolymph arrives at the sinuses that are scattered throughout the body, where exchange of substances takes place. After passing the gills, the hemolymph return to the heart by means of three wide non-

valved openings (10). A large part of the cephalothorax in penaeid shrimp is occupied by the hepatopancreas. The main functions of the hepatopancreas are absorption of nutrients, storage of lipids and production of digestive enzymes (11). One of the heamolymph vessel that leaves the heart ends in the lymphoid organ, where the hemolymph is filtered. This organ is located ventro-anteriorly to the hepatopancreases. The central nervous system of crustacean is ladder-like of the assembled nerve cells called ganglia, joined across the midline and a separated longitudinally from one another by paired connectives (12).

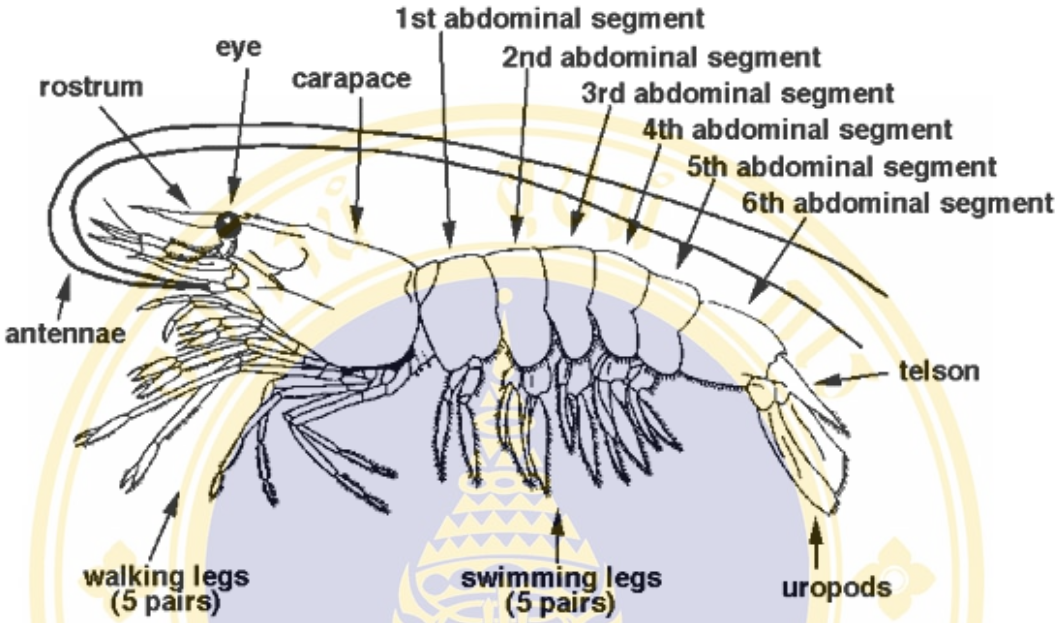

Figure 1. Lateral view of the external morphology of *Panaeus monodon* (7)

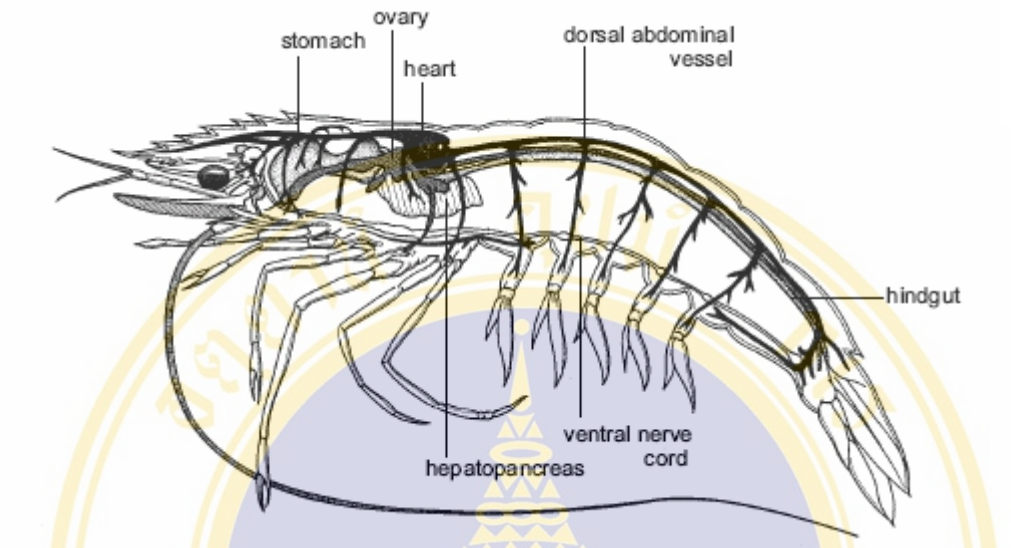

Figure 2. Lateral view of the internal morphology of *Panaeus monodon* (9)

1.2 Viral pathogen of the penaeid shrimps

During the past decade, shrimp agricultural activity has been destructively affected by two major viruses that caused high mortality rates, namely yellow head virus and white spot syndrome virus.

1.2.1 Yellow head virus (YHV)

Yellow head virus (YHV) was first found in *P. monodon* in Thailand in 1990. Histopathological analysis of infected shrimp revealed widespread cellular necrosis in the gills, connective tissues, hemocytes, hematopoietic tissues, and lymphoid organ, and thus strongly indicated a preferential infection of cells of ectodermal or mesodermal origins (13-15). The yellow head virus has been identified to order Nidovirals, family Roniviridae, genus Okavirus (16-18). This virus is a rod-shape virus, enveloped with peplomer and a tubular helical nucleocapsid containing a positive sense single-stranded RNA (17). In natural infection, the affected shrimp showed the yellowish color on the cephalothorax areas, called yellow head disease (YHD), resulting from the underlying yellow hepatopancreas showing through the translucent carapace. This disease can be found in black tiger shrimp in the weight range of 5 to 15 g (25 to 70 days). The shrimp that is infected with YHV usually dies within 2-3 days (15).

1.2.2 White spot syndrome virus (WSSV)

White spot syndrome (WSS) is a viral disease which affects most of the commercially cultivated marine shrimp species worldwide. The virus was first found in *P. japonicus* in northern Taiwan in 1992 (19), followed by Japan in 1993 (20). This virus is enveloped nucleocapsids with bacilliform morphology, containing double-stranded DNA, and a tail-like extension at one end. Typical signs of the diseased shrimp were reddish and pinkish-red discoloration of the body, including obvious white spots on the inside of the carapace, appendages and the inside body surface. The cumulative mortality of white spot syndrome-infected shrimp reaches 100% within 2-7 days.

1.3 Penaeid shrimp cell culture

Panaeid shrimp cell culture technology was developed for use in the studies of growth characteristics and analysis of penaeid viruses (21). Explant cell cultures have been obtained from various tissues and organs of the penaeid shrimp, including the lymphoid (Oka) organ (22-25), the primary target for YHV in the whole animal. The cell derived from the lymphoid organ were found to proliferate rapidly and remain stable for long period of time (2-3 weeks) (26). Primary cell cultures of the lymphoid organ are susceptible to YHV which produce cytopathic effects (CPE) that include rounding of cells and their detachment from the substrate which occurs as early as 3 days post-inoculation for YHV (27).

The lymphoid organ of penaeid shrimp is located on both left and right sides of the antero-dorsal surface of the hepatopancreases (22, 28). Because of its unique location and its relatively small size, identification and dissection of the organ is not easy, especially when small size shrimps (less than 10 g) are used. The optimal size of shrimp to be used for the preparation of primary lymphoid cell culture is between 20 and 30 g. Animals weighing over 30 g are generally not recommended because the cells from their organs appear to be more senescent and degenerate faster despite the fact that their Oka organs are relatively much larger (27).

1.4 General background of RNA interference (RNAi) pathway

RNA interference or RNAi was identified in many organisms, such as *Drosophila melanogaster*, *Neurospora crassa* and *Arabidopsis thaliana* (29). The RNAi is known as a sequence-specific gene silencing process in which double-stranded RNA (dsRNA) induces silencing of cognate mRNA. In plant, this phenomenon is called post-ranscriptional gene silencing (PTGS), whereas quelling (or co-suppression) is known as similar process in fungi (*Neurospora crassa)*. In PTGS, dsRNA from virus or transgene can trigger the post-transcriptional degradation of homologous cellular RNA (30). In quelling, dsRNA from transgene can trigger the silencing of homologous chromosomal loci simultaneously (30). In the PTGS pathway, dsRNA trigger the silencing through the synthesis of complementary RNA (cRNA) by the action of dsRNA-dependent RNA polymerase (RdRP) (30-31). Then the antisense cRNA stranded are hybridized to target RNA which induce the cleavage, modification or

degradation of target mRNA (Figure 3). In the RNAi pathway, the double-stranded RNA could originate from several sources; for examples, aberrant transcript of high copy transgenes, viral RNA and *in vitro* synthesized dsRNA that is experimentally injected or transfected into the cells (32). The model of the RNAi pathway is shown in Figure 4 (33). Firstly, a long dsRNA is cleaved into small interfering RNA fragments (siRNAs) of about 21-23 nucleotides by the action of an RNase-III-like dsRNA-specific ribonuclease, namely Dicer (34). The cleavage of long dsRNA by dicer utilizes ATP and generates the siRNA product with two-base 3' overhangs and 5'phosphate (35-37). Subsequently, the double-stranded siRNA is incorporated into a multiprotein complex known as the RNA-induced silencing complex (RISC) which contains an Argonaute protein as the major constituent. The double-stranded siRNA in RISC is unwound by ATP-dependent reaction into single-stranded siRNA and resulting in activated RISC. The activated RISC is guided by its single-stranded siRNA component to the target transcript by complementary base-pairing. The target mRNA is then cleaved by the action of endoribonuclease provided by the Argonaute protein, followed by further degradation with cellular exoribonucleases (38).

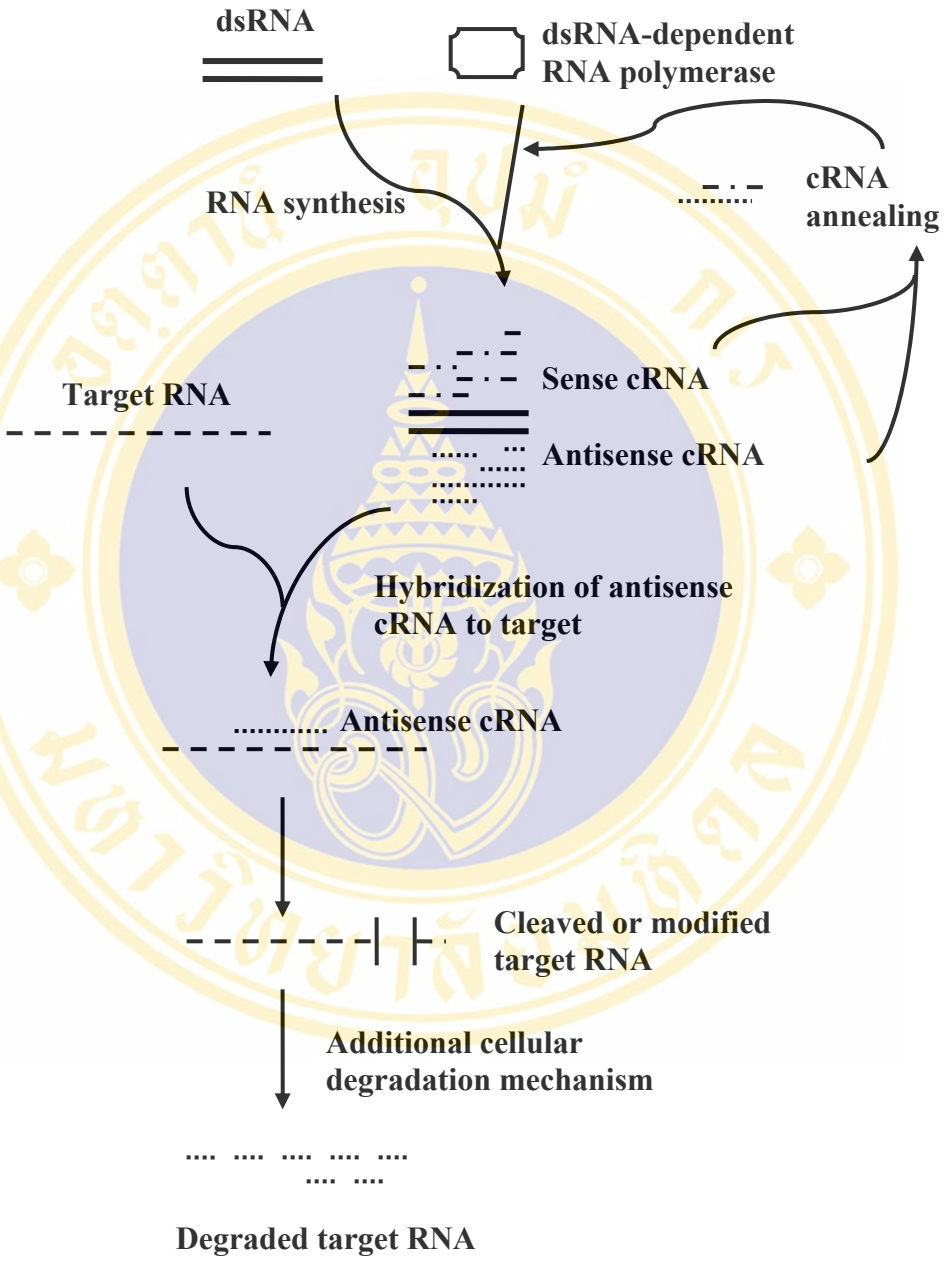

Figure 3. The model of the post-transcriptional gene silencing pathway in plant (Modified from (30))

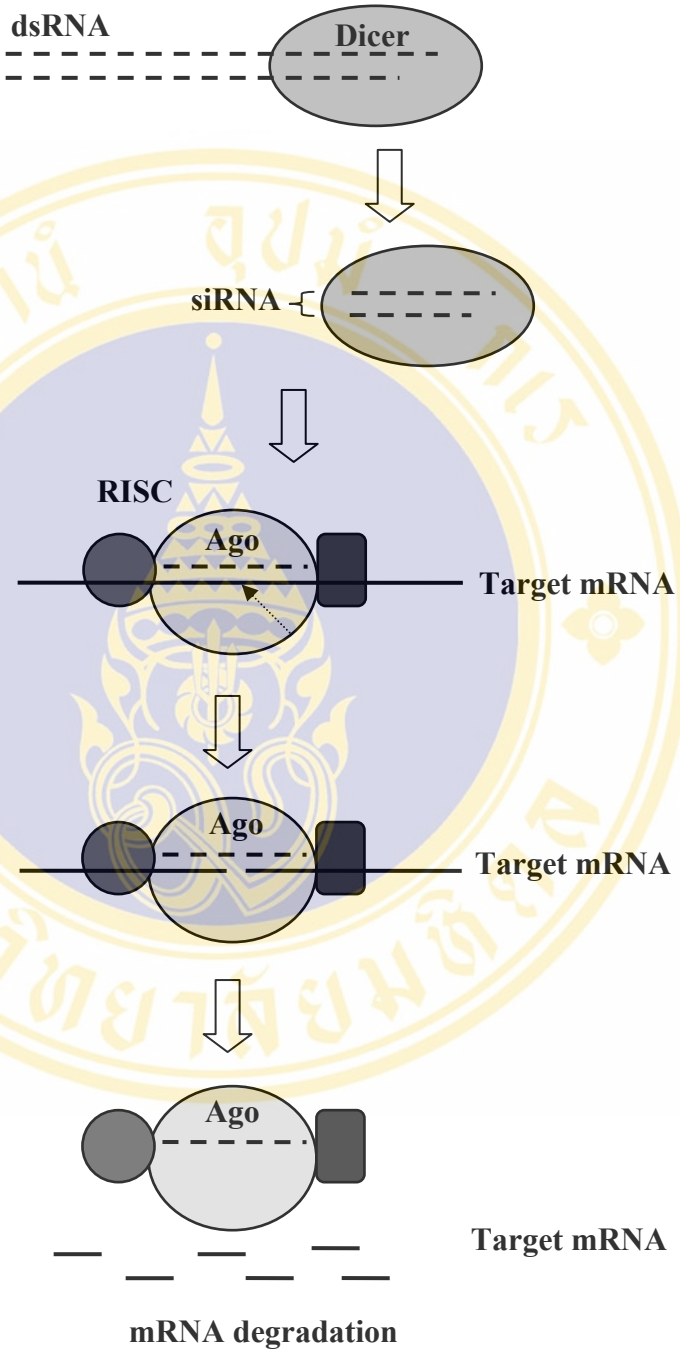

Figure 4. The model of the RNA interference (RNAi) pathway (Modified from (33))

1.5 The essential component in the RNAi pathway

1.5.1 General background of Dicer protein

Dicer protein is a member of the RNase class III family which recognizes double-stranded RNA template and digest them to small size RNA (siRNA). The cleavage by Dicer produces the siRNA products with the 5' phosphate and 3' hydroxyl termini. The Dicer enzyme composes of 4 domains; an amino-terminal helicase domain, two RNase III domains, a dsRNA binding domain and a PAZ domain (the conserved domain that is also found in Argonaute family (Figure 5) (39). The dsRNA binding domain recognizes 2' hydroxyl of the sugar of dsRNA template (40). The cleavage of dsRNA substrate occurs from the dimerization forming between the active site in each monomer of the RNase III domain. Particularly, one catalytic site cuts each strand of dsRNA resulting in the cleavage of dsRNA cleavage into siRNA (41). The size of ~21-23 nt siRNA is specified by the distance of dsRNA between the PAZ domain (which bind to 2 nt 3' overhang of dsRNA) and the active site of RNase III domains to create the suitable site of siRNA product (Figure 6) (41). Besides, the function of Dicer is co-ordinated with dsRNA-binding cofactor (dsRBD cofactor), such as, R2D2 in Drosophila (42). This dsRBD cofactor binds to the siRNA and facilitates siRNA loading into RISC to encourage the mRNA degradation (42-43).

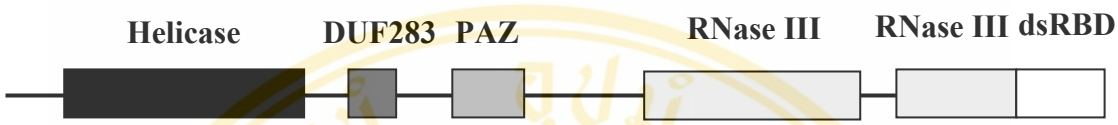

Figure 5. The domain structure of RNAse III family in *H. sapiens* (Modified from (43))

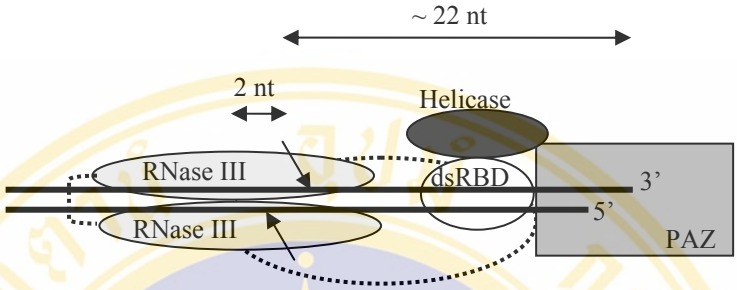

Figure 6. Model of catalytic cleavage of Dicer enzyme (Modified from (43))

1.5.2 General background of Argonaute protein

Argonaute is a protein family that is present in a wide range of organisms, such as plant, Drosophila, *C. elegan* and human (44). The number of Argonaute protein varies in different species. For instances, Drosophila contain 4 Argonaute proteins which are Piwi, Aubergine (or Sting), dAgo1 and dAgo2 (44), human contain 8 Argonaute proteins which are divided into 2 subfamilies that are 4 of PIWI subfamily (PIWIL1/HIWI, PIWIL2/HILI, PIWIL3 and PIWIL4/HIWI2) and 4 of eIF2C/AGO subfamily (EIF2C1/hAGO1, EIF2C2/hAGO2, EIF2C3/hAGO3 and EIF2C4/hAGO4) (45) and Arabidopsis has 10 Argonaute proteins, but only two of them, AGO1 and ZWILLE, have been studied in detail (44).

Argonaute proteins play primary roles in developmental control, and some of them are also involved in mRNA degradation pathway via RNA interference (RNAi). The Argonaute family members vary in both biological functions and expression in specific tissues (44). For example, two Argonaute proteins in Drosophila, Piwi and Aubergine, are required for the germline development. In contrast, the other two Argonautes, dAgo1 and dAgo2, were demonstrated for their function in RNAi pathway (44). dAgo1 is required for the efficient RNAi as demonstrated by the dAgo1 mutant that exhibited the decrease in the ability of mRNA degradation in respond to dsRNA *in vitro*, whereas dAgo2 is shown biochemically to be the important component in RISC (44). In Arabidopsis, Ago1 is shown to be involved in post-transcriptional gene silencing. Opposing to Ago1, another Argonaute family in Arabidopsis called ZWILLE does not function in post-transcriptional silencing but is demonstrated to be essential for cell division in development (44).

Argonaute protein is composed of 1,000 amino acids which contain 2 conserved domains, an N-terminal PAZ domain and a C-terminal PIWI domain (Figure 7) (44). The structure of PAZ domain consists of three parts (Figure 8), six-stranded β-barrel as a central domain, two α-helices which cap on top of the central barrel and a domain composing of a long β-hairpin and a short α-helix position below the central part (45). The central β-barrel contains aromatic amino acid residues which conserved within the PAZ domain family. This part functions as RNA-binding domain by binding to the two nucleotide 3’ overhang of siRNA (46). Another conserved domain, the PIWI domain, displays conserved structure to an RNase H family. This

family of RNase produces the cleavage product with the 5' phosphate and the 3' hydroxyl group in the reqiurement of divalent metal ions (43, 47-48). The structure of PIWI domain composes of five-stranded-β sheet surrounding with α-helices (Figure 9). This enzyme family contains three conserved carboxylic group, DDE (two aspartates and one glutamate) which situated on β sheet region for forming the active site. The first two carboxylated residues are located at the same positions among RNase H family while the third residue shows variation in its position (49). Mutation in the two conserved aspartate residues cause the inactivation of RISC in mRNA cleavage (50).

In the RNAi process, Argonaute functions as the enzyme in RISC with the activity of conserved PAZ and PIWI domains. From the beginning, PAZ domain recognizes 3' end of the siRNA strand originated from dsRNA cleavage by Dicer (49). The 5' end of the mRNA target enters into the cleft between PAZ domain and N-terminal domain and forms the complementary base-paring to the siRNA (Figure 10). This cleft contains the positively charge for appropriate binding of the negatively charge of the RNA strand (49). Then the catalytic RNase H-like enzyme in the PIWI domain cleave the mRNA target at the position to the center of the guide siRNA (49).

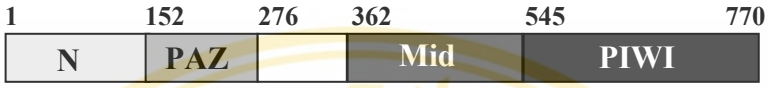

Figure 7. Domain structure of Argonaute protein in *P. furiosus* (Modified from (49))

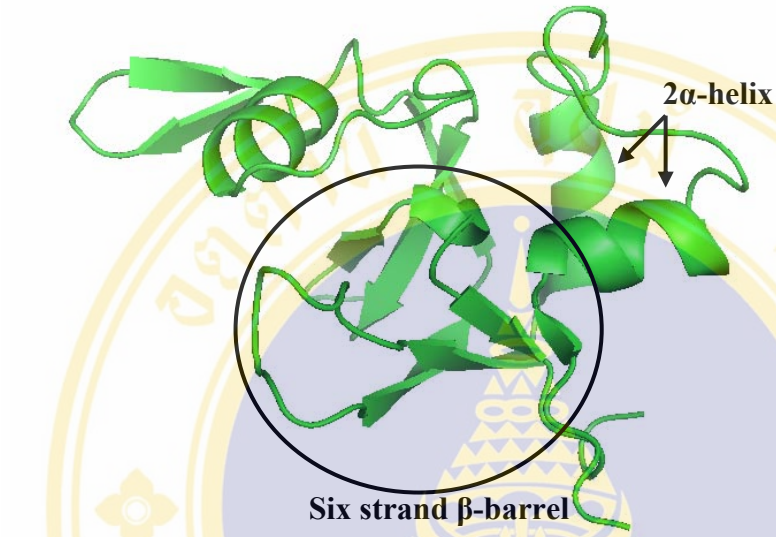

Figure 8. The structure of *D. melanogaster* Argonaute 2 PAZ domain family (Accession number: MMDB 27919, 1T2SA0 chain A, 110513)

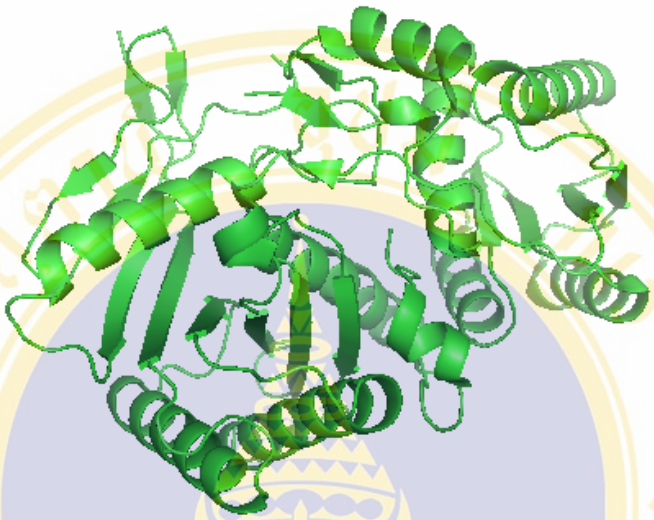

Figure 9. The structure of *P. furiosus* Argonaute PIWI domain (Accession number: MMDB 31372, 1W9H , 127717)

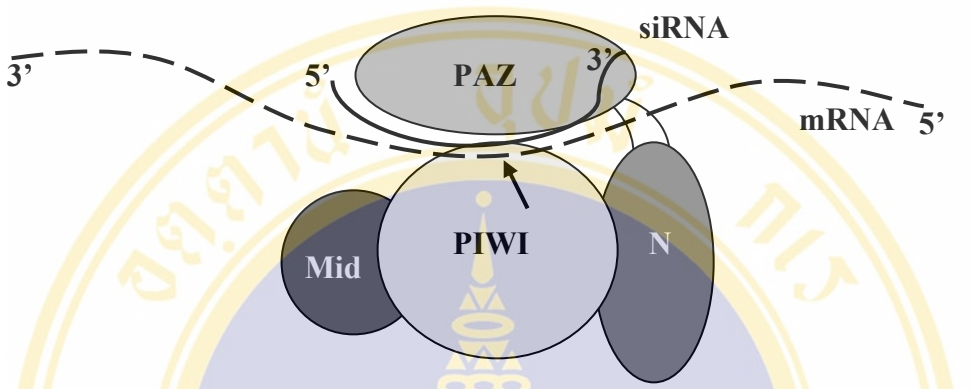

Figure 10. Model of mRNA degradation guided with siRNA by Argonaute protein of *P. furiosus* (Modified from (49))

1.6 Other components in the RNAi pathway

Two RNA binding proteins, the VIG protein, the human homolog of FMRP (fragile X mental retardation protein), dFXR and tudor staphylococcal nuclease (Tudor-SN) are shown to associate with RISC (51-52). The first protein, VIG, is encoded from the intron of *vasa* gene which is conserved in *C. elegans*, *Arabidopsis*, mammals and *S. pombe* (51). The VIG protein is composed of RGG box which functions in binding to RNA (51). In the Drosophila S2 cells, VIG functions in the maintaining of the silencing efficiency. The suppression level of VIG inhibits about 50% RNAi activity (51). Besides, VIG shares high similarity to the human phosphoprotein ki-1/57 which is a substrate of the protein kinase and thus is implicated in chromatin remodeling and transcriptional gene silencing (52-53). The second protein, dFXR, is encoded from the locus on the X chromosome which silenced in Fragile X syndrome (51). In Drosophila, dFXR protein functions in repressing of the translation of an mRNA encoding the microtubule-associated protein. Similar to the VIG protein, the Fragile X family also contains an RGG box which is suitable for binding of RNA (51). The third protein, tudor staphylococcal nuclease (Tudor-SN) is composed of staphylococcal nuclease (SNase) domain and a Tudor domain (54). The homolog of this protein is also discovered in *C. elegans*, *Arabidopsis*, mammals and *S. pombe* (54). SNase exhibits the nuclease activity that produces the product containing 5' hydroxyl group and 3'phosphate (55-56) similarly to the tudor domain that also displays the nuclease activity (52). However, tudor-SN is responsible for cleavage of both RNA and DNA strand and it cleaves the target independent to the sequence. This is in contrast to the characteristic of RISC which has no DNase activity and acts in highly sequence specific cleavage (54). However, the specific role of these three proteins in the RNAi pathway are still unclear.

1.7 The RNAi pathway and developmental function of Argonaute protein

Besides the function in RNAi pathway, some of the Argonaute proteins also play role in developmental control. In plant, *A. thilania*, Argonaute protein AGO1 functions in both RNAi pathway and development. The *ago1* mutants showed the defect in RNAi pathway (sensitive to viral infection) and phenotypic abnormalities (for example, abnormal infertile flowers and leaves) (44). In *D. melanogaster*, one of the

Argonaute proteins, Piwi is required for germline development and transgene-mediated co-suppression (44). Mutant in *piwi* affects the germline development by causing insufficient in the number of germline stem cell in the adult stage and inhibits post-transcriptional gene-silencing pathway (PTGS) (44).

1.8 The RNAi pathway, DNA methylation and chromatin remodeling

The RNAi pathway affects the centromeric silencing via methylation of histone H3 and the formation of condensed heterochromatin (57). In the process, transcription of centromeric region leads to the formation of dsRNA which is then processed into siRNA by the RNAi pathway (58). The siRNA then binds to the methyl-transferase and forms complementary base-paring to homologous centromeric sequence (58). This causes the histone methylation at the centromeric region and activates the condense heterochromatin formation (58). The compact structure of the heterochromatin then causes the transcriptional gene silencing (59). Mutation in Argonaute protein, Dicer and RNA polymerase II caused the lacking of histone methylation which mediated the loss of centromeric silencing. For example, in Arabidopsis, there are two genes that are responsible for DNA methylation, MET1 and DDM1. MET1 encodes the DNA methyltransferase while DDM1 encodes the protein that is involved in chromatin remodeling. Mutation in MET1 and DDM1 reduced the level of gene methylation and also cause negative impact to PTGS which is corresponded to the decrease in transgene methylation (60).

1.9 The RNAi pathway and antiviral defense

The RNAi machinery can be developed as a tool in antiviral defense in many organisms (61). The viral dsRNA can inhibit viral expression or viral replication by mRNA cleavage. For instance, in Drosophila S2 cell, co-transfection with the full-length of Flock house virus (FHV) RNA and dsRNA corresponding to the FHV sequence causes the decrease in the accumulation of FHV RNA (61). Moreover, infection of Drosophila S2 cell with FHV virus resulting in the production of siRNA which sequence specific to FHV and the reduction of FHV RNA level (62). Therefore, FHV acts as both the target and the initiator of RNA silencing (62). Conversely, viruses can develop the mechanism to defense RNAi in host cells by producing the

RNAi-suppressing protein (63). For example, the viral protein p19 in plant (VP19) can inhibit RNAi in the host cell by preventing the unwinding of duplex siRNA to single-stranded siRNA (64-65). This caused the unincorporation of siRNA into RISC and block the RNAi pathway in the cell (66).

2.1 RNAi pathway and the microRNA pathway

The evolutionarily conserved RNAi pathway also involved with the microRNA (miRNA) pathway (67). MicroRNA is encoded within plant and animal genomes and plays widespread roles in growth and development of specific tissue (68). It has been shown to be involved in the control of cell death and cell proliferation in flies, haematopoietic differentiate in mammals, neuronal pattern in nematodes, leaf and flower development in plants (69). MicroRNA is the small non-coding RNA that regulates gene expression of homologous transcript at the level of translational efficiency and stability of partial or fully sequence-complementary mRNA (68). The silencing by microRNA can initiate degradation of mRNA in plant or translation inhibition in animal (68). For example, in Arabidopsis, the miRNA (miRNA171/miRNA39) show the perfect complementarity to the mRNA target and direct the sequence-specific mRNA degradation (70). Alternatively, in *C. elegan*, two miRNA, *lin-4* and *let-7*, regulated the endogenous gene which is involved in developmental timing by forming partial complementary to 3' untranslated region of target mRNA, *lin-14* and *lin*-41 (71-74). In Figure 11, microRNA gene is transcribed from RNA polymerase II in nucleus and produced the long primary transcript called pri-microRNA which is composed of several hundred nucleotides long (43, 75). Pri-microRNA is processed by another class of RNase III enzyme called Drosha. Drosha is composed of long N-terminal region, two RNase III domains and double-stranded RNA binding domain (dsRBD) (43, 75) . Drosha required a hairpin dsRNA with a loop of greater than 10 nucleotides as a specific substrate. This enzyme is associated with double-stranded RNA binding protein called Pasha which recognized the active site of RNase III domain of Drosha (43). The Drosha/Pasha complex activated the cleavage of 30 base pairs from the 10 nt loop resulting in the ~70 nucleotides stem loop product called pre-miRNA which contains 2 nucleotides 3' overhang at the terminus (43, 75). The pre-miRNA is then exported from the nucleus to the cytoplasm

by exporting factor, exportin-5, which directly and specifically binds to the pre-miRNA (43, 76). In the cytoplasm, Dicer enzyme recognizes 2 nucleotides 3' overhang of Pre-miRNA by using PAZ domain and generates the ~21-23 nucleotides mature miRNA (43). The mature miRNA is then transferred into RISC which has the Argonaute protein binding to the 5'end and the 3'end of mature miRNA by using PIWI and PAZ domain, respectively, similar to the siRNA (75). In human cell, Argonaute protein, eIF2C2, and two ribonucleoprotein complex of the ATP-dependent RNA helicase , Gemin 3 and Gemin 4 proteins, are found to be co-immunoprecipitate with miRNA in the RISC activity assay (77). In *C. elegan*, two Argonaute proteins, Alg-1 and Alg-2 are required for miRNA function similar to Rde-1 in siRNA function (78, 79). In Arabidopsis, AGO1 is required for miRNA function and PTGS (80). The perfectly match miRNA can act as a siRNA in the production of mRNA cleavage and degradation (81). However, binding of imperfect complementary miRNA to the 3' untranslated region of target gene cause the translational suppression which inhibits the expression at the level of protein synthesis (81). Conversely, imperfect complementary siRNA to the mRNA target can induce the translational inhibition as miRNA function (81). In mammalian cell culture, siRNA can repress gene expression by forming the partial base-pairing to the 3'UTR of target mRNA without the effect to the mRNA stability (77). Therefore, the function of siRNA and miRNA in gene silencing, either trigger the degradation of target gene or activation of translational repression, depends on the degree of the complementarity to the target gene (71-74, 82-83)

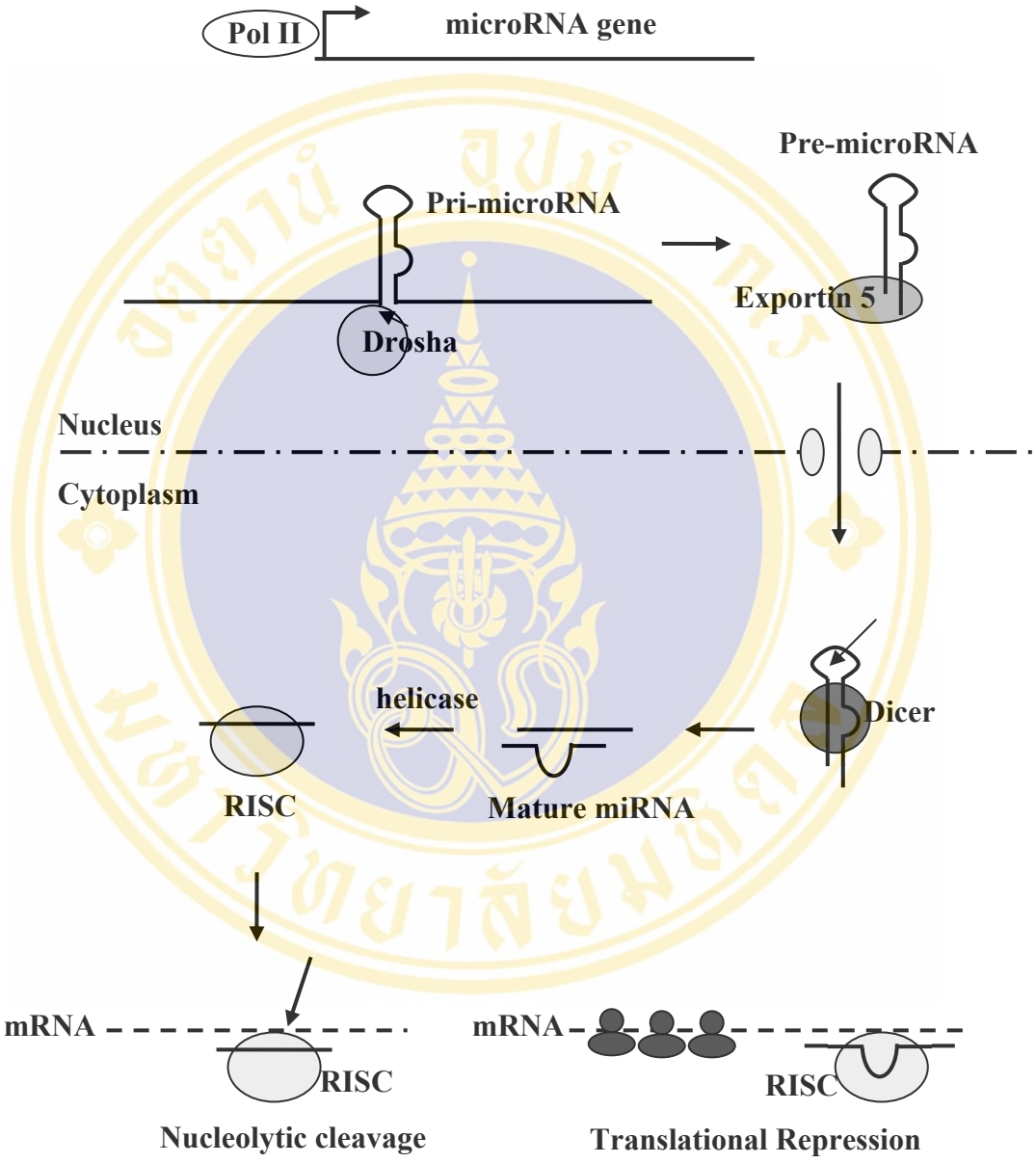

Figure 11. The model of the microRNA (miRNA) pathway (Modified from (43))

CHAPTER II
OBJECTIVE

2.1 Rationale

Penaeus monodon or the black tiger shrimp, is the export product that has high commercial value in Thailand. However, the shrimp farming in our country has encountered several problems with viral infectious diseases, such as, diseases from Yellow Head Virus and white spot syndrome virus, which cause a collapse in shrimp production and thus affect the economy of our country. As such, the mechanism of RNA interference has been developed to control viral replication in the shrimp. Therefore, understanding of the function of Argonaute protein which is a key component in RISC will improve the understanding of RNAi pathway that has become a potential way to prevent viral infectious disease in this economically important species.

2.2 Objective

The objectives of this thesis are

- To clone and characterize Argonaute cDNA that encodes Argonaute protein from *P. monodon*

- To investigate whether Argonaute plays role in RNAi pathway in *P. monodon*.

CHAPTER III
MATERIALS

3.1 Materials

3.1.1 Bacterial strain

Escherichia coli, DH5α [*supE*44Δ*lac*U169(Φ80 lacZ ΔM15)*hsdR*17 *recA*1 *endA*1 *gyrA*96 *thi*-1 *relA*1] was used as a host for plasmid propagation.

3.1.2 Culture media

3.1.2.1 Bacterial culture media

-LB medium : 1.0% (w/v) tryptone, 0.5%(w/v) yeast extract, 1.0% (w/v) NaCl, pH 7.5

-LB agar : LB broth with 2.0%(w/v) agar

The *E. coli* transformants were grown in LB/Ampicillin medium containing 100 μg/ml Ampicillin.

-SOB medium : 2% (w/v) bacto tryptone, 0.5% (w/v) yeast extract, 10 mM NaCL, 2.5 mM KCL, 10 mM $MgCl_2$ and 10 mM $MgSO_4$

3.1.2.2 Primary cell culture medium

-Leibovitz's L-15 medium : Leibovitz's L-15 powder, 1% D-Glucose and 0.5% NaCl, pH 7.5

-Washing medium : 2X-Leibovitz's L-15 medium, 1% D-Glucose, 0.5% NaCl, 200 IU/ml penicillin, and 200 ug/ml streptomycin

-Working medium : 2X-Leibovitz's L-15 medium, 1% D-Glucose, 0.5% NaCl, 200 IU/ml penicillin, and 200 ug/ml streptomycin supplemented with 15% (v/v) fetal bovine serum, 15% shrimp meat extract and 5% (v/v) lactabumin

3.2 Enzymes and accessory buffers

Restriction enzymes and other modification enzymes were purchased from New England Biolabs, USA; Promega, USA; Gibco BRL, USA. The restriction enzymes used in this study are listed in Table1.

Table 1. Restriction enzymes and optimal condition for digestion

Enzymes	Recognition sequences	Optimal condition Buffer/Incubation Temperature
*Eco*R I	G^{v}AATTC	H/37°C
Nco I	C^{v}CATGG	H/37°C
Pst I	CTGCA^{v}G	H/37°C
Sal I	G^{v}TCGAC	D/37°C
Xba I	T^{v}CTAGA	D/37°C
Xho I	C^{v}TCGAG	D/37°C

Note: In the second coloumn, ^{v} indicates the cleavage site

Buffer D : 6 mM Tris-HCl (pH 7.9), 6 mM $MgCl_2$, 150 mM NaCl, 1 mM DTT

Buffer H : 90 mM Tris-HCl (pH 7.5), 10 mM $MgCl_2$, 50 mM NaCl

3.3 Cloning vectors

The pGEM®-T Easy (Promega) and pUC 18 (kindly provided Miss Supattra Treerattrakool) were used as cloning vectors. The detail about these vectors is given in Figure 1 and 2 and Table 2.

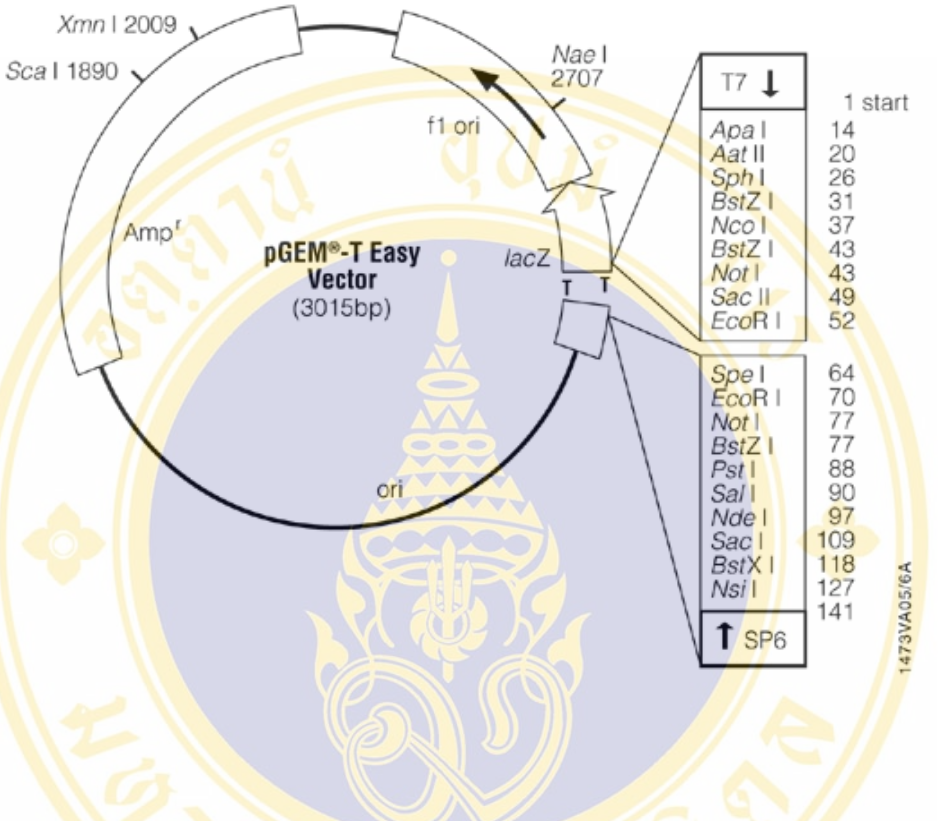

Figure 12. The physical map of pGEM®-T Easy vector (Promega)

The pGEM®-T Easy vector is suitable for cloning of PCR product. It contains a 3' terminal thymidine added to both ends, which is compatible with a single deoxyadenosine overhang at 3' end of PCR product generated by certain thermostable polymerases.

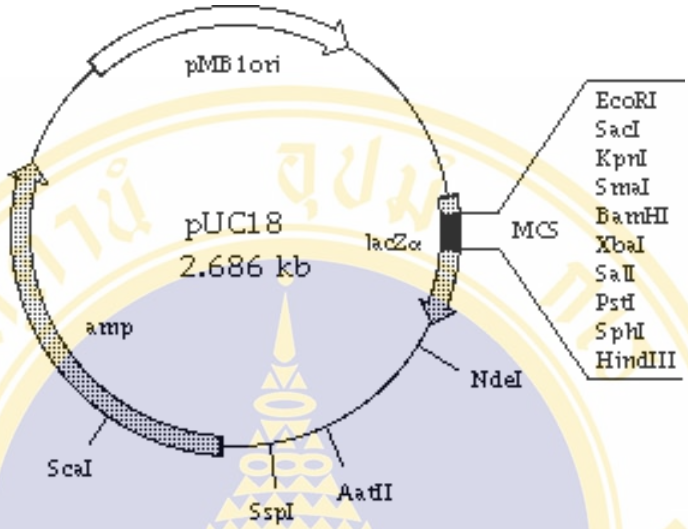

Figure 13. The physical map of pUC 18 vector

The pUC 18 vector is suitable for cloning of DNA fragment. It contains multiple-cloning sites on *lac Z* region. The DNA fragment insertion can be verified by using plates containing IPTG and X-Gal.

Table 2. Cloning vectors and descriptions

Plasmids	Description	Marker in *E. coli*	Figure
pGEM®-T Easy	-contain a single 3'terminal thymidine at both end of linearized vector which make the high efficiency of the ligation -contain the *lac Z* reporter gene and multiple cloning site	*lac Z* and *Amp*^{r}	1
pUC 18	-contain *lac* promoter for expression of cloned DNA -containing the *lac Z* reporter gene and multiple cloning site	*lac Z* and *Amp*^{r}	2

3.4 Miscellaneous

-Deoxynucleotide Triphosphate (dNTPs) Promega

-RiboMAX™ Large Scale RNA production System Promega

–T7 and SP6 RNA polymerase

-QIAquick Gel Extraction Kit QIAGEN

-QIAprep Spin Miniprep Kit QIAGEN

-MEGAscript® RNAi Kit Ambion

3.5 Oligonucleotides

The oligonucleotide primers were custum-ordered from Proligo Singapore Pty Ltd. The sequence of all oligonucleotides are shown in Table 3 and the recognition sites of restriction enzymes are underlined.

Table 3. The detail of oligonucleotide primers

Experiment	Primer name	Sequence (5'-3')	Tm (°C)
Reverse transcription	PRT	*Eco*R I *Hind* III *Xba* I *Bam*H I CCGGAATTCAAGCTTCTAGAGGATCCTT(T)$_{14}$	69.9
Reverse transcription	PM-1	*Eco*R I *Hind* III *Xba* I *Bam*H I CCGGAATTCAAGCTTCTAGAGGATCC	60.5
3'RACE	AGO1	CA(gA)CC(I)Tg(CT)TT(CT)Tg(CT)AA(gA)TA(CT)gC	48
3'RACE	RISC2R	gT(Ag)Tg(Ag)Tg(AgTC)C(gT)(TC)TT(TC)Tg	50
3'RACE	AGO/S1	TCTACAAGTCTACGCGGTTC	60
3'RACE	AGO/S2	ATGAGAGAGGCTTGCATAAA	56
5'RACE	dAGOF1	CCCTCGCAGTGGAAGATGATG	57
5'RACE	5'AGOR1	AGTGTCACCCACACGCTTCAC	55
5'RACE	5'RACE4	CCCTTAATTTCTTTTGTGAACTTGA	53
Coding sequence	AGOExF	*Eco*R I *Sal* I TGGAATTCGTCGACAAAAGAATGTACCCTGTTGGGCAGC	76
coding sequence	AGOExR	*Xba* I ACTCTAGATTAAGCAAAGTACATGACTCTGTTTG	59
dsRNA template	PAZ-F	TTTATGTGTGAAGTGTTAGATATTCGAG	53
dsRNA template	PAZ-R	CATGGTAGATGTCTGCATGTCTGT	53
dsRNA template	PIWI-F	CAGCTTGTATGTGTTGTTCTACCAGG	56
dsRNA template	PIWI-R	GAGATGATAACGAGCCCTGAAGG	56
dsRNA template	dsAGOF1	ACGTGACAGGGTGTTCAAGGTAG	55
dsRNA template	dsAGOR1	TGTATTGCATCATAAGGAATGGTTC	54
dsRNA template	dsAGOF2	AGACAGAATGGATCAACAACAC	48
dsRNA template	dsAGOR2	TGAGCAGCTCCTTCACCATAG	52

3.6 Shrimp specimens

Black tiger shrimps (*P. monodon*) were purchased from shrimp farms in Chachoengsao, Phatumthani, Samutprakarn and Samutsongkharm provinces of Thailand.

CHAPTER IV
METHODS

4.1 Amplification of a cDNA encoding Argonaute protein of *Penaeus monodon* (Pem-AGO)

4.1.1 First strand cDNA synthesis via reverse transcription (RT)

The total RNA from the lymphoid organ of *P. monodon* (kindly provided by Miss Supattra Treerattrakool) was used as a template to generate first-strand cDNA in a reverse transcription reaction. Total RNA (about 1 μg) was mixed with 500 nM of oligo-dT (PRT) primer in a final volume of 5 μl RNase-free water. The mixture was heated at 70°C for 5 min and quickly chilled on ice for 5 min. Then the following components were added to the mixture; 4 μl of 5X Improm-II™ reaction buffer, 2.4 μl of 25 mM $MgCl_2$,1 μl of dNTP mix (10 mM each), 0.5 μl of 40 unit RNasin ribonuclease inhibitor (Promega), 1 μl of Improm-II™ Reverse-Transcriptase (Promega) and RNase-free water to a final volume of 20 μl. The reaction was incubated at 25 °C for 5 min to allow binding of oligo-dT primer to the poly A of mRNA template. Then the temperature was raised to 42°C for 60 min to synthesize the first stranded DNA, and finally the reverse transcription reaction was inactivated at 70°C for 15 min. These incubation steps were performed in a GeneAmp®PCR System 2400 Thermal Cycler (PE applied Biosystems).

4.1.2 Amplification of partial Pem-AGO cDNA (fragment 1) by Polymerase chain reaction (PCR)

The first strand cDNA was subjected to the amplification of the partial cDNA encoding Argonaute protein using degenerate primers, AGO1 and RISC2-R. The PCR reaction was performed in the volume of 25 μl containing of 17.75 μl of RNase-free water, 2.5 μl of 10X thermophilic polymerase reaction buffer, 2 μl of 25

mM $MgCl_2$, 0.5 µl of dNTP mix (10 mM each), 0.5 µl of 10 µM AGO1 upstream primer, 0.5 µl of 10 µM RISC2-R downstream primer and 1 µl of the first strand cDNA. After incubating the mixture at 94°C for 3 min, 0.25 µl of 1.25 unit Taq DNA polymerase (Promaga) was added. Amplification was performed with 35 reaction cycles, each comprising of denaturation at 94°C for 30 sec, annealing at 48°C for 30 sec and extension at 72°C for 1 min. The last PCR cycle was followed by a 7 min extension at 72°C for 7 min.

4.1.3 Amplification of the 3' region (fragment 2) of Pem-AGO cDNA by 3' Rapid Amplification of cDNA ends (3'RACE)

The first strand cDNA was subjected to amplification of the 3' end of Argonaute cDNA using specific primers, AGO/S1 and AGO/S2. The PCR reaction was the same as described earlier for the first amplification using degenerate primers, except that 0.5 µl of 10 µM AGO/S1 and 0.5 µl of 10 µM PM-1 primers were used instead of AGO1 and RISC2-R respectively. The amplification step was performed as the previous step, except that the annealing was carried out at 55°C. Then, the nested PCR conducted by AGO/S2 and PM-1 primers was amplified to increase specificity using the same condition, except the annealing temperature at 50°C was used.

4.1.4 Amplification of the 5' region of Pem-AGO cDNA

4.1.4.1 Amplification of partial 5' sequence (fragment 3) of Pem-AGO cDNA

The first strand cDNA from 4.1.1 was used as a template to amplify partial 5' region of Pem-AGO cDNA using two specific primers; dAGOF1 which was designed from the conserved nucleotide sequence of *D. melanogaster*'s Argonaute 1 and 5'AGOR1 which was designed from the nucleotide sequence of the 3'RACE fragment. The PCR reaction was set up as previous step with 0.5 µl of 10 µM dAGOF1 and 0.5 µl of 10 µM 5'AGOR1 primers and the annealing took place at 55°C.

4.1.4.2 Amplification of the 5' end of Pem-AGO cDNA (fragment 4) by 5'RACE

4.1.4.2.1 First strand cDNA synthesis via reverse transcription (RT)

The total RNA from the lymphoid organ of *P. monodon* was used as a template to generate the first strand cDNA in a reverse transcription reaction similar to 2.1.1 except that 500 nM of 5'RACE 1 primer was used in the reaction instead of oligo-dT primer.

4.1.4.2.2 Tailing of the cDNA with dATP

The poly A tail was added to the 3'end of the first strand cDNA by the action of terminal deoxynucleotidyl transferase (Promega). The final volume of 25 µl contained 10 µl of the RT product from 2.3.2.1, 10 mM of dATP and 5 µl of 5X TdT buffer [100 mM cacoadylate buffer (pH 6.8), 1 mM $CoCl_2$ and 0.1 mM DTT]. The mixture was incubated at 94ºC for 3 min and chilled on ice. The reaction was added with 15 unit (1 µl) of terminal deoxynucleotidyl transferase and incubated at 37ºC for 20 min. Finally, the reaction was inactivated by further incubated at 65ºC for 10 min.

4.1.4.2.3 Amplification of the 5'end of Argonaute cDNA by PCR

The dATP-tailed first strand cDNA was subjected to amplification using 5'RACE 4 gene specific primer, designed from the conserved nucleotide sequence, and oligo-dT primer in the PCR reaction as described in previous steps with the annealing temperature of 55°C.

4.2 Amplification of the cDNA coding sequence of Argonaute protein by Phusion™ DNA polymerase

The first-strand cDNA generated by oligo-dT primer from 4.1.1 was used as a template to amplify the coding sequence of Argonaute cDNA using 5'and 3'gene specific primers, AGOEx-F and AGOEx-R, that were designed based on the sequence from the start and stop codons of the 5' and 3' RACE products, repectively. The PCR reaction was performed in the volume of 25 µl composing of 12.5 µl of RNase-free

water, 5 µl of 5X thermophilic polymerase reaction buffer, 0.75 µl of DMSO, 0.5 µl of dNTP mix (10 mM each), 0.5 µl of 10 µM AGOEx-F upstream primer, 0.5 µl of 10 µM AGOEx-R downstream primer and 1 µl of the first strand cDNA. After incubating the mixture at 98°C for 3 min, 0.25 µl of 1.25 unit Phusion™ DNA polymerase was added. Amplification was performed with 35 cycles, each comprising of denaturation at 98°C for 10 sec, annealing at 55°C for 30 sec and extension at 72°C for 90 sec. The last PCR cycle was followed by an extension at 72°C for 10 min.

4.3 Agarose gel electrophoresis

Gel electrophoresis was used for determining the size of PCR products. To prepare the gel, 1% (w/v) or appropriate amount of agarose in 1X TBE buffer [45 mM Tris-borate, 1 mM EDTA] was melted and poured into edge-sealed plastic tray. A comb was inserted in order to form the sample slot. After the agarose gel was completely set (20-30 min at room temperature), the comb was carefully removed and the gel was installed on the platform in the electrophoresis chamber containing 1X TBE buffer. The DNA samples were mixed with 30% (v/v) gel-loading buffer [25% (v/v) glycerol, 60 mM EDTA, 0.25% (W/V) Bromophenol Blue] and slowly loaded into the slots of the submerged gel. The electrophoresis was carried out with a constant voltage at 80 V for 90 min. After electrophoresis, the gel was stained with a staining solution containing 2.5 µg/ml of ethidium bromide (EtBr) and destained with water for 10-15 min. The DNA pattern was visualized under UV light [Gel Doc model 1000 (BIO-RAD, USA)] and photographed.

4.4 Purification of DNA using QIAquick Gel Extraction Kit (QIAGEN)

The expected DNA fragment was excised from agarose gel with a clean razor blade under a long wavelength UV light for the shortest possible time. The gel slice was transferred to a microcentrifuge tube and the volume of the gel was approximately determined (0.1 g equals approximately 100 µl). Then the DNA fragment was purified using a QIAquick GEL Extraction Kit following the manufacturer's protocol. Three volumes of QG buffer were added to 1 volume of the gel, then the mixture was incubated at 50°C for 10 min or until the gel slice was completely dissolved. The

mixture was transferred to the QIAquick column inserted in 2 ml collection tube. The column was centrifuged at 13,000 rpm for 1 min at room temperature. The flow-through solution was discarded. The 0.5 ml of QG buffer was added to the column and centrifuged for 1 min as the previous step. After the flow-through solution was removed, the column was washed by adding 0.75 ml of PE buffer and centrifuged for 1 min. In order to collect the eluted DNA, the column was placed on a fresh microtube and 20 μl of EB buffer was applied. The column was left at room temperature for 10 min before centrifugation. Finally, the concentration of the eluted DNA was determined by agarose gel electrophoresis.

4.5 DNA ligation

The purified DNA fragment was ligated to the plasmid vector as follows. The ligation mixture was performed using the catalytic reaction of T4 DNA ligase to regenerate phosphodiester bonds between 3'-hydroxyl and 5'-phosphate termini in DNA. A final volume of 10 μl reaction contained a mixture of digested plasmid vectors and the DNA fragments at the molar ratio of 1:3 in 1X Ligase Reaction Buffer [50 mM Tris-HCL, pH 7.6, 10 mM $MgCl_2$, 1 mM ATP, 1 mM DTT, 5%(W/V) polyethylene glycol-8000] and 1 unit T4 DNA ligase. The ligation was incubated at 4°C for 12-16 hr.

4.6 Preparation of competent cells

A single colony of *E. coli* strain DH5α was inoculated into 25 ml of SOB medium, pH 7.0 [2% (w/v) bacto tryptone, 0.5% (w/v) yeast extract, 10 mM NaCL, 2.5 mM KCL, 10 mM $MgCl_2$ and 10 mM $MgSO_4$] in 250 ml flask. The cells were incubated at 18ºC with vigorous shaking for 24 h. The overnight culture was transferred into 250 ml of SOB medium and incubated at 18ºC with vigorous shaking until OD_{600} reached 0.4-0.6. The culture was placed on ice for 10 min before transferred to 500 ml centrifuge bottle and centrifuged at 2,500 x g, 4ºC for 10 min. The cell pellet was resuspended in 80 ml of ice-cold TB buffer, pH 6.7 (10mM PIPES, 55 mM $MnCl_2$, 15 mM $CaCl_2$ and 250 mM KCL), incubated on ice for 10 min and centrifuged at 2,500 x g, 4ºC for 10 min. The cells were resuspended in 20 ml of ice-cold TB buffer. Dimethyl sulfoxide (DMSO) was added with gently swirling to a final

concentration of 7% (v/v) then the culture was incubated on ice for 10 min. The resulting competent cells were stored at -80ºC as 200 µl aliquots in microtubes.

4.7 Transformation of competent *E.coli* DH5α

The ligation products or plasmid DNA were used for transformation to *E. coli* cells. A volume of 10 µl of ligation product was transferred to 100 µl of competent cells, mixed gently by flicking the tube and incubated on ice for 30 min. The cells were heat-shocked at 42°C for exactly 90 sec and immediately chilled on ice for 2 min. Then 900 µl of LB medium was added and the mixture was incubated at 37°C with shaking for 1 hr. The transformed cells were collected by centrifugation at 13,000 x g for 30 sec and suspended in 600 µl of LB medium. Finally, 200 µl of suspended cells were spread on each LB agar plates containing 100 µg/ml of ampicillin. The transformants were allowed to grow by incubation at 37°C overnight.

4.8 Plasmid extraction from *E. coli* using CTAB method

Plasmids were prepared based on the use of the cationic detergent cetyltrimethylammonium bromide (CTAB) for DNA precipitation. A single colony of bacteria was inoculated in 3 ml of LB medium containing 100 µg/ml ampicillin. After overnight growth in a 37°C shaker incubator, cells were harvested in a 1.5 ml microcentrifuge tube by spinning at 13,000 x g for 30 sec. Then, the pellets were suspended in 350 µl of STET buffer [8% (w/v) sucrose, 50 mM EDTA, 0.1% (w/v) Triton X-100, 50 mM Tris-HCL, pH8.0]. After vortexing, 25 µl of lysozyme solution (10 mg/ml) was added and the mixture was incubated at room temperature for 5-10 min. The samples were then placed in a boiling waterbath for 45 sec, followed immediately by incubating on ice for 30 sec and then centrifuged at 13,000 x g for 10 min. After discarding the pellet, 35 µl of 5% (w/v) CTAB solution was added and then centrifuged at 13,000 x g for 10 min. The supernatant was removed and 300 µl of 1.2 M NaCl was added to resuspend the pellet. After vortexing, 1 µl of 10 mg/ml RNase A was added with incubation at 37°C for 1 hr. Then, the proteins were removed by adding an equal volume of phenol/chloroform and mixed by shaking for 30 sec. The samples were subsequently centrifuged at 13,000 x g for 10 min to separate the

aqueous phase from the organic phase. The clear aqueous phase was transferred to a new tube. Then 2 volumes of pre-cooled absolute ethanol was added and incubated at -30°C for 20 min. The DNA pellets were recovered by centrifugation at 13,000 x g, 4°C for 10 min. Finally, the DNA pellets were washed with 70% ethanol, air dried, and resuspended in 15-20 µl of milli-Q water.

4.9 Plasmid DNA extraction using QIAprep Spin Miniprep Kit (QIAGEN)

The overnight bacterial culture was collected by centrifugation at 13,000 x g for 30 sec at room temperature, and the supernatant was discarded. The cell pellet was resuspended with 250 µl of Buffer P1 and then added with 250 µl of Buffer P2. The mixture was gently mixed by inverting the tube for 4-6 times. A volume of 250 µl of Buffer N3 was added and the tube was gently inverted for 4-6 times, then centrifuged at 13,000 rpm for 10 min. The supernatant was transferred to the QIAprep spin column and centrifuged at 13,000 rpm for 1 min. The flow-through solution was discarded and 750 µl of Buffer PE was added. After centrifugation for 1 min, the flow-through was removed and the additional centrifugation for 1 min was required to remove the residual wash buffer. The QIAprep column was placed in a fresh 1.5 ml microcentrifuge tube and the plasmid DNA was eluted by adding 20 µl of Buffer EB [10 mM Tris-Cl (pH 8.5)], left standing for 1 min and followed by centrifugation for 1 min to collect DNA solution.

4.10 Screening for recombinant clones by restriction enzyme analysis

After plasmid DNA was extracted from *E. coli* cells, the recombinant plasmids were digested with appropriate restriction enzymes. The final volume of 20 µl contained 2 µl of 10X Buffer H, 0.5 µl of 10 unit of restriction enzyme, 1 µl (1 µg) of plasmid DNA and RNase-free water to final volume 20 µl. The reaction was incubated at 37°C for 1 hr. Then, the pattern of digested DNA was analyzed by electrophoresis on 1% agarose gel.

4.11 DNA Sequencing and data analysis

The DNA sequences of selected clones were determined at DNA sequencing service either Macrogen (www.macrogen.com) or Institute of Molecular Biology and Genetics (Mahidol University). The sequencing data were compared against the nucleotide sequences in all non-redundant databases using the blastn program at www. ncbi.nlm.nih.gov/blast. The nucleotide sequences were translated to amino acid sequences using the transeg program at www.mb.mahidol.ac.th/ tools/EMBOSS, and the amino acid sequences were searched for homology using the blastp program at www. ncbi.nlm.nih.gov. Multiple sequence alignments were later performed using the Vector NTI , Clustal X and GeneDoc programs.

4.12 Amplification of short DNA templates for the synthesis of double-stranded RNA by Vent DNA polymerase (Biolabs)

The small DNA templates for double-stranded RNA (dsRNA) synthesis were amplified using first strand cDNA synthesized by oligo-dT primer as a template. Three sets of forward and reverse specific primers, dsAGOF1-dsAGOR1, dsPIWIF-dsPIWIR and dsPAZF-dsPAZR were designed from non-conserved (the first pair) and conserved region (second and third pair) in the coding sequence of Argonaute cDNA, respectively. The amplification was performed in the volume of 25 µl containing of 15.75 µl of RNase-free water, 2.5 µl of 10X thermophilic polymerase reaction buffer, 0.5 µl of dNTP mix (10 mM each), 2.5 µl of 10 µM of µpstream primer (dsAGOF1, dsPIWIF or dsPAZF), 2.5 µl of 10 µM of downstream primer (dsAGOR1, dsPIWIR or dsPAZR) and 1 µl of the first strand cDNA. After incubating the mixture at 95°C for 3 min, 0.25 µl of 1.25 unit Vent DNA polymerase was added. Amplification was performed with 35 cycles, each comprising of denaturation at 93°C for 10 sec, annealing at 45°C (dsAGOF1-dsAGOR1) or at 50°C (dsPIWIF-dsPIWIR and dsPAZF-dsPAZR) for 10 sec and extension at 72°C for 1 min. The last PCR cycle was followed by a final extension at 72°C for 7 min.

4.13 Amplification of the short DNA template for the synthesis of double-stranded RNA by Taq DNA polymerase

The third pairs of primer, dsPAZ-F and dsPAZ-R, were designed from conserved PAZ domain of Argonaute cDNA. The amplification was performed in the volume of 25 µl containing of 17.75 µl of RNase-free water, 2.5 µl of 10X thermophilic polymerase reaction buffer, 2 µl of 25 mM $MgCl_2$, 0.5 µl of dNTP mix (10 mM each), 0.5 µl of 10 µM AGO1 µpstream primer, 0.5 µl of 10 µM RISC2-R downstream primer and 1 µl of the first strand cDNA. After incubating the mixture at 94°C for 3 min, 0.25 µl of 5 unit Taq DNA polymerase (Promaga) was added. Amplification was performed with 35 reaction cycles, each comprising of denaturation at 94°C for 30 sec, annealing at 48°C for 30 sec and extension at 72°C for 1 min. The last PCR cycle was followed by a 7 min extension at 72°C for 7 min.

4.14 Synthesis of double-stranded RNA by *in vitro* transcription using Ribomax™ Large Scale RNA Production System-T7 RNA polymerase (Promega)

The PCR product from 3.14 was then ligated to pGEM®-T Easy vector and transformed into *E. coli* DH5α as described in 3.7 and 3.8. The direction of the insert fragment was determined by DNA sequencing. The clone that contained the insert in either forward and reverse direction related to the T7 promoter were selected as a template for *in vitro* transcription of the sense or antisense.

4.14.1 *In vitro* transcription of sense and antisense-strand RNA

A plasmid DNA template was linearized with an appropriate restriction enzyme (*Sal* I) before subjected to *in vitro* transcription to produce an RNA of defined length. The linearized DNA was heated in a waterbath at 65°C to inactivate the enzyme followed by ethanol precipitation. Then the template was used in the synthesis of RNA by setting up the reaction at room temperature. The reaction was performed in 100 µl reaction mixture containing 20 µl of T7 Transcription 5X Buffer (400 mM of HEPES-KOH (pH 7.5), 120 mM of $MgCl_2$, 10 mM of spermidine and 200 mM of DTT), 30 µl of rNTPs (25 mM each of ATP, CTP, GTP, UTP), 40 µl of 10 µg of linear DNA template, 10 µl of T7 RNA polymerase. The reaction was mixed and

incubated at 37°C for 4 hr. Then 10 µl of RNase-Free DNase (1u/ug) was added to the reaction to remove the DNA template following transcription. The sample was incubated at 37°C for 15 min. Then 1 volume of TE (10 mM of Tris-HCL, pH 8.0 and 1 mM of EDTA, pH 4.5)-saturated phenol:chloroform:isoamyl alcohol (25:24:1) was added. The reaction was vortexed for 1 min and centrifuge at 13,000 x g, 4°C for 2 min. The upper aqueous phase was transferred to a fresh microtube and added with 1 volume of chloroform:isoamyl alcohol (24:1). The reaction was vortexed for 1 min and centrifuge similar to the previous step. After the upper aqueous phase was transferred to a fresh microtube, 0.1 volume of 3M Sodium Acetate (pH 5.2) and 1 volume of isopropanol was added and placed on ice for 5 min. The reaction was centrifuged at 13,000 x g, 4°C for 10 min followed by washing with 1 ml of 70% ethanol. After centrifugation at 13,000 x g, 4°C for 5 min, the supernatant was discarded and the pellet was air-dried and resuspended with 50 µl of RNase-free water.

4.14.2 Synthesis of double-stranded RNA

Two direction of single-stranded RNA (sense and antisense) from the previous step were annealed to synthesize double-stranded RNA. The annealing reaction contained 20 µl of 5X annealing buffer (100 mM of Potassium acetate, 30 mM of HEPES-KOH (pH 7.4) and 30 mM of MgOAC), the equal concentration of sense and antisense single-stranded RNA and RNase-free water to a final volume of 100 µl. The sample was heated to denature at 90°C for 2 min. The temperature was gradually decreased to 37°C and hold for 1 hr. The reaction was placed at room temperature for another 1 hr. The sample was analyzed on agarose gel electrophoresis and store at -20°C.

4.14.3 Digestion of remaining single-stranded RNA in the double-stranded RNA reaction

The excess single-stranded RNA that remained after the annealing reaction was degraded by digestion with RNase A. The digested reaction containing 2 µl of 5X RNaseA buffer (300 mM of Sodium acetate, 100 mM of Tris, pH 8.0 and 5 mM of EDTA, pH 8.0), 2-5 µg of double-stranded RNA, 1 µl of 0.1ug/ul RNase A

and the RNase-free water to 10 µl. The reaction was incubated at 37°C for 10 min. The sample was analyzed on agarose gel electrophoresis.

4.14.4 Precipitation of double-stranded RNA from the enzymatic reaction

The equal volume of TE-saturated phenol:chloroform:isoamyl alcohol (25:24:1) was added to the digestion reaction. The reaction was vortexed for 1 min and centrifuge at 13,000 x g, 4°C for 5 min. The upper aqueous phase was transferred to a new tube and added with equal volume of chloroform. The mixture was vortexed for 1 min and centrifuge similar to the previous step. After the upper aqueous phase was transferred to a fresh microtube, 0.1 volume of 3M Sodium Acetate (pH 5.2) and 1 volume of isopropanol was added and incubated at -30°C for 1 hr. The sample was centrifuged at 13,000 x g, 4°C for 15 min. The supernatant was removed and 1 ml of 70% ethanol was added to the pellet. After centrifugation at 13,000 x g, 4°C for 5 min, the supernatant was discarded and the pellet was air-dried and resuspended with 50 µl of RNase-free water.

4.15 *In vivo* stem-loop production (Bacterial expression) of double-stranded RNA of yellow head virus (YHV) and green fluorescense protein (GFP)

The single colony of YHV (or GFP) pET3a plasmid (obtained from Miss Supansa Yodmuong) was inoculated into 4 ml of LB medium (1.0% (w/v) tryptone, 0.5% (w/v) yeast extract, 1.0% (w/v) NaCl, pH 7.5) containing 12 µg/ml of tetracyclin and 100 µg/ml of Ampicillin and incubated at 37°C overnight with vigorous shaking. The 0.5 ml of overnight culture was transfered into 50 ml of 2XYT medium and incubated at 37°C with vigorous shaking until OD_{600} reached 0.6-0.7. Then the culture was induced with 0.4 mM IPTG for 4 hr until OD_{600} reached 1.0. The cell was centrifuged at 6,000 x g, 4ºC for 10 min to collect the pellet and resuspended in 0.1% SDS in PBS. The sample was boiled for 2 min followed by RNase A digestion to degrade the loop from the double-stranded RNA. The reaction was supplied with 5X RNase A buffer and 50 µg of RNase A. After the reaction was incubated at 37°C for 15 min, the double-stranded RNA was isolated with TRI-REAGENT®. The 5 ml of TRI-REAGENT® was added to the reaction and mixed by vortexing. The 1 ml of

chloroform was added and incubated at room temperature for 15 min. The mixture was centrifuged at 10,000 x g for 10 min at 4ºC. The upper phase was collected and added with 2.5 ml of isopropanol for precipitation at -20ºC for overnight. Then the mixture was centrifuged at 10,000 x g for 15 min at 4ºC. The supernatant was discarded and 1 ml of 75% ethanol was added to the pellet followed by centrifugation at 7,500 x g for 5 min at 4ºC. Finally, the pellet was resuspended with 150 mM NaCl and stored at -20ºC.

4.16 Determination of RNA concentration and purity

The concentration and purity of RNA was determined by using spectrophotometer at wavelength 260 nm and 280 nm. The final RNA concentration was measured by spectrophotometer at wavelength 260 nm and was calculated by the following formula.

RNA concentration (µg/µl) = [A_{260} x (dilution factor) x 40] / 1000

The RNA purity was determined by the absorbance ratio of A_{260}/A_{280}. A ratio of 1.8-2.0 indicated that RNA samples were relatively pure.

4.17 Electrophoresis of RNA

The RNA sample was analyzed in 1.2% agarose gel containing 0.48 g of agarose, 2.2 ml of 37% formaldehyde, 4 ml of 10x MOPS buffer (200 mM of MOPS, 50 mM of sodium acetate and 10 mM of EDTA) and 33.8 ml of DEPC-water. The prepared RNA sample [3 µl of the RNA samples (3 µg), 9.5 µl of RNA loading buffer (360 µl of formamide, 80 µl of 10X MOPS buffer, 130 µl of 37% formaldehyde, 50 µl of sterile water, 50 µl of EtBr (10 mg/ml), 40 µl of sterile glycerol and 40 µl of saturated Bromophenol Blue in sterile water)] were heated at 65º C for 15 min and loaded onto the gel immersed in 1X MOPS buffer. The pattern of RNA was visualized under UV light.

4.18 RNA isolation

The lymphoid cell (or a pair of lymphoid organs) was homogenized in 600 µl of TRI-REAGENT®. After homogenization, 200 µl of chloroform was added and incubated at room temperature for 15 min. The mixture was centrifuged at 12,000 x g for 10 min at 4ºC. The upper phase was collected and added with 500 µl of isopropanol for precipition at -20ºC for overnight. Then the mixtue was centrifuged at 12,000 x g for 15 min at 4ºC. The supernatant was discarded and 1 ml of 75% ethanol was added to the pellet followed by centrifugation at 7,500 x g for 10 min at 4ºC. Finally, the pellet was resuspended with RNase-free water and stored at -80ºC.

4.19 Preparation of the primary cell culture from the lymphoid (Oka) organ of *P. monodon*

Primary cell cultures from the lymphoid (Oka) organ of *P. monodon* were established as described by Kasornchandra et al. (1999) and Assavalapsakul et al. (2003). The lymphoid organs, located at the anterior-ventral surface of hepatopancrease were dissected out from freshly killed *P. monodon*. The pooled lymphoid was washed five times in washing solution [2X-Leibovitz's L-15 medium, 1% of D-Glucose, 0.5% of NaCl, 5% lactabumin, 200 IU/ml penicillin, and 200 µg/ml streptomycin]. Then the collected tissue was transferred to working solution [2X-Leibovitz's L-15 medium, 1% of D-Glucose, 0.5% of NaCl, 200 IU/ml penicillin, and 200 µg/ml streptomycin supplemented with 15% (v/v) fetal bovine serum, 15% shrimp meat extract and 5% (v/v) lactabumin] in the cultured plate and minced into cell suspensions. Then the primary cell was transferred to 96-well tissue culture plate and incubated at 28ºC. Propagation of the cells was observed daily under an inverted microscope.

4.20 Transfection of double-stranded RNA into primary lymphoid cell using TransMessenger™ Transfection Reagent

TransMessenger Transfection Reagent was used to transfect double-stranded RNA into eukaryotic cells. The reagent is based on the lipid formulation which is composed of the specific RNA-condensing reagent (or Enhancer R), an RNA-condensing buffer (or Buffer EC-R) and TransMessenger Transfection Reagent. In the

first step, the double-stranded RNA was condensed with the specific RNA-condensing reagent (Enhancer R) in an RNA-condensing buffer (Buffer EC-R) in the ratio of 1 μg of double-stranded RNA to 2 μl of Enhancer R. The mixture was vortexed and incubated at room temperature for 5 min. In the second step, TransMessenger Transfection Reagent was added to the condensed double-stranded RNA in the ratio of 1 μg of double-stranded RNA to 2 μl of TransMessenger Reagent. The mixture was vortexed and followed by incubating at room temperature for 10 min to allow the forming of TransMessenger-RNA complexes. Then 150 μl of medium (without serum or antibiotic to avoid RNase contamination) was added, mixed by pipetting and dropped on the cell plate. The plate was swirled gently to distribute the transfection solution and incubated at 26 ºC for 3 hr before removing the reagent. After the cell was washed with the antibiotic-free medium, the growth medium was added and followed by incubating at 26 ºC further. The cell was collected at different time point, 24 h, 48h and 72 h, for RT-PCR analysis.

CHAPTER V
RESULTS

5.1 Cloning of a cDNA encoding Argonaute protein of *P. monodon* (Pem-AGO)

In order to obtain the nucleotide sequence of *P. monodon*'s Argonaute (Pem-AGO) cDNA, four overlapping partial cDNA fragments that comprise the entire length of Pem-AGO cDNA were cloned by the combination of RT-PCR and RACE strategies. Briefly, the first partial cDNA fragment (fragment 1) was cloned by RT-PCR with degenerate primers that were designed from the conserved sequences of Argonaute proteins. Then the nucleotide sequence of fragment 1 was used to design specific primers for 3' RACE to amplify fragment 2 that contains the information at the 3' end of the cDNA. The third fragment (fragment 3) containing partial 5' sequence upstream of the fragment 1 was subsequently cloned by using specific primer to fragment 1 and another primer that was designed based on *Drosophila*'s AGO1 nucleotide sequence. Finally the 5' sequence of Pem-AGO was completed by 5' RACE amplification of fragment 4. The relative locations of each fragments along the Pem-AGO cDNA is shown as diagram in Figure 14-15.

5.1.1 Amplification of partial cDNA (fragment 1) of Pem-AGO using degenerate primers

Total RNA from the lymphoid organ was reverse-transcribed into cDNA using PRT primer. Then, the amplification of the partial cDNA of Argonaute protein was performed with degenerate primers, AGO1 and RISC2-R primers which were designed based on the conserved sequences among Argonaute proteins from several species (Table 4). The PCR product of the expected size about 800 bp was obtained (Figure 16). This PCR fragment was recovered from the gel, cloned into pGEM®-T Easy vector and transformed to *E. coli* DH5α.

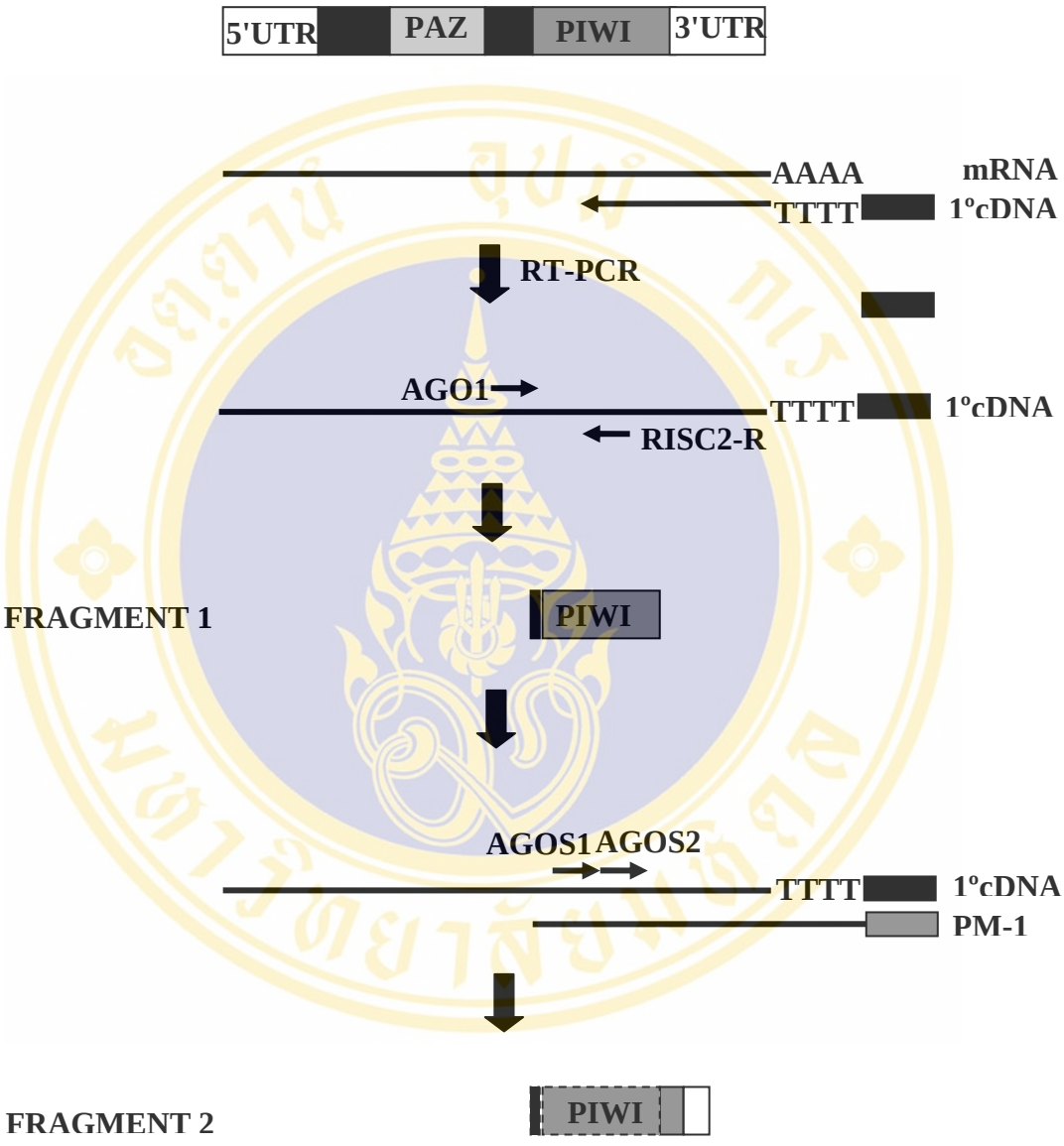

Figure 14. A schematic diagram representation of the amplification of fragments 1 and 2 of Pem-AGO cDNA

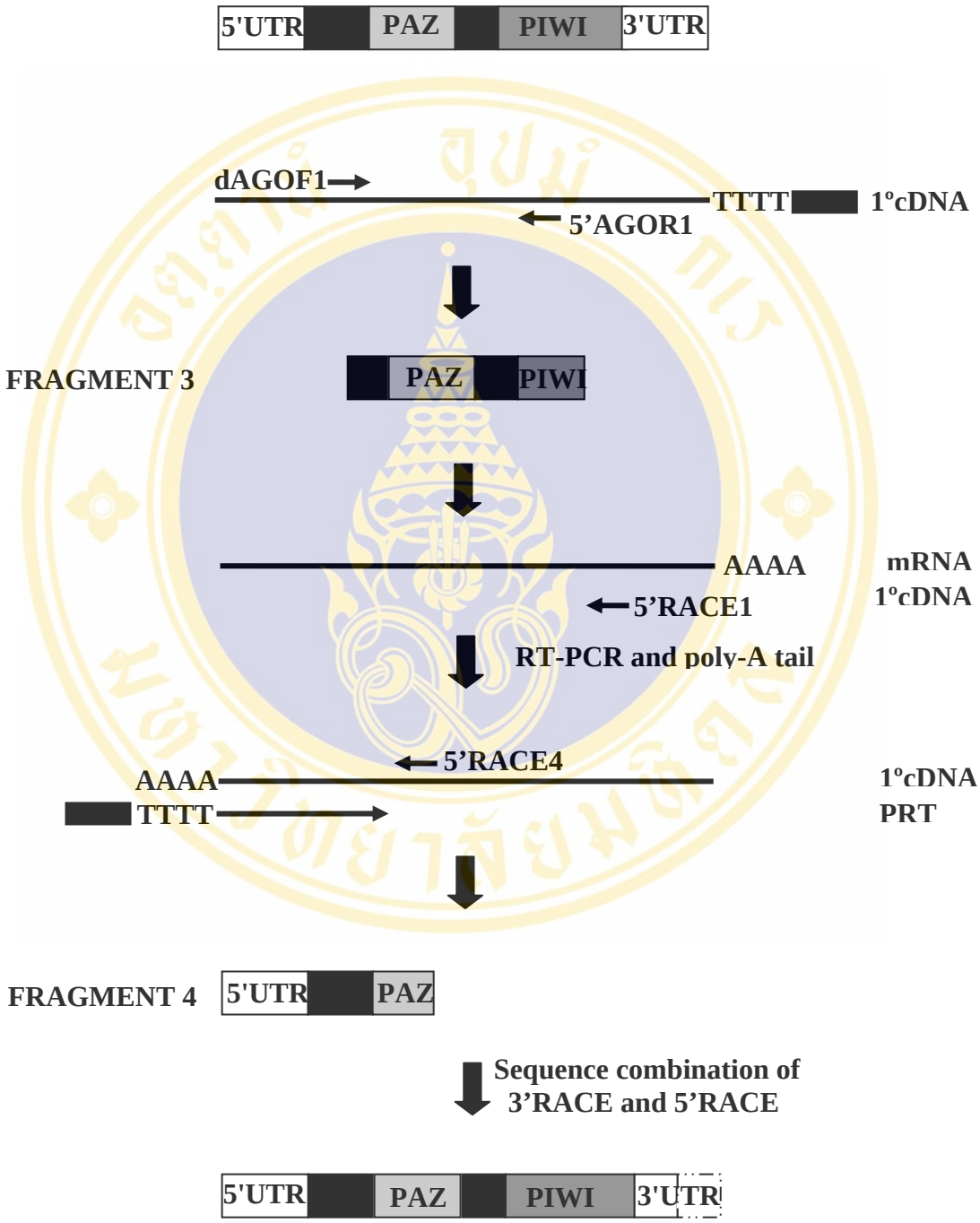

Figure 15. A schematic diagram representation of the amplification of fragments 3 and 4 of Pem-AGO cDNA

Argonaute Species	AGO1	RISC2-R
argo-A	QPAIPFIS	**QKRHHTR**
zwille-A	EPVIPIYS	**QKRHHTR**
argo1-D	**QPCFCKYA**	**QKRHHTR**
eIF2C2-H	**QPCFCKYA**	**QKRHHTR**
argo1-C	**QPCFCKYA**	**QKRHHTR**

Table 4. Two degenerate primers designed from conserved amino acid blocks of Argonaute protein from different species (shown in bold)

Argo-A and zwille-A are Argonaute protein of *A. thilania*, argo1-D are Argonaute protein of *D. melanogaster*, eIF2C2 are Argonaute protein of *H. sapiens*, argo1-C are Argonaute protein of *C. elegan*.

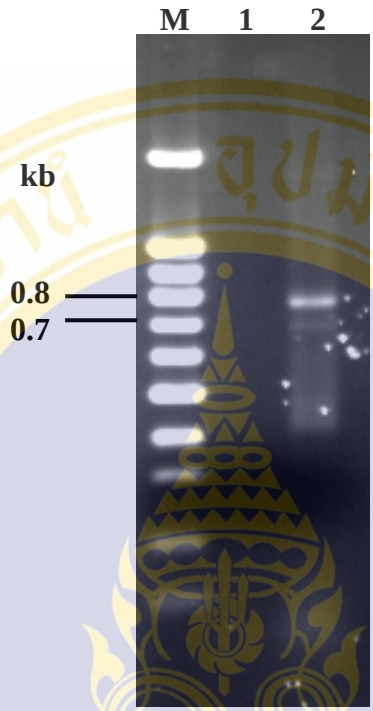

Figure 16. The PCR product of the fragment 1 of Pem-AGO cDNA

Total RNA from the lymphoid organ was used as a template for RT-PCR with AGO1 and RISC2-R primers. The amplification products were fractionated on 1.2% agarose gel electrophoresis. Lane M is 100 bp DNA ladder. Lane 1 is the negative control which contained no cDNA template in the reaction. Lane 2 is the PCR product of fragment 1 that was amplified from AGO1 and RISC2-R primers.

5.1.2 cDNA cloning and screening of recombinant clones

Twenty recombinant clones were screened by restriction enzyme analysis with restriction endonuclease, *Eco*R I. The patterns of digestion products of some recombinant clones were shown in Figure 17. The clones that contained the correct insert fragment would generated 2 bands, a 3 kb of the vector and a 800 bp of the insert. Three recombinant clones, no. 1, 5, and 8 harboring the insert fragment of the correct size were selected for further characterization.

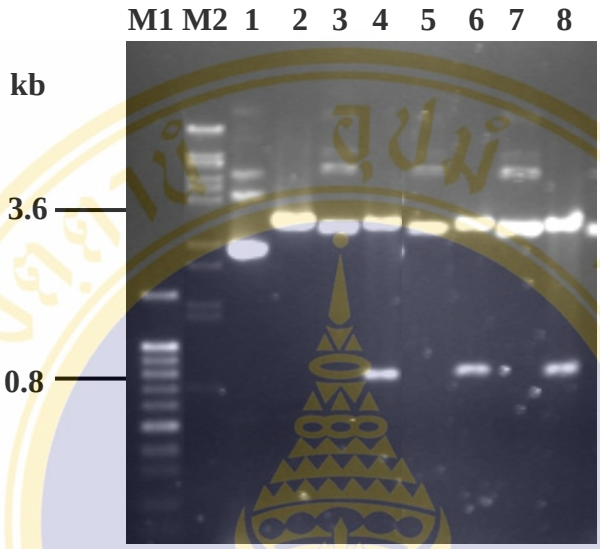

Figure 17. Screening of recombinant clones containing fragment 1 by restriction enzyme analysis

Randomly picked recombinant clones were digested with *Eco*R I. Lanes M1 and M2 are 100 bp DNA ladder and *λBstE* II marker, respectively. Lanes 1 and 2 are undigested and *Eco*R I-digested plasmid of the blue colony that contains the vector alone. Lanes 3, 5 and 7 represent undigested plasmids of the white colonies number 1, 5 and 8, respectively where as the *Eco*R I-digested plasmids of clones number 1, 5 and 8 were shown in lanes 4, 6 and 8, respectively.

5.1.3 Sequence analysis of recombinant clones

The plasmids of the 3 selected clones were subjected to nucleotide sequencing. The nucleotide sequences of these clones were compared by Clustal X program. The sequence comparison showed that all three clones had almost identical nucleotide sequences except for a nucleotide substitution at position 62 in clone no. 1 (Figure 18). Searching for significant similarity by blastn program (www.ncbi.nlm.nih.gov/blast) showed that the consensus nucleotide sequence shared the highest sequence similarity to *Drosophila melanogaster* Argonaute 1, dAGO1 (CG6671-PB) at 78% identity. Similar result was obtained where the blastp search revealed a 81% identity between the deduced amino acid sequence of fragment 1 to the amino acid sequence of dAGO1 (Figure 19).

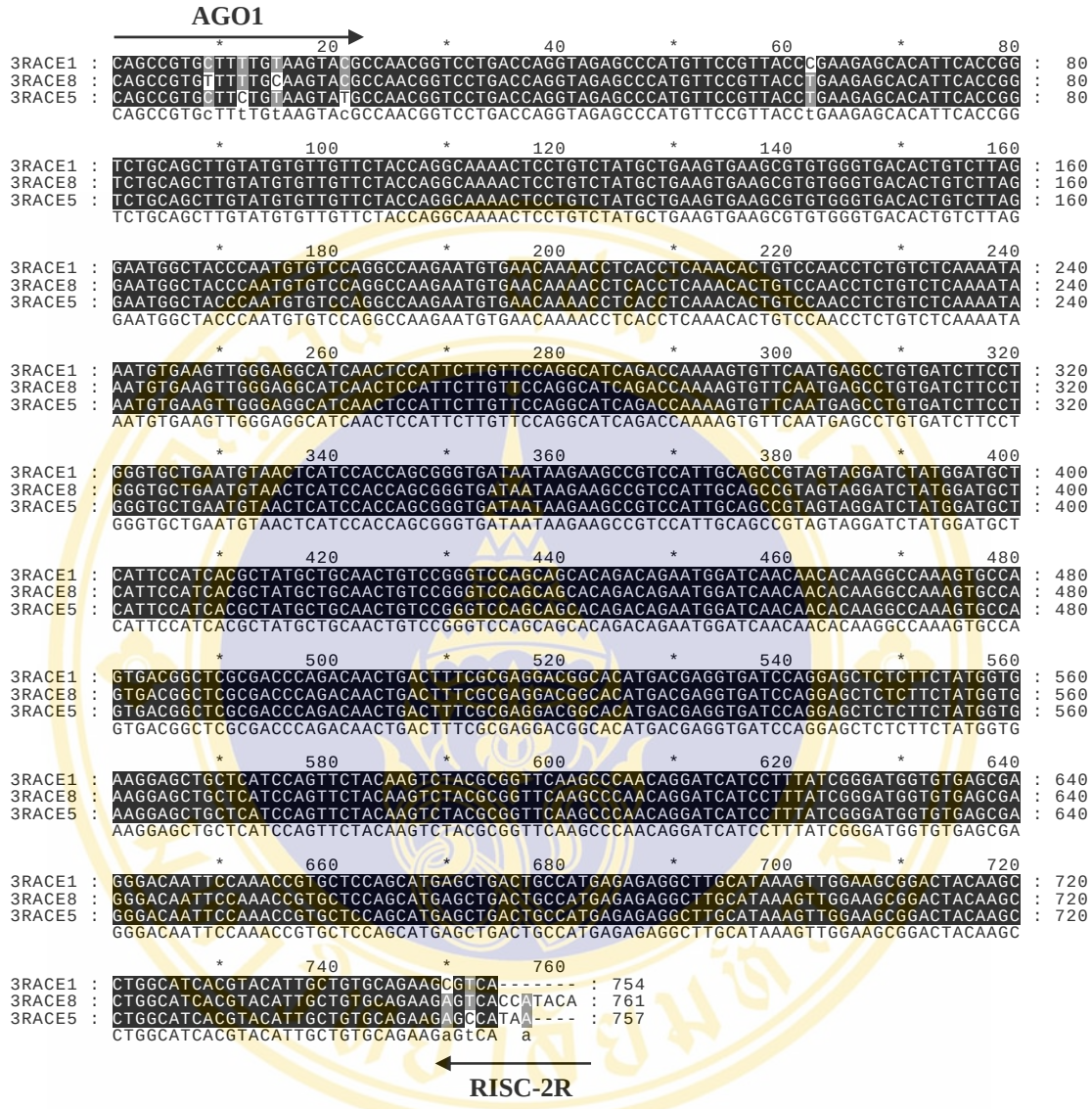

Figure 18. An alignment of nucleotide sequences of the fragment 1 of Pem-AGO cDNA among the three individual clones

The alignment was conducted by Clustal X program. The arrows indicate the nucleotide sequences of the two degenerate primers, AGO1 and RISC2-R. The nucleotides that are identical in all sequences are highlighted in black whereas grey color indicates the positions at which variations in the nucleotide are found. The consensus sequence among the three clones is shown in the bottom line of each block.

***Drosophila melanogaster* CG6671-PB, isoform B (AGO1) mRNA, complete cds**

Length = 950, Score = 391 bits (1004), Expect = 1e-107

Identities = 203/250 (81%), Positives = 211/250 (84%), Gaps = 28/250 (11%)

```
Query  1    QPCFCKYANGPDQVEPMFRYLKSTFTGLQLVCVVLPGKTPVYAEVKRVGDTVLGMATQCV  180
            QPCFCKYA GPDQVEPMFRYLK TF GLQLV VVLPGKTPVYAEVKRVGDTVLGMATQCV
Sbjct  578  QPCFCKYATGPDQVEPMFRYLKITFPGLQLVVVVLPGKTPVYAEVKRVGDTVLGMATQCV  637

Query  181  QAKNVNKTSPQTLSNLCLKINVKLGGINSILVPGIRPKVFNEPVIFLGADVTHPPAGDNK  360
            QAKNVNKTSPQTLSNLCLKINVKLGGINSILVP IRPKVFNEPVIFLGADVTHPPAGDNK
Sbjct  638  QAKNVNKTSPQTLSNLCLKINVKLGGINSILVPSIRPKVFNEPVIFLGADVTHPPAGDNK  697

Query  361  KPSIAAVVGSMDAHPSRYAATVRVQQHRQNGSTTQGQSASDGSRPRQLTFARTAHDEVIQ  540
            KPSIAAVVGSMDAHPSRYAATVRVQQHRQ                          E+IQ
Sbjct  698  KPSIAAVVGSMDAHPSRYAATVRVQQHRQ--------------------------EIIQ  730

Query  541  ELSSMVKELLIQFYKST-RFKPNRIILYRDGVSEGQFQTVLQHELTAMREACIKLEADYK  717
            ELSSMV+ELLI FYKST  +KP+RIILYRDGVSEGQF  VLQHELTA+REACIKLE +Y+
Sbjct  731  ELSSMVRELLIMFYKSTGGYKPHRIILYRDGVSEGQFPHVLQHELTAIREACIKLEPEYR  790

Query  718  PGITYIAVQK  747
            PGIT+I VQK
Sbjct  791  PGITFIVVQK  800
```

Figure 19. An example of identity search results of the fragment 1 of Pem-AGO cDNA by the blastp program

The consensus nucleotide sequence of fragment 1 of Pem-AGO cDNA was submitted to blastp program. The result showed that the deduced amino acid sequence of the fragment 1 exhibited an identity of 81% to a corresponding amino acid sequence of Argonaute 1 of *D. melanogaster* [Accession:NP_523734.1].

5.2 Amplification of the 3' end (fragment 2) of Pem-AGO cDNA

In order to obtain the nucleotide sequence at the 3' end of Pem-AGO cDNA, the 3'RACE strategy was employed. Two specific primers, AGO/S1 and AGO/S2, were designed from the sequence of the fragment 1 obtained in the previous step. The first-strand cDNA synthesized from PRT primer was used as template to amplify the 3' end of Pem-AGO cDNA. The first round amplification was performed with AGO/S1 and PM-1 primers. The PCR product longer than 700 bp was obtained (Figure 20A). Then, the nested PCR conducted by AGO/S2 and PM-1 primers produced the band between 600 bp and 700 bp in size (Figure 20B). This nested PCR fragment was recovered from the gel, cloned into pGEM® –T Easy vector and transformed into *E. coli* DH5α.

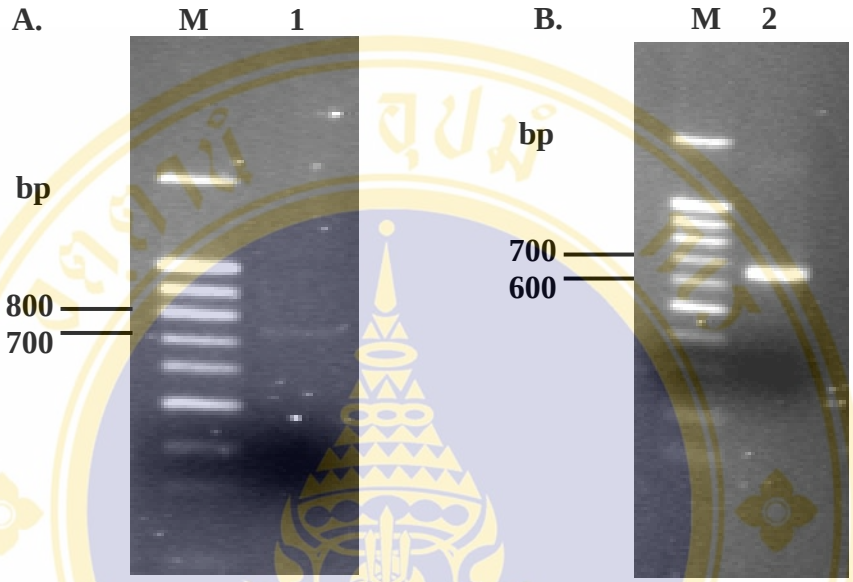

Figure 20. PCR products from 3' RACE (fragment 2)

The amplification products were fractionated on 1% agarose gel electrophoresis. Lane M is 100 bp DNA ladder. Lane 1 is the PCR products from the first round amplification with AGO/S1 and PM-1 primers (A) and the second round amplification (nested) with AGO/S2 and PM-1 primers (B).

5.2.1 Screening of recombinant clones containing fragment 2 and sequencing analysis

After the recombinants were screened by *Eco*R I digestion (Figure 21), two recombinant clones, no.6 and 8 harboring the insert fragment of correct size were selected for DNA sequencing as the previous steps. The nucleotide sequences of the two clones were compared by Clustal X program. The sequence comparison showed that the two clones had almost identical nucleotide sequences except for nucleotide substitution at positions 229, 301, 324, 326, 530 and 555 (Figure 22). Of these nucleotide variations, only the substitution at positions 326 did not change the encoded amino acids. The nucleotide sequence of the two primers, AGO/S2 and PM-1 were detected, but neither the poly A sequence upstream of the PM-1 primer nor the poly A signal at the 3' end was found. Searching for significant similarity by blastp program (www.ncbi.nlm.nih.gov/blast) showed that this fragment 2 contains a coding sequence at the C-terminal of Pem-AGO as well as the partial sequence of 3'UTR. The identity of 90% was found between the deduced amino acid sequence of fragment 2 and the amino acid sequences of *Drosophila melanogaster* Argonaute 1 (CG6671-PB) (Figure 23).

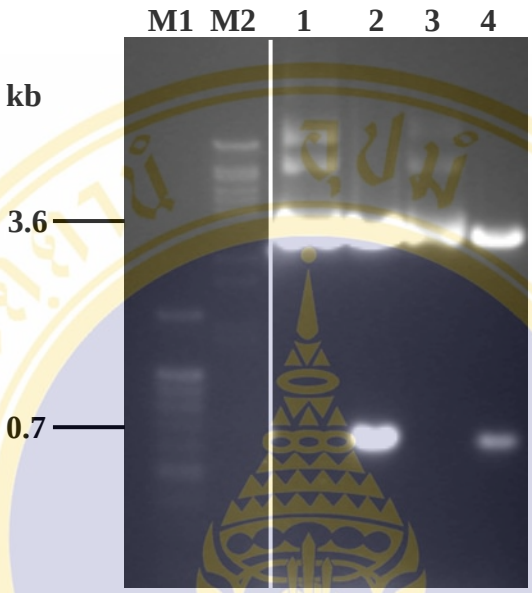

Figure 21. Screening of recombinant clones containing fragment 2 of Pem-AGO cDNA by restriction enzyme analysis

The recombinant clones were randomly picked and digested with *Eco*R I Lane M1 and M2 are 100 bp DNA ladder and *λBst*E II marker, respectively. Lanes 1 and 3 are the undigested plasmid of the recombinant clones number 6 and 10 whereas lanes 2 and 4 represent the *Eco*R I-digested plasmids from clones 6 and 10, respectively .

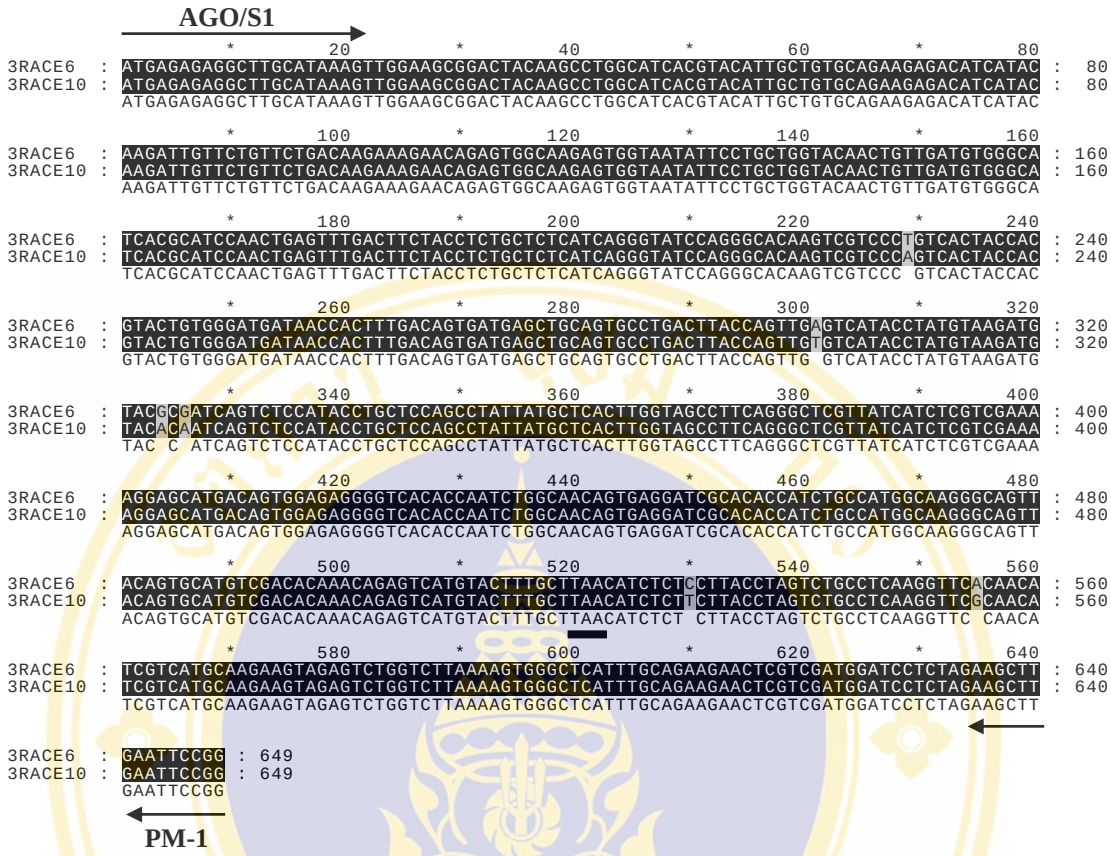

Figure 22. An alignment of nucleotide sequences of the fragment 2 of Pem-AGO cDNA of the two individual clones

The alignment was conducted by Clustal X program. The arrows represent the nucleotide sequences of the two primers, AGO/S2 and PM-1. The stop codon (TAA) was underlined. The nucleotides that are identical between the two sequences are highlighted in black. The consensus sequence was shown in the bottom line.

***Drosophila melanogaster* CG6671-PB, isoform B (AGO1) mRNA, complete cds**

Length = 950, Score = 340 bits (871), Expect = 3e-92

Identities = 157/173 (90%), Positives = 165/173 (95%), Gaps = 0/173 (0%)

```
Query  1    MREACIKLEADYKPGITYIAVQKRHHTRLFCSDKKEQSGKSGNIPAGTTVDVGITHPTEF  180
            +REACIKLE +Y+PGIT+I VQKRHHTRLFC++KKEQSGKSGNIPAGTTVDVGITHPTEF
Sbjct  778  IREACIKLEPEYRPGITFIVVQKRHHTRLFCAEKKEQSGKSGNIPAGTTVDVGITHPTEF  837

Query  181  DFYLCSHQGIQGTSRPCHYHVLWDDNHFDSDELQCLTYQLSHTYVRCTRSVSIPAPAYYA  360
            DFYLCSHQGIQGTSRP HYHVLWDDNHFDSDELQCLTYQL HTYVRCTRSVSIPAPAYYA
Sbjct  838  DFYLCSHQGIQGTSRPSHYHVLWDDNHFDSDELQCLTYQLCHTYVRCTRSVSIPAPAYYA  897

Query  361  HLVAFRARYHLVEKEHDSGEGSHQSGNSEDRTPSAMARAVTVHVDTNRVMYFA  519
            HLVAFRARYHLVEKEHDSGEGSHQSG SEDRTP AMARA+TVH DT +VMYFA
Sbjct  898  HLVAFRARYHLVEKEHDSGEGSHQSGCSEDRTPGAMARAITVHADTKKVMYFA  950
```

Figure 23. An example of identity search results of the fragment 2 of Pem-AGO by blastp program

The nucleotide sequence of the clone number 6 was submitted to blastp program. The result showed that the deduced amino acid sequence of the fragment 2 exhibited an identity of 90% to the corresponding sequence of Argonaute protein in *D. melanogaster*. [Accession : NP_523734.1]

5.3 Amplification of the 5' end of Pem-AGO cDNA

5.3.1 Further amplification of partial 5' fragment of Pem-AGO cDNA (fragment 3)

Amplification of the partial 5' region was conducted using the cDNA that was synthesized by PRT primer as a template. 5'AGOR1 primer that was designed from the nucleotide sequence of the previously obtained fragment 1 of Pem-AGO cDNA and dAGOF1 primer, designed from the conserved nucleotide sequence of *D. melanogaster*, were used in the PCR reaction. The product of about 1 kb was obtained (Figure 24). The PCR fragment was recovered from the gel and cloned into pGEM®-T Easy vector. The recombinant clones were screened by *Eco*R I digestion and two clones, number 4 and 7, were selected randomly for sequencing (Figure 25). The alignment of nucleotide sequences between the two recombinant clones were shown in Figure 26. Variations of the nucleotides between the two clones were found at positions 195, 372, 436, 505, 741 and 941, however the encoded amino acids were affected only by the variation at positions 436, 505 and 941. Figure 27 shows the identity between the deduced amino acid sequence of the fragment 3 and Argonaute 1 of *D. melanogaster* at 88% by blastp searching.

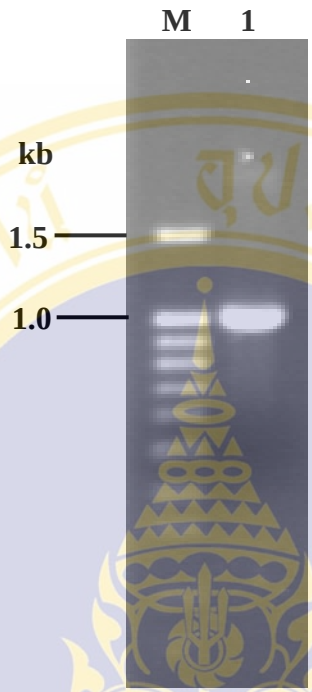

Figure 24. The PCR product of the fragment 3 of Pem-AGO cDNA

The amplification products were fractionated on 1% agarose gel electrophoresis. M is 100 bp DNA ladder. Lane 1 is the PCR product that was amplified from 5'AGOR1 and dAGOF1 primers.

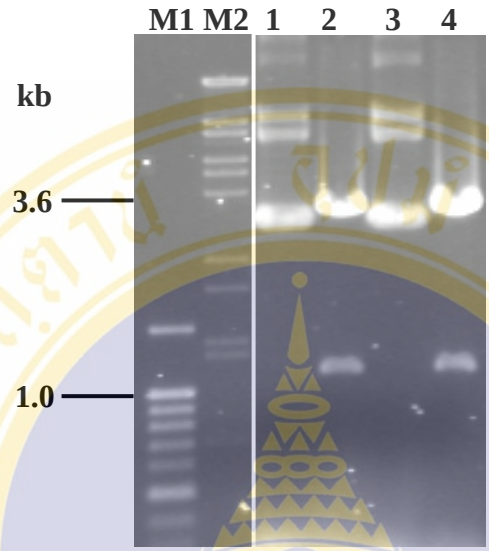

Figure 25. Screening of recombinant clones containing the fragment 3 of Pem-AGO by restriction enzyme analysis

Randomly picked recombinant clones were digested with *Eco*R I. Lane M1 represents 100 bp DNA ladder and lane M2 is λ*Bst*E II marker. The undigested plasmids of the recombinant clones number 4 and 7 are shown in lanes 1 and 3 whereas the *Eco*R I-digested plasmids are loaded in lanes 2 (clone number 4) and 4 (clone number 7), respectively.

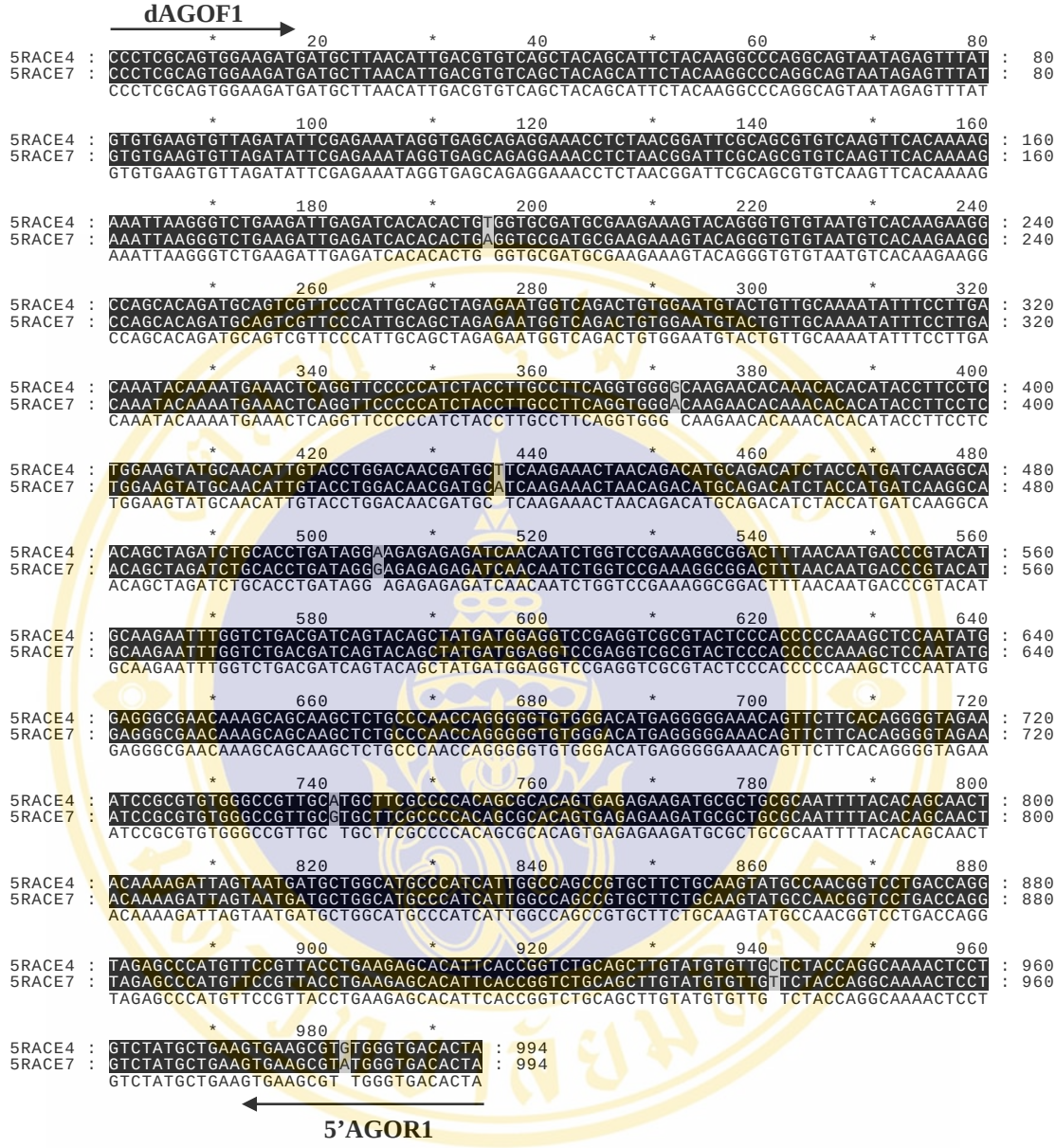

Figure 26. An alignment of nucleotide sequence from the fragment 3 of Pem-AGO cDNA between two recombinant clones

The alignment was conducted by Clustal X program. The arrows represent the nucleotide sequences of the two primers, dAGOF1 and 5’AGOR1. The nucleotide residues that are identical in all sequences are highlighted in black whereas grey color indicates the nucleotide residues that contained the variation between the two clones.

***Drosophila melanogaster* CG6671-PB, isoform B (AGO1) mRNA, complete cds**

Length = 950, Score = 621 bits (1601), Expect = 1e-176

Identities = 306/346 (88%), Positives = 317/346 (91%), Gaps = 15/346 (4%)

```
Query  1    PSQWKMMLNIDVSATAFYKAQAVIEFMCEVLDIREIGEQRKPLTDSQRVKFTKEIKGLKI  180
            PSQWKMMLNIDVSATAFYKAQ VI+FMCEVLDIR+I EQRKPLTDSQRVKFTKEIKGLKI
Sbjct  283  PSQWKMMLNIDVSATAFYKAQPVIDFMCEVLDIRDINEQRKPLTDSQRVKFTKEIKGLKI  342

Query  181  EITHCGAMRRKYRVCNVTRRPAQMQSFPLQLENGQTVECTVAKYFLDKYKMKLRFPHLPC  360
            EITHCG MRRKYRVCNVTRRPAQMQSFPLQLENGQTVECTVAKYFLDKY+MKLR+PHLPC
Sbjct  343  EITHCGQMRRKYRVCNVTRRPAQMQSFPLQLENGQTVECTVAKYFLDKYRMKLRYPHLPC  402

Query  361  LQVGQEHKHTYLPLEVCNIVPGQRCFKKLTDMQTSTMIKATARSAPDRKREINNLVRKAD  540
            LQVGQEHKHTYLPLEVCNIV GQRC KKLTDMQTSTMIKATARSAPDR+REINNLV++AD
Sbjct  403  LQVGQEHKHTYLPLEVCNIVAGQRCIKKLTDMQTSTMIKATARSAPDREREINNLVKRAD  462

Query  541  FNNDPYMQEFGLTISTAMMEVRGRVLPPPKLQYGGR-----TKQQ----------ALPNQ  675
            FNND Y+QEFGLTIS +MMEVRGRVLPPPKLQYGGR     T QQ          A PNQ
Sbjct  463  FNNDSYVQEFGLTISNSMMEVRGRVLPPPKLQYGGRVSTGLTGQQLFPPQNKVSLASPNQ  522

Query  676  GVWDMRGKQFFTGVEIRVWAVACFAPQRTVREDALRNFTQQLQKISNDAGMPIIGQPCFC  855
            GVWDMRGKQFFTGVEIR+WA+ACFAPQRTVREDALRNFTQQLQKISNDAGMPIIGQPCFC
Sbjct  523  GVWDMRGKQFFTGVEIRIWAIACFAPQRTVREDALRNFTQQLQKISNDAGMPIIGQPCFC  582

Query  856  KYANGPDQVEPMFRYLKSTFTGLQLVCVALPGKTPVYAEVKRVGDT  993
            KYA GPDQVEPMFRYLK TF GLQLV V LPGKTPVYAEVKRVGDT
Sbjct  583  KYATGPDQVEPMFRYLKITFPGLQLVVVVLPGKTPVYAEVKRVGDT  628
```

Figure 27. An example of identity search result of the fragment 3 of Pem-AGO by blastx program

The nucleotide sequence of the clone number 4 containing the fragment 3 of Pem-AGO cDNA was submitted to blastp program. The deduced amino acid sequences of the fragment 3 shared an 88% identity to Argonaute 1 protein of *D. melanogaster* [Accession : NP_523734.1].

5.4 Amplificatiom of the 5'end (fragment 4) of Pem-AGO cDNA by 5'RACE

Further amplification of the 5' region was conducted by 5'RACE. 5'RACE1 primer that was designed from the nucleotide sequence of the fragment 1 of Pem-AGO cDNA was used to synthesize the first stranded cDNA by the action of reverse transcriptase. Then the cDNA template was tailed with dATP by terminal deoxynucleotide transferase. The tailed cDNA was used as a template to amplify the 5'end by using 5'RACE4 primer, designed from the sequence in the fragment 1 of Pem-AGO cDNA, in combination with PRT primer. The result showed that the PCR product about 1.2 kb was amplified (Figure 28). This fragment was purified and cloned into pGEM®-T Easy vector. After screening the recombinant clones with restriction enzyme *Eco*R I (Figure 29), the clones with correct insert size, clones number 4 and 21, were subjected to nucleotide sequencing. The nucleotide sequence alignment showed variations in nucleotide between the two clones at positions 56, 230, 266, 545, 779 (Figure 30). Additionally, the nucleotides 319 to 327 of clone number 4 were absent in the other clone. The putative start codon was detected at position 93. Searching for significant similarity by blastp program showed that the deduced amino acids sequence of the fragment 4 shared high sequence similarity to *Drosophila melanogaster* Argonaute 1 (CG6671-PC) at 78% identity (Figure 31).

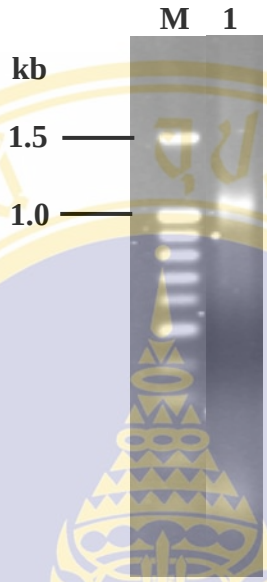

Figure 28. The PCR product from the fragment 4 of Pem-AGO cDNA

The amplification products were fractionated on 1% agarose gel. M is 100 bp DNA ladder and lane 1 is the PCR product that was amplified from 5'RACE 4 and PRT primers.

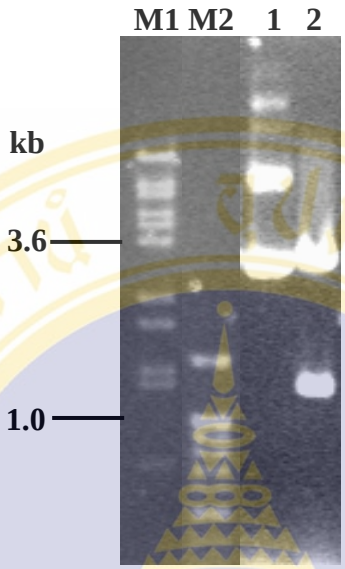

Figure 29. Screening for recombinant clones containing the fragment 4 of Pem-AGO cDNA by restriction enzyme analysis

Plasmid DNA from randomly picked recombinant clones were digested with *Eco*R I. Lane M1 and M2 are λ*Bst*E II and 100 bp DNA ladder, respectively Randomly picked recombinant clones were digested with *Eco*R I. The undigested plasmids of the recombinant clones number 4 is shown in lanes 1 whereas the *Eco*R I-digested plasmids are loaded in lanes 2.

.

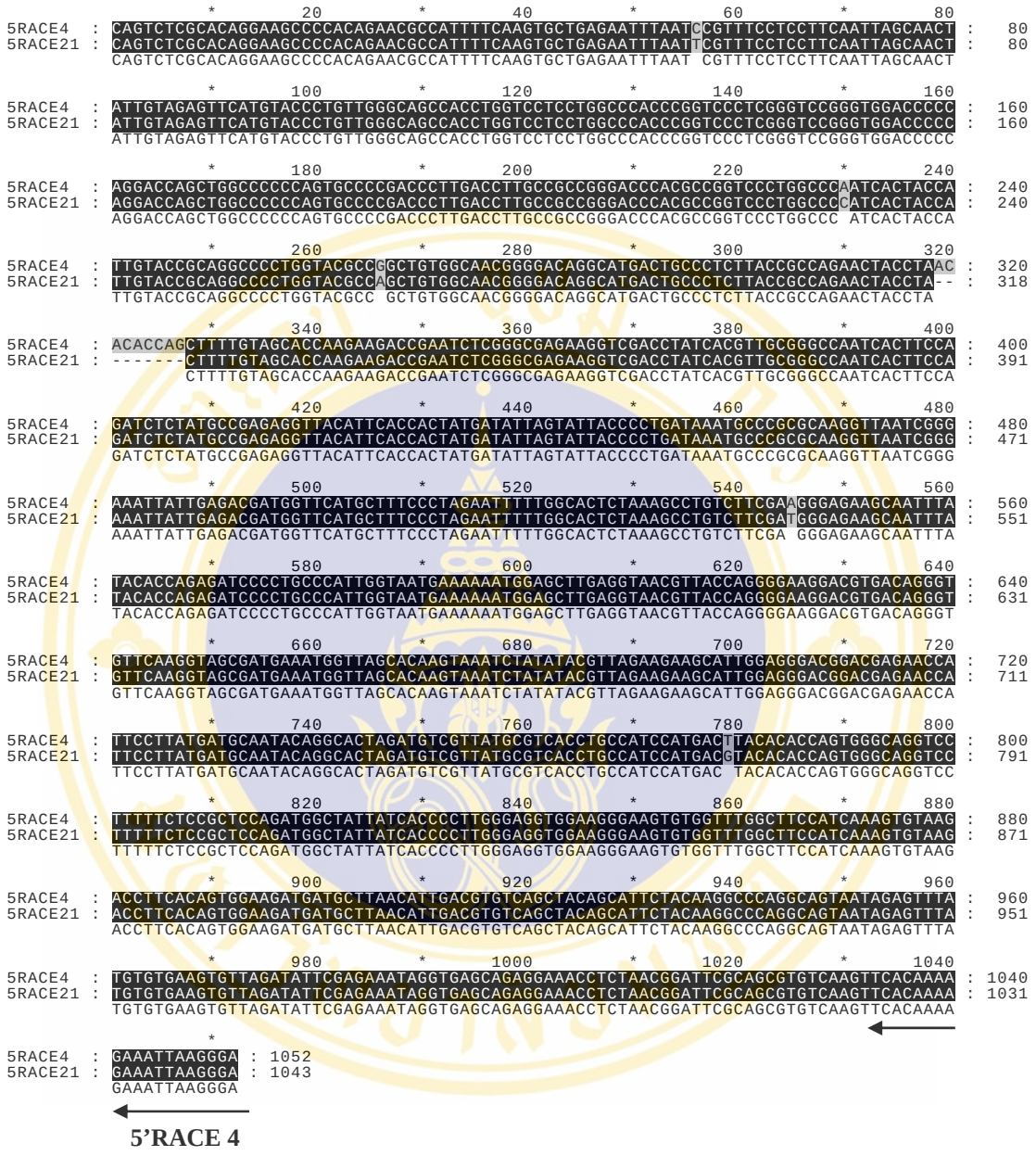

Figure 30. An alignment of nucleotide sequences of the fragment 4 of Pem-AGO cDNA between two recombinant clones

The alignment was conducted by Clustal X program. The arrow represents the nucleotide sequences of the primers, 5'RACE 4. The nucleotide residues that are identical in all sequences are highlighted in black whereas grey color indicates the nucleotide residues that contain the variation.

***Drosophila melanogaster* CG6671-PB, isoform B (AGO1) mRNA, complete cds**

Length = 950, Score = 340 bits (871), Expect = 5e-92

Identities = 157/200 (78%), Positives = 177/200 (88%), Gaps = 6/200 (3%)

```
Query  261  TPAVATGTGMTALLPPELPNTPAFVAPRRPNLGREGRPITLRANHFQISMPRGYIHHYDI  440
            TPA+AT T      P   P+ P F  PRRPNLGREGRPI LRANHFQ++MPRGY+HHYDI
Sbjct  82   TPAIATAT------PATQPDMPVFTCPRRPNLGREGRPIVLRANHFQVTMPRGYVHHYDI  135

Query  441  SITPDKCPRKVNREIIETMVHAFPRIFGTLKPVFEGRSNLYTRDPLPIGNEKMELEVTLP  620
            +I PDKCPRKVNREIIETMVHA+ +IFG LKPVF+GR+NLYTRDPLPIGNE++ELEVTLP
Sbjct  136  NIQPDKCPRKVNREIIETMVHAYSKIFGVLKPVFDGRNNLYTRDPLPIGNERLELEVTLP  195

Query  621  GEGRDRVFKVAMKWLAQVNLYTLEEALEGRTRTIPYDAIQALDVVMRHLPSMTYTPVGRS  800
            GEG+DR+F+V +KW AQV+L+ LEEALEGRTR IPYDAI ALDVVMRHLPSMTYTPVGRS
Sbjct  196  GEGKDRIFRVTIKWQAQVSLFNLEEALEGRTRQIPYDAILALDVVMRHLPSMTYTPVGRS  255

Query  801  FFSAPDGYYHPLGGGREVWF  860
            FFS+P+GYYHPLGGGREVWF
Sbjct  256  FFSSPEGYYHPLGGGREVWF  275
```

Figure 31. An example of identity search result of the fragment 4 of Pem-AGO by blastp program

The nucleotide sequence of the clone number 4 containing the fragment 4 of Pem-AGO cDNA was submitted to blastp program. The deduced amino acid sequences of the fragment 4 shared an 78% identity to Argonaute 1 protein of *D. melanogaster* [Accession : NP_523734.1].

5.5 Amplification of the coding sequence of Argonaute cDNA with Phusion® Taq DNA polymerase.

From the previous cloning steps, four overlapping fragments (fragments 1 - 4) of Pem-AGO cDNA were obtained. The virtual transcript of Pem-AGO cDNA was obtained by the combination of the nucleotides sequences of these four cDNA fragments using vector NTI program. In order to verify whether this virtual transcript of Pem-AGO is really existed in *P. monodon*, an attempt to clone the putative entire coding sequence of Pem-AGO cDNA was made. Two specific primers, AgoC-F and AgoC-R, were designed from the 5' end (the first ATG codon that is in-frame with the translated product) and the 3' end (TAA) of the coding region of the combined Pem-AGO sequence. The cDNA template generated with PRT primer was used in the reaction with Phusion® Taq DNA polymerase. The PCR product of the expected size about 2.8 kb was obtained (Figure 32). The nucleotide sequences of two recombinant clones, COD1 and COD3, containing this Pem-AGO cDNA were compared in Figure 33. The comparison indicated that the sequences of these two clones were nearly identical except for one nucleotide substitution at position 1,530. Moreover, the region of 9 nucleotides at positions 227 to 235 was found in one clone but not the other. This is the same region that was detected in the two clones of fragment 4 as shown in Figure 30.

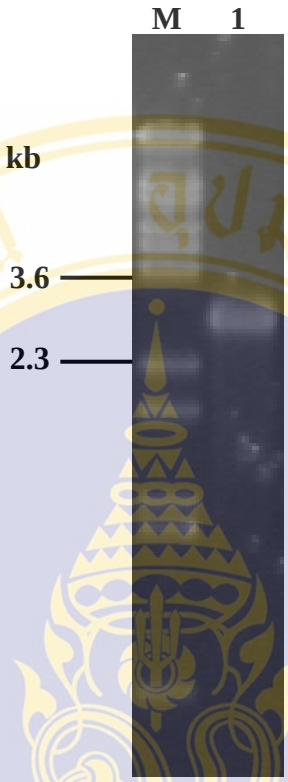

Figure 32. The PCR product from the coding sequence of Pem-AGO

The amplification products were fractioned on 0.8% agarose gel electrophoresis. M is 100 bp DNA ladder. Lane 1 is the PCR product that was amplified with Phusion® Taq DNA polymerase using AgoC-F and AgoC-R primers.

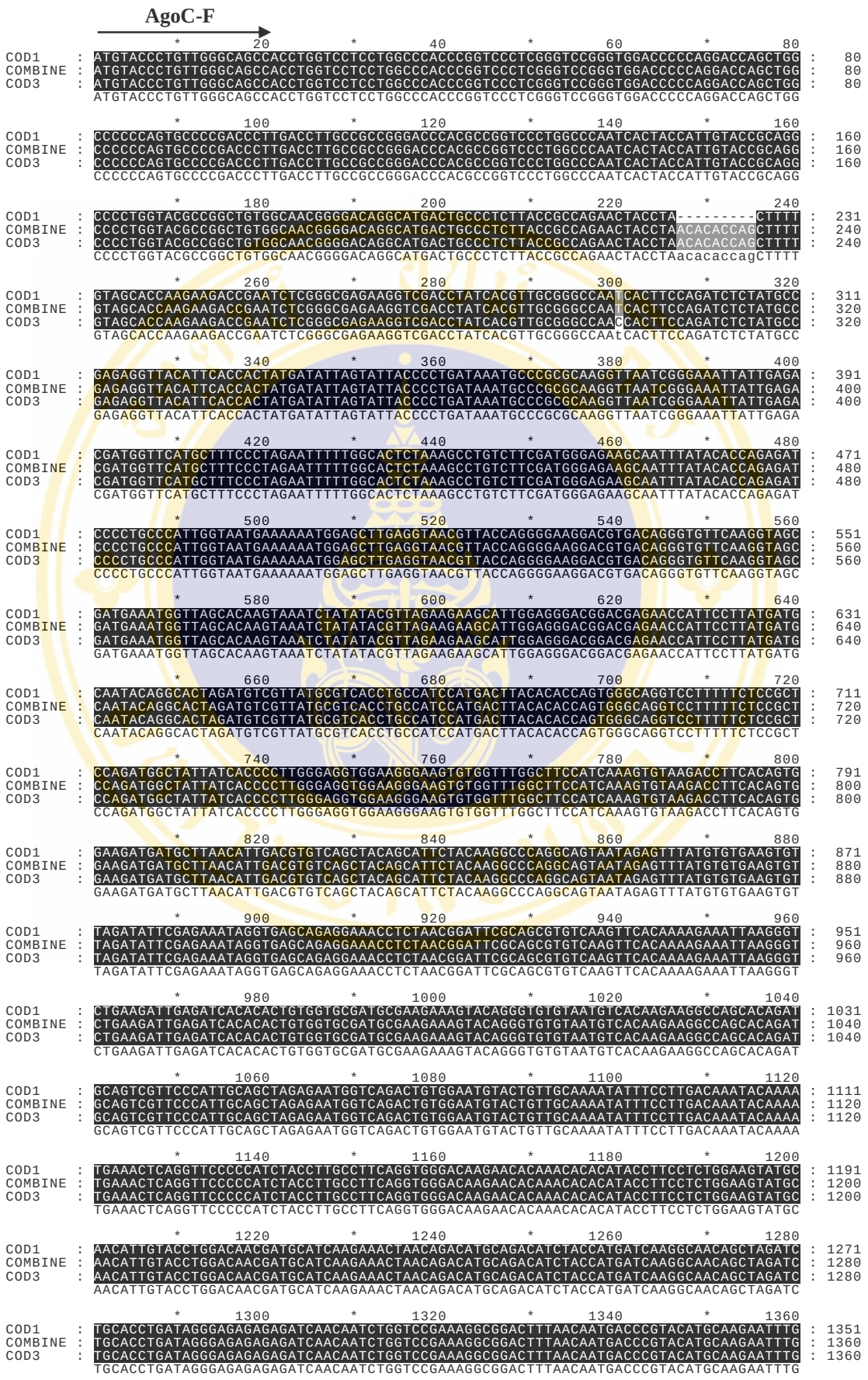

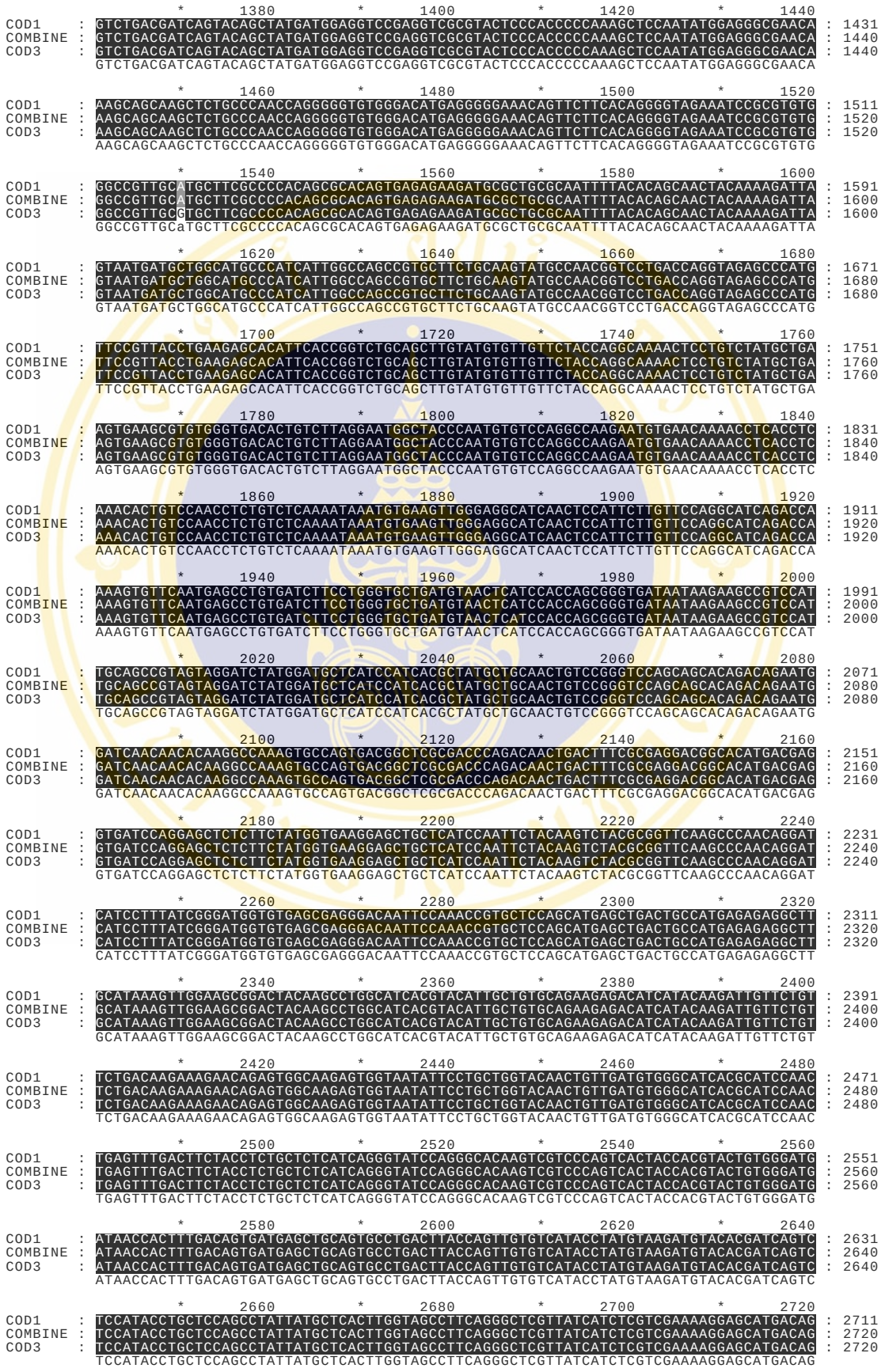

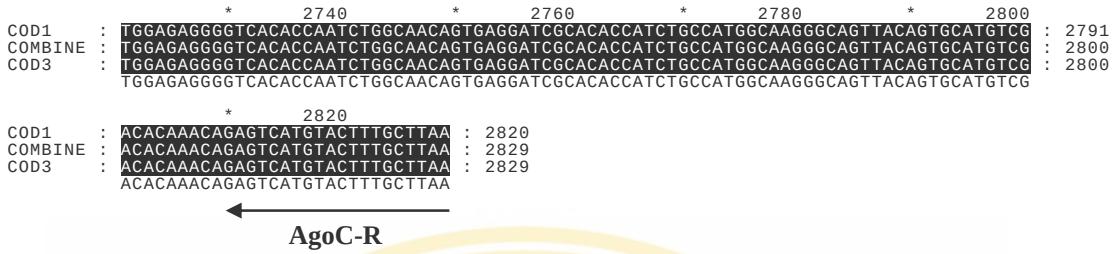

Figure 33. The alignment of nucleotide sequence between the coding sequence of Pem-AGO cDNA and the combined four overlapping fragment

The alignment was conducted by Clustal X program. The arrows indicate the nucleotide sequences of the two primers, AgoC-F and AgoC-R. The nucleotides that are identical in all sequences are highlighted in black whereas grey color indicates the positions at which variation nucleotide are found. The consensus sequence was shown in the bottom line of each block.

5.5.1 Analysis of Pem-AGO sequence

The entire coding sequence of Pem-AGO is either 2,820 or 2,829 nucleotides long depending on whether or not it contains the 9-nuclotide region at position 227 to 235. The nucleotide and the deduced amino acid sequence of Pem-AGO is shown in Figure 34. Analysis by blastp program has identified two signature domains of the Argonaute family in the Pem-AGO sequence. The PAZ domain of Pem-AGO was 139 amino acids long found at position 289 to 428 while the PIWI domain span amino acid 572 to 901 was 329 amino acids in length.

MYPVGQPPGPPGPPGPSGPGGPPGPAGPPVPRPLTLPPGPTPVPGPITTIVPQAPGTP
AVATGTGMTALLPPELP**NTPA**FVAPRRPNLGREGRPITLRANHFQISMPRGYIHHYDI
(---T)
SITPDKCPRKVNREIIETMVHAFPRIFGTLKPVFEGRSNLYTRDPLPIGNEKMELEVT
LPGEGRDRVFKVAMKWLAQVNLYTLEEALEGRTRTIPYDAIQALDVVMRHLPSMTYTP
VGRSFFSAPDGYYHPLGGGREVWFGFHQSVRPSQWKMMLNIDVSATAFYKAQAVIE**FM**
CEVLDIREIGEQRKPLTDSQRVKFTKEIKGLKIEITHCGAMRRKYRVCNVTRRPAQMQ
SFPLQLENGQTVECTVAKYFLDKYKMKLRFPHLPCLQVGQEHKHTYLPLEVCNIVPGQ
RCFKKLTDMQTSTMIKATARSAPDRKREINNLVRKADFNNDPYMQEFGLTISTAMMEV
RGRVLPPPKLQYGGRTKQQALPNQGVWDMRGKQFFTGVEIRVWAVACFAPQRTVREDA
LRNFTQQLQKISNDAGMPIIGQPCFCKYANGPDQVEPMFRYPKSTFTGL**QLVCVVLPG**
KTPVYAEVKRVGDTVLGMATQCVQAKNVNKTSPQTLSNLCLKINVKLGGINSILVPGI
RPKVFNEPVIFLGADVTHPPAGDNKKPSIAAVVGSMDAHPSRYAATVRVQQHRQNGST
TQGQSASDGSRPRQLTFARTAHDEVIQELSSMVKELLIQFYKSTRFKPNRIILYRDGV
SEGQFQTVLQHELTAMREACIKLEADYKPGITYIAVQKRHHTRLFCSDKKEQSGKSGN
IPAGTTVDVGITHPTEFDFYLCSHQGIQGTSRPSHYHVLWDDNHFDSDELQCLTYQLC
HTYVRCTQSVSIPAPAYYAHLVAFRARYHLVEKEHDSGEGSHQSGNSEDRTPSAMARA
VTVHVDTNRVMYFA

Figure 34. The deduced amino acid sequence of Pem-AGO entire coding sequence

Dot line represents to the three deleted amino acid sequences in one clone. Two conserved domain, PAZ and PIWI in the Pem-AGO were shown in highlight.

5.5.2 Comparison between the Argounaute proteins of *P. monodon* and *D. melanogater*

The alignment between Pem-AGO and its highest similar protein, *Drosophila* Argonaute 1 (dAGO1) was conducted by clustal X program and was shown in Figure 35. The two proteins were very similar, especially in the conserved PAZ and PIWI domains. However, the PIWI domain of Pem-AGO contained an extra 81 amino acids when compare to that of dAGO1.

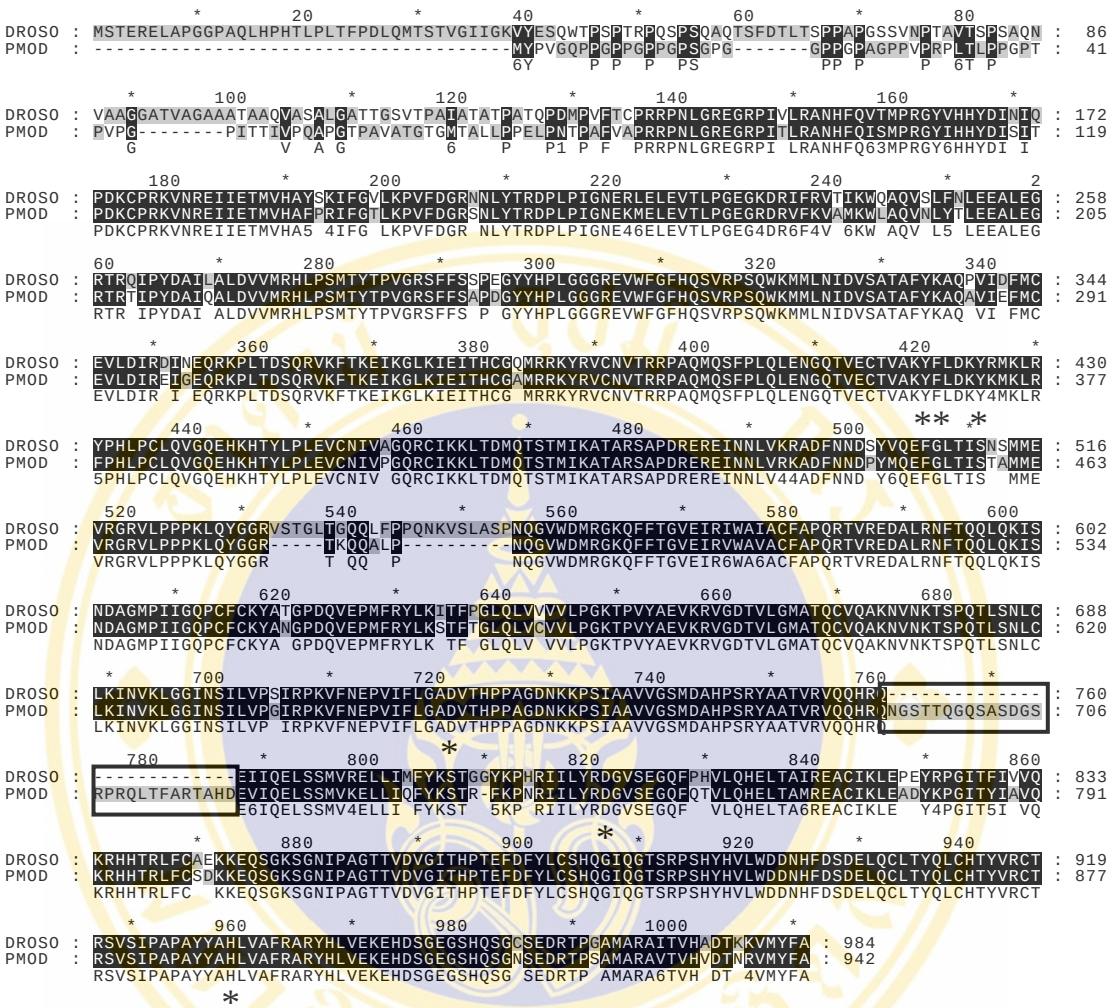

Figure 35. The alignment of amino acid sequence between Pem-AGO and *Drosophila* Argonaute 1 (dAGO1)

The deduced amino acid sequence of clone no.3 was aligned to the amino acid sequence of *D. melanogaster* by Clustal X program. The extra 81 amino acids of Pem-AGO in the PIWI domain were shown in rectangular. The asterisks * indicated the conserved amino acid sequences containing in PAZ and PIWI domain of dAGO1 and Pem-AGO.

5.6 Preparation of double-stranded RNA

The function of Pem-AGO in RNAi could be determined by studying the efficacy of RNAi in the cells in which Pem-AGO transcript is not expressed or expressed at low level. Such Pem-AGO depleted cells could be generated by the introduction of dsRNA that corresponds to Pem-AGO transcript into the cells.

5.6.1 Amplification of the templates for *in vitro* transcription

The double-stranded RNA corresponding to particular regions in the Pem-AGO sequence was designed for knocking down Pem-AGO transcript in order to characterize the function of Pem-AGO in the RNAi pathway.

Three pairs of primers were designed from the coding sequences of Pem-AGO cDNA in order to amplify the short DNA template for the synthesis of double-stranded RNA (Figure 36). The dsAGO-F1 and dsAGO-R1 primers were designed to amplify the 111 base pairs region corresponding to the non-conserved sequence from the 5'region of Pem-AGO cDNA, called ds1 fragment. The second pair was dsPIWI-F and dsPIWI-R that amplify the conserved sequence of 129 base pairs located in the PIWI domain, called dsPIWI fragment. The third pair, PAZ-F and PAZ-R was used for amplification of the 417 base pairs region of the conserved PAZ domain, call dsPAZ. After PCR amplification, the products of the expected size for each template (Figure 37) were individually cloned into pGEM®- T Easy vector. The recombinant clones of the three fragments were screened and the nucleotide sequences were confirmed. The recombinant clones containing the insert in either sense or antisense directions related to the T7 promoter in the vector were obtained for all three fragments. The correct sequences of the sense and antisense templates of each fragment were verified by DNA sequencing.

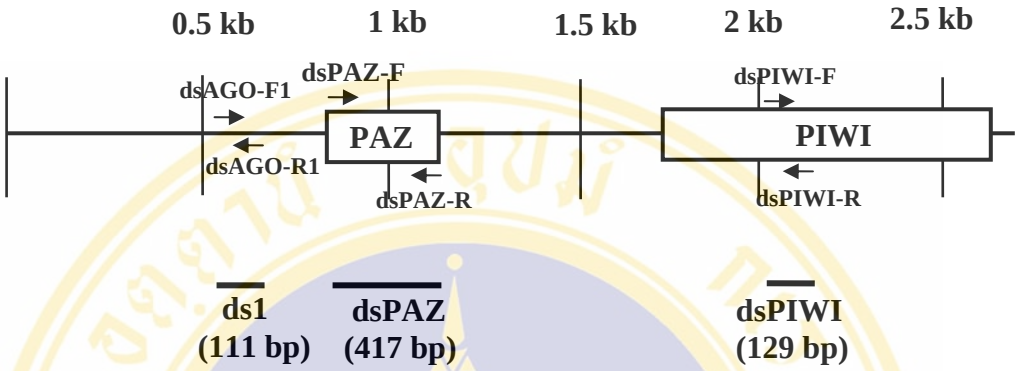

Figure 36. The schematic diagram representing the primers for amplification of DNA templates for *in vitro* transcription of single-stranded RNA

Three pairs of primers were designed to amplify the templates for ds1 (dsAGO-F1 and dsAGO-R1), dsPIWI (dsPIWI-F and dsPIWI-R) and dsPAZ (dsPAZ-F and dsPAZ-R) from the coding sequences of Pem-AGO cDNA. The regions of the three dsRNA were shown as black lines under the diagram.

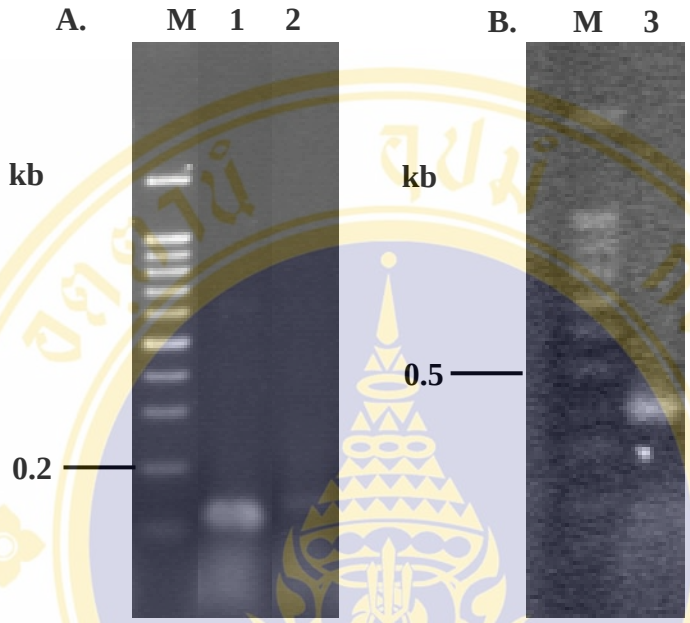

Figure 37. The amplification of DNA templates for *in vitro* transcription of single-stranded RNA

The cDNA clones containing the coding sequence of Pem-AGO was used as a template for PCR amplification. The amplification products were fractionated on 1.5% agarose gel. M is 100 bp DNA ladder. Lane 1 and lane 2 in (A) are the PCR product that was amplified with dsAGOF1-dsAGOR1 primers (ds1) and dsPIWI-F-dsPIWI-R primers (dsPIWI). Lane 3 in (B) is the PCR product that was amplified with dsPAZ-F and dsPAZ-R primers (dsPAZ).

5.6.2 *In vitro* transcription and annealing of dsRNA

The plasmid DNA containing ds1, dsPIWI and dsPAZ fragments in both directions were extracted from *E. coli* cells by using QIAGEN column. Then the plasmids were linearized with *Sal* I which is located in the multiple cloning sites of the pGEM®- T Easy vector and 3'downstream of the insert fragment. The linearized plasmids were used to transcribe single-stranded RNA by *in vitro* transcription reaction using Ribomax™ Large Scale RNA Production system of T7 RNA polymerase (Promega) which transcribed from the T7 promoter through to insert fragment and ended at the *Sal* I site. After both the sense and antisense single-stranded of ds1, dsPIWI and dsPAZ were obtained, the concentration of single-stranded RNA was determined by spectrophotometer and gel electrophoresis. The equal concentration of sense and antisense single-stranded RNA were used for the annealing reaction to synthesize double-stranded RNA of the three fragments. The annealed dsRNA products showed a major band with several other discrete bands that may represent different multimeric form of the annealing products (Figure 38 and 39). In order to prove whether the products of the annealing reaction really existed in the form of dsRNA, these annealing products were treated with RNase A, the enzyme that selectively degrade only single-stranded RNA. The RNase A-treated products appeared as a single band of the smaller size than the major band seen from the untreated products (Figure 38 and 39). This result confirmed that the three dsRNA of Pem-AGO were obtianed.

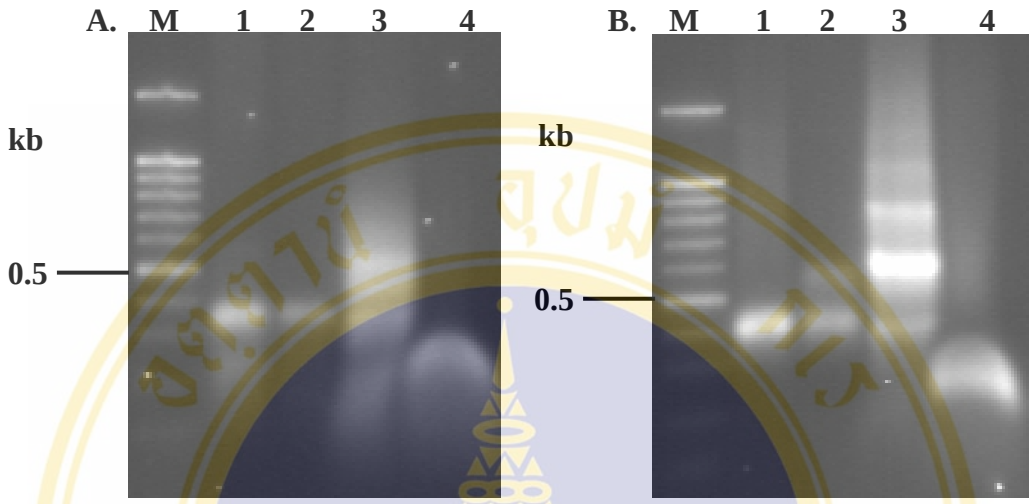

Figure 38. The single-stranded RNA from *in vitro* transcription and double-stranded RNA from the annealing reaction of ds1 and dsPIWI fragments

Plasmid DNA containing short DNA templates in sense and antisense directions were transcribed to single-stranded RNA by *in vitro* transcription. Sense and antisense single-stranded RNA of ds1 (A) and dsPIWI (B) were heated before loading in lane 1 and 2, respectively. Lane 3 is double-stranded RNA from the annealing reaction. Lane 4 is double-stranded RNA after treated with RNaseA.

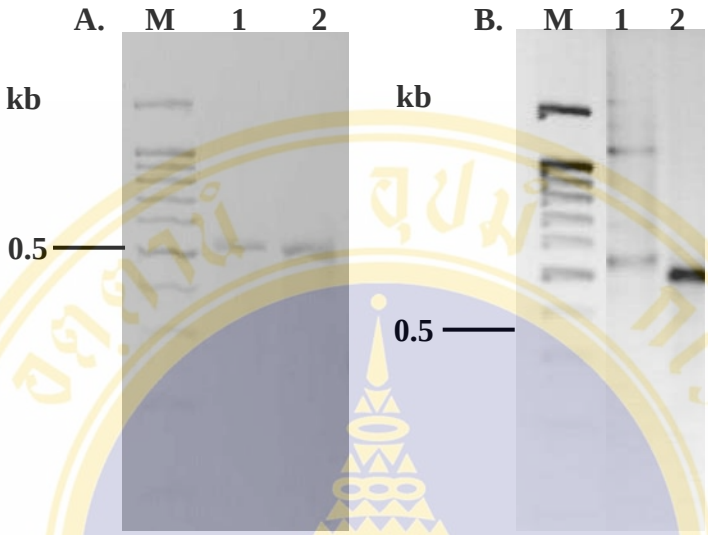

Figure 39. The single-stranded RNA from *in vitro* transcription and double-stranded RNA from the annealing reaction of dsPAZ fragment

A) Plasmid DNA containing short DNA template in sense and antisense directions were transcribed to single-stranded RNA by *in vitro* transcription. Sense and antisense single-stranded RNA were heated before loading in lane 1 and 2, respectively

B) Lane 1 is double-stranded RNA from the annealing reaction. Lane 2 is double-stranded RNA which after treated with RNaseA.

5.7 Reduction in the expression level of Pem-AGO in the Lymphoid (Oka) cell culture by Pem-AGO dsRNAs

Three double-stranded RNAs, ds1, dsPIWI and dsPAZ, corresponding to different regions of Pem-AGO sequence were used to transfect the primary lymphoid (Oka) cell culture of *P. monodon* in order to determine the function of Pem-AGO in RNAi pathway. Each double-stranded RNA was transfected into the Oka cell culture at the concentration of 2 μg per 1 ml in a 24-well culture plate. The remaining dsRNA in the culture medium was washed at one and a half hour after transfection. The cells were collected at 24 and 48 h for detection of the level of Pem-AGO expression by RT-PCR (Figure 40). The Pem-AGO transcript was amplified by the primers that target the coding region of the PIWI domain. The level of Pem-AGO expression in each sample was compared to the level of actin transcript of the same sample. The control cells that were not transfected with any dsRNA showed the highest level of Pem-AGO transcript. The percentages of Pem-AGO transcript (after normalized with the actin) in each sample comparing with that of the control cells were shown as a bar graph in Figure 41-42. The result from duplicated experiments showed that at 24 h post-transfection the cells that received ds1, dsPIWI and dsPAZ expressed Pem-AGO transcript at the level of 73, 77 and 69% of the control cell, respectively. The cells transfected with unrelated dsRNA of the green fluorescent protein (dsGFP) although expressed lower level of Pem-AGO than the control cells, the level of Pem-AGO expression is still higher than that in the cells transfected with any one of the Pem-AGO dsRNA. A more than not reduction in the level of Pem-AGO transcript in the cells transfected with ds1, dsPIWI and dsPAZ was observed after transfection for 48 h. However, the effect of dsGFP on Pem-AGO transcript was not determined at this time point. These results demonstrated that dsRNAs from Pem-AGO sequence were able to deplete, although not completely, the level of Pem-AGO expression in the cells.

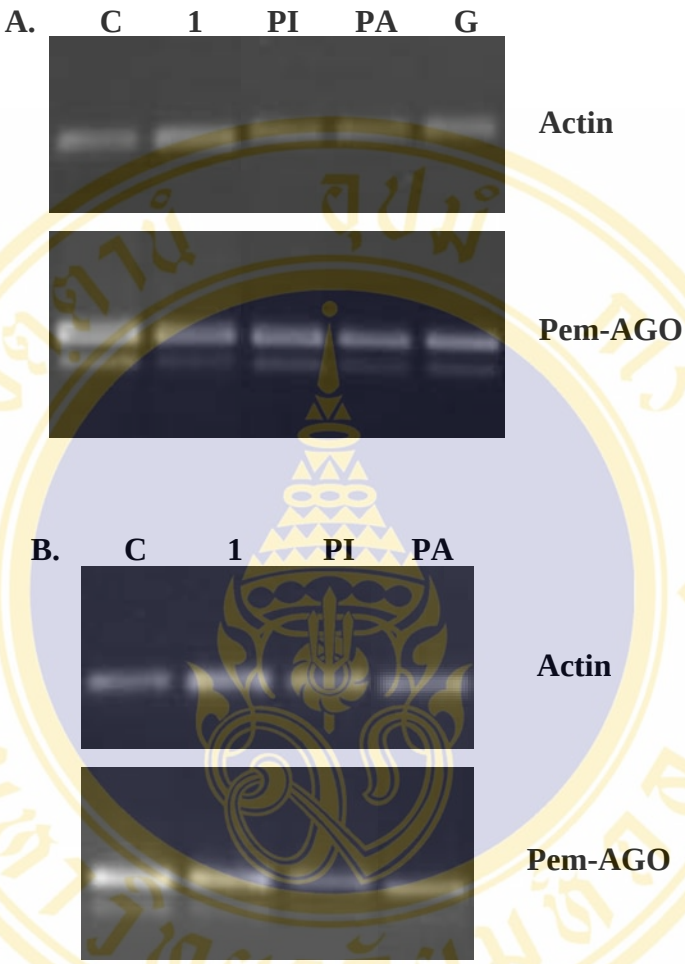

Figure 40. RT-PCR detection of Pem-AGO transcript in the Oka cell culture after transfected with Pem-AGO specific dsRNAs

The Oka cells were transfected with either Pem-AGO specific dsRNAs; ds1, dsPIWI and dsPAZ or unrelated dsRNA, dsGFP. The control cells were transfected with the buffer alone. Total RNA was extracted from the cells at 24 h (A) and 48 h (B) post transfection. The upper panel represents the actin transcript and the lower panel shows the Pem-AGO transcript that was amplified by PIWI-F and PIWI-R primers. C is the control cells whereas 1, PI, PA and G represent the cells transfected with ds 1, dsPIWI, ds PAZ and dsGFP, respectively.

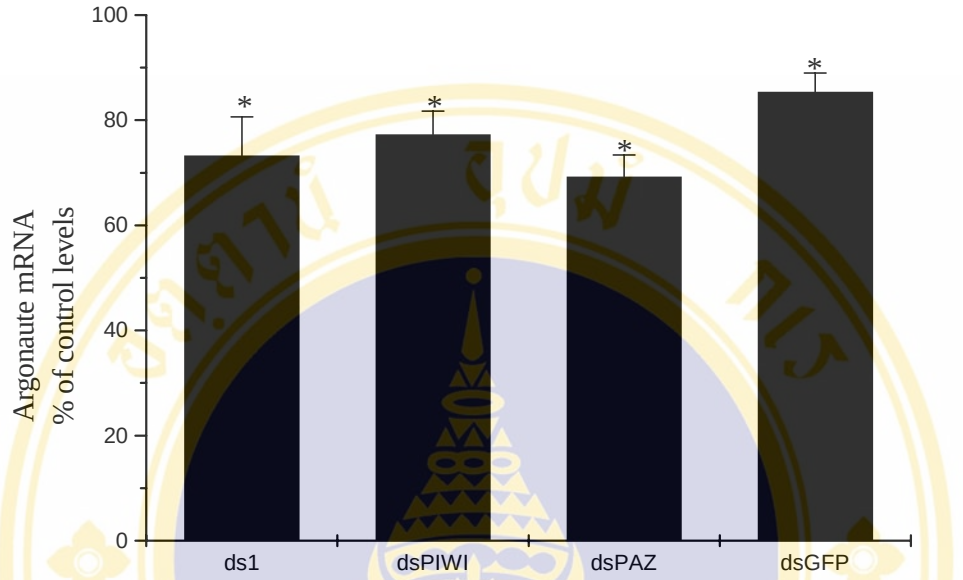

Figure 41. The percentages of knockdown Pem-AGO transcript after 24 h double-stranded RNA transfection

The value of the band intensity of Argonaute (PIWI) and actin are measured by using Scion Image program. The values are expressed as mRNA levels of Argonaute (PIWI)/actin which normalized to 100% level. The Y axis indicated the relative of PIWI/ACTIN. The X axis showed the oka cell culture that transfected with four different double-stranded RNAs. The data are from independently duplicated experiments and plotted as means $\pm$SEM (Standard error of the mean). * Indicated a significant difference between control cell and dsRNA-transfected cell at $P < 0.05$ by using one-way ANOVA test.

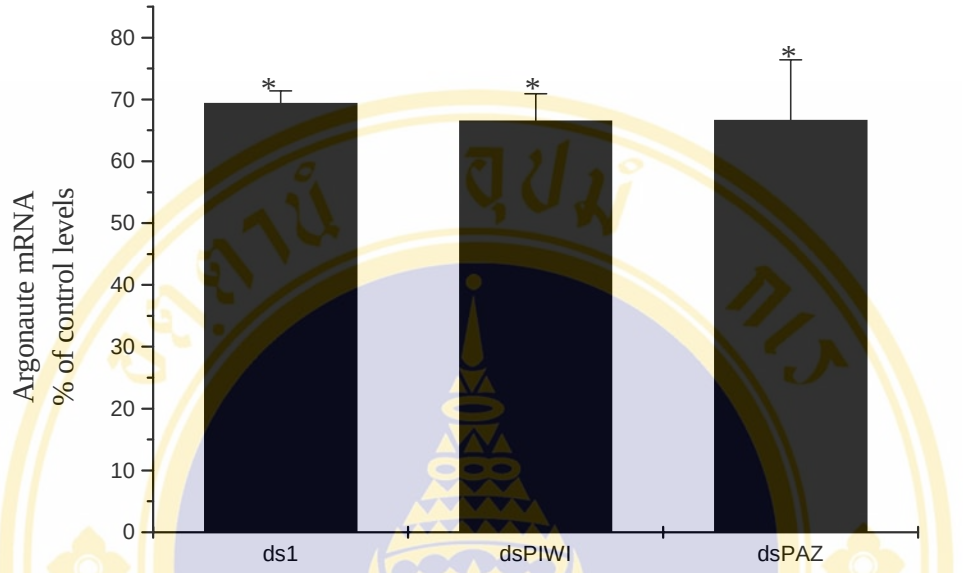

Figure 42. The percentages of knockdown Pem-AGO transcript after 48 h double-stranded RNA transfection

The value of the band intensity of Argonaute (PIWI) and actin are measured by using Scion Image program. The values are expressed as mRNA levels of Argonaute (PIWI)/actin which normalized to 100% level. The Y axis indicated the relative of PIWI/ACTIN. The X axis showed the oka cell culture that transfected with three different double-stranded RNAs. The data are from independently duplicated experiments and plotted as means ±SEM (Standard error of the mean). * Indicated a significant difference between control cell and dsRNA-transfected cell at $P < 0.05$ by using one-way ANOVA test.

5.8 Determination of the efficacy of RNAi pathway in Pem-AGO depleted cells

5.8.1 The effect on silencing endogenous gene

To determine the effect on RNAi pathway in Pem-AGO depleted cells, the double-stranded RNA corresponding to an endogenous gene, the serotonin (5-hydroxytryptamine, 5-HT) receptor (kindly provided by Dr. Chalermporn Ongvarrasopone) was co-transfected with individual dsRNA of Pem-AGO (one microgram each) into the Oka cell culture. The cells were collected at 72 h after transfection, and the transcription level of both Pem-AGO mRNA and 5-HT receptor mRNA were detected by RT-PCR. The levels of Pem-AGO transcript in the cells that were co-transfected with either ds1 and dsPIWI, ds1 and dsRNA of 5-HT receptor (ds5-HTR) or dsPIWI and ds5-HT were not different from that of the control cells (no dsRNA), but lower than that of the ds5-HTR-transfected cells (Figure 43, middle panel). The ds5-HTR triggered the decrease in the expression of 5-HT receptor to about 15% of that in the control cells. However, the transcription level of 5-HT receptor was recovered to considerable extent in the cells that were co-transfected with ds1 or dsPIWI and ds5-HT, whereas the cells receiving only ds1 and dsPIWI exhibited the same level of 5-HT receptor transcript as the control cells (Figure 43, bottom panel).

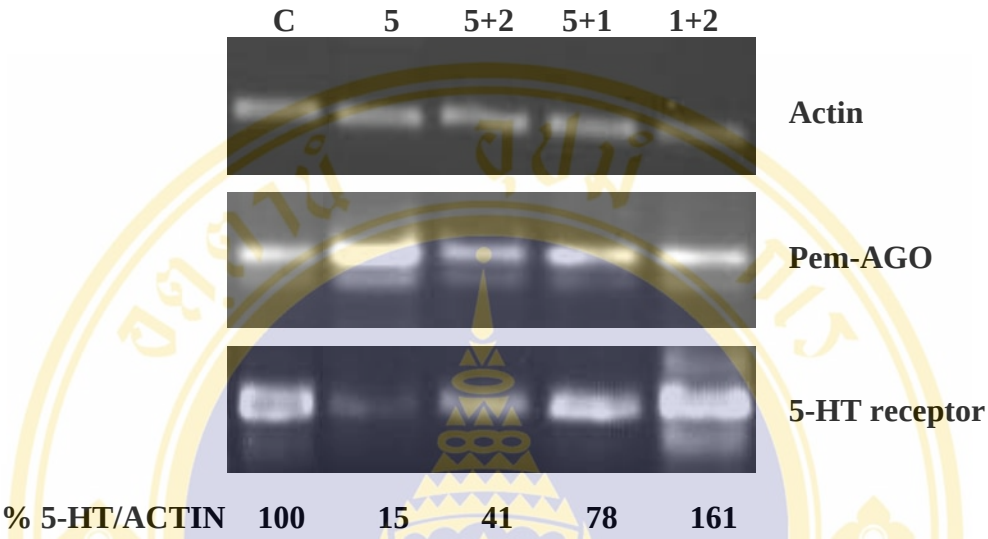

Figure 43. RT-PCR detection of 5-HT receptor transcript in the Oka cells after co-transfected with Pem-AGO specific dsRNA and 5-HT receptor dsRNA

The Oka cells were either trnasfected with ds5-HT-R alone or co-transfected with ds5-HT-R and ds1 or dsPIWI of Pem-AGO. The cells were collected for RT-PCR at 72 h after transfection. The actin transcript is shown in the top panel. The middle and bottom panels represent the RT-PCR products of Pem-AGO (using PIWI-F and PIWI-R primers) and 5-HT receptor (using YR5-HTFULL and YR3RACE primers), respectively. C is the control cells that received no dsRNA, whereas 5, 5+2 and 5+1 represents the cells that were transfected with ds5-HTR alone, ds5-HTR together with dsPIWI and ds5-HT-R together with ds1, respectively. Similarly, 1+2 represents the cells that were co-transfected with ds1 and dsPIWI of Pem-AGO. The numbers at the bottom represent the percentage of 5-HT-receptor mRNA level in each sample comparing with the control.

5.8.2 The effect on silencing exogenous gene

The double-stranded RNA harboring the sequence of the protease gene of the yellow head virus (dsYHV) has been shown to be capable of preventing the replication of YHV in the Oka cells (84). Therefore, the potency of Pem-AGO depleted cells to prevent YHV replication upon the presence of dsYHV was investigated. The dsYHV was used to co-transfect into the Oka cell culture with each of Pem-AGO dsRNA (one microgram each) and followed by infection with 10^{-5} titer of YHV at 40 h after transfection. The transcription level of Pem-AGO and the replication of YHV in the cells were detected by RT-PCR at 72 h post infection (Figure 44). The result showed that the level of Pem-AGO transcript in each sample was not different (Figure 43, middle panel). High level of YHV transcript, as detected by RT-PCR using the primers that were specific to the helicase gene of YHV was detected only in the control cells that was infected with YHV without transfection with either Pem-AGO or YHV dsRNA. The cells that received dsYHV prior to YHV infection produced dramatically detection level of YHV transcript. Similar level of YHV transcript to that of dsYHV-transfected cells was also detected in the cells into which dsYHV had been co-transfected with dsPIWI and dsPAZ. However, it should be noted that YHV may replicate more efficiently in dsYHV and ds1-transfected cells as the level of YHV transcript was slightly higher than that in the cells co-transfected with dsYHV and any of the other two Pem-AGO dsRNA (Figure 44, bottom panel).

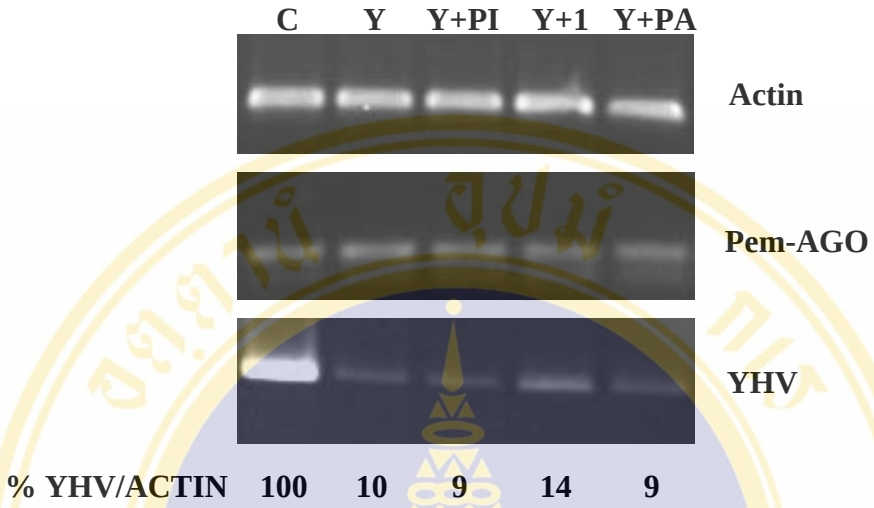

Figure 44. RT-PCR detection of YHV transcript in the Oka cell culture after transfected with different dsRNAs and followed by YHV infection

The Oka cells were transfected with different dsRNAs at 40 h before infected by 10^{-5} titer of YHV. The cells were harvested at 72 h after YHV infection. The actin transcript is shown in the top panel. The middle and bottom panel represent the transcripts of Pem-AGO and YHV (amplified with Hel-F and Hel-R primers), respectively. C is the untransfected cells, whereas Y represents the dsYHV-transfected cells. The cells in which dsYHV was co-transfected with dsPIWI, ds 1and dsPAZ were depicted as Y+PIWI, Y+1 and Y+PA, respectively. The numbers at the bottom represent the percentage of YHV mRNA level in each sample comparing with the control.

CHAPTER VI
DISCUSSION

Argonaute is a family of proteins that plays a primary role in developmental control. In addition, several of Argonaute proteins are shown to be a key component in the RNA-mediated gene silencing mechanism in a variety of species ranging from nematode to human (29). The number of Argonaute proteins varies from one organism to another. In general, Argonaute protein is classified into two major groups; the proteins that are responsible for developmental control and the proteins that are associated with RNAi function. For example, in human, two subfamilies of Argonaute protein are characterized, the PIWI subfamily and eIF2C/AGO subfamily (45). The PIWI subfamily functions in the maintenance of stem cell differentiation. Alternatively, the eIF2C/AGO subfamily is associated with siRNA and RISC that are related to the RNAi pathway. In the RNAi pathway, Argonaute protein acts as the major component in RISC which guides the degradation of cognate mRNA directing by siRNA. Recently, RNAi has been demonstrated for its potential in preventing viral replication in the shrimp *P. monodon* (85). Since the knowledge about RNAi in the shrimp is very limited, characterization of Argonaute protein and its functional role in RNAi could pave the way to a better understanding of this promising pathway for viral control in the shrimp.

In this study, 3'RACE and 5'RACE stratergy were used to clone the coding sequence of Argonaute cDNA from *P. monodon* (Pem-AGO). The function of Pem-AGO in the RNAi pathway was characterized by investigating the potency of RNAi to knock down specific gene in *P. monodon*'s primary Oka cell culture that were depleted in Pem-AGO expression.

In the cloning strategy, the degenerate primers were designed from the conserved sequence of Argonaute proteins from *A. thaliana*, *D. melanogaster*, *H. sapiens* and *C. elegan* in order to amplify the Argonaute cDNA (Pem-AGO) of *P. monodon*

The 3'UTR sequence obtained by 3'RACE was incomplete because the poly A sequence at the 3'end from the sequence analysis was not found. This could occur from non-specific binding of the primer sequence (PM-1) at the internal site within the 3'UTR region. Such internal binding would block the amplification from the PM-1 primer that binds to its corresponding sequence in the oligo (dT)-containing primer, PRT, that recognize the poly A at the 3' end of cDNA.

The 5' end amplification with 5'RACE strategy gave two types of product that were distinguished base on the presence or the absence of nine nucleotides at position 319-327 (Figure 30). This leads to the loss of three amino acids in one type and the change in the next amino acid residue when compared between the deduced amino acid sequences from both fragments. The presence of two different sequences either with or without the nine nucleotides discussed above was confirmed by amplification of the entire coding sequence of Pem-Ago cDNA (Figure 33). This suggested that there are at least two variants of Pem-Ago cDNA in *P. monodon*.

The amplification of the fragment 1 of Pem-AGO in this study gave only a single band of the products and analysis of three recombinant clones containing the fragment 1 showed the same nucleotide sequence. However, in previous work that aimed at cloning this cDNA fragment, a shorter product of fragment 1 has been also obtained (Apinunt Udomkit, Personal communication). This shorter fragment 1 has the deletion of eighty-one nucleotides (27 amino acids) in the coding sequence for the PIWI domain (Appendix 1). However, an attempt to clone the entire coding region of the Pem-AGO cDNA containing this deletion was not successful. One possible reason for this is that the short form of Pem-AGO, if really existed, may be expressed at much lower level than the longer form as could be observed in later experiments in this thesis. When the transcript of Pem-AGO was detected by RT-PCR with the primers PIWI-F and PIWI-R, two bands of the product were produced, and the amount of the smaller fragment was always less than that of the longer one (Appendix 2).

Because the PIWI domain is conserved in Argonaute protein family and this domain exhibits similar structure to that of RNaseH domain (49). The PIWI domain is responsible for the endonuclease activity in RISC that cleaves the mRNA target. The active site for RNaseH family normally contains the three catalytic residues called the DDE (aspartate, aspartate and glutamate) motif which are conserved in several species

(49). Although the region of 81 bases deletion in the PIWI domain of the short Pem-AGO does not include these conserved catalytic residues, the missing of the 81 nucleotides might disturb the proper conformation and thus affect the formation of the active site among the three catalytic residues that is suitable for catalytic reaction of the PIWI domain. However, the function of the short form of Pem-AGO is still not known. It is possible that this short form might display different function from the Pem-Ago that is characterized in this study.

The information of the overlapping fragments of Pem-AGO obtained earlier was used to design specific primers in order to amplify the entire coding sequence of Pem-AGO cDNA. The 2,829 bp (939 amino acids) of the coding sequence of Pem-AGO was successfully amplified. This Pem-AGO sequence was closest (at 85% identity) to the Argonaute protein 1 (dAgo1) of *D. melanogaster*. The Pem-Ago sequence contained the two conserved domains of Argonaute family, PAZ and PIWI. PAZ domain of Pem-AGO is 417 base pair long and PIWI is 987 base pair in length. The amino acid sequence of Pem-AGO PAZ and PIWI domains were 94.7% and 99.7 %, respectively, identical to the consensus sequence of both domains (Appendix 3-4). The nuclear magnetic resonance solution structure of the PAZ domain of dAgo1 depicted that the characteristic fold of this domain is centered around six-stranded β-barrel core (46). The surface of β-barrel structure and the appendage (α-helix and β-hairpin) form the conserved nucleotide binding site (Tyr 386, Phe 387 and Tyr 391) which bind to the 2 nucleotide-3'overhang of the siRNA. Mutation in the conserved residues in the binding site in dAgo1 showed the 50% decrease in RNA binding. This conserved RNA-binding site was also found in the Pem-AGO sequence (indicated by the asterisks in Figure 35) suggesting the conserved function between dAgo1 and Pem-AGO. The other conserved domain, the PIWI domain, adopts structural similarity to the RNaseH enzyme family which contains three conserved catalytic residues, Asp-Asp-Glu (DDE) in the active site (49). Mostly, the positions of two aspartates are invariant, but the third amino acid, glutamate varies in the position among RNase H family. However, the third residue in the catalytic site of the PIWI domain of human Argonaute (hAgo2) was demonstrated to be the histidine instead of glutamate. This catalytic triad, DDH (instead of DDE), was also found in Pem-AGO sequence at conserved positions (indicated by asterisks in Figure 35). This catalytic site was

proposed to function as the metal ion binding site that is required for the activity of RNaseH enzyme in the mRNA cleavage reaction. Mutation of the two aspartates and histidine, but not the glutamate, in hAgo2 inactivated the mRNA cleavage *in vitro*. This suggested that these three residues are coordinated with the metal ion and accomplished the mRNA cleavage activity.

The conserved positions of the residues that are critical for the function of Argonaute in both PAZ and PIWI domain implies the possible role of Pem-AGO in the RNAi pathway. In order to provide a supporting evidence for this implication, the involvement of Pem-AGO in RNAi mechanism in *P. monodon* was determined. One approach to characterize the function of Argonaute in RNAi is to assay for RNAi efficiency in the cells that are defective in Argonaute expression. Such Argonaute-depleted cells could be generated either by gene knockdown (85) or by siRNA-mediated gene silencing (86)

In *P. monodon*, an attempt to characterize the function of Argonaute protein was made. Although the continuous cell line from penaeid tissues has not been successfully established, primary cell culture could be prepared from various tissues of penaeid shrimp (16). From the variety of tissues, the cells from lymphoid (Oka) organ were found to proliferate more rapidly and remain stable for long periods of time (2-3 weeks). Furthermore, the repression of specific gene by dsRNA has been demonstrated in the primary lymphoid cell culture (25). Additionally, the result in this study also showed the high level of expression of Pem-AGO in the lymphoid organ (Appendix 2). Taken together, the primary Oka cell culture was considered for investigation of Pem-AGO function in RNAi.

In the characterization of Pem-AGO function, three regions located in the coding sequence of Pem-Ago were selected to synthesize three double-stranded RNAs; ds1, dsPIWI and dsPAZ. The ds1 is corresponded to the sequence 5' upstream of the PAZ domain. This region is not conserved among different Argonaute proteins, therefore ds1 is expected to specifically knockdown only the Pem-AGO sequence identified in this study. Alternatively, dsPIWI and dsPAZ were synthesized from the conserved sequences in the PIWI and PAZ domains, respectively, and thus should target all the Argonaute transcripts that contain similar PAZ and PIWI sequences. The Oka cell culture that was transfected with 2 μg of ds1, dsPIWI and dsPAZ for 24 h showed the

27%, 23% and 31% reduction in Pem-AGO transcript level comparing with the Pem-AGO transcription the control cells. At 48 h after transfection the cells that were transfected with all three types of Pem-AGO dsRNA exhibited similar levels of reduction at approximately 30% of that in the control cells (Figure 40-42). The result suggested that three dsRNAs of Pem-AGO showed comparable level of activity in the inhibition of Pem-AGO mRNA expression in the Oka cells. The efficacy of siRNA generated from long dsRNA to silence the target mRNA depends on several factors such as the 5' end thermodynamic stability of the anti-sense strand and the accessibility to the target sequence (87). The results of Pem-AGO silencing by dsRNA in this study are similar to that of the knockdown of the rat Argonaute (GERp95) by specific siRNA in which approximately 50% depletion in GERp95 mRNA level was observed at 24 and 48 h after transfection (86). One possible explanation for this incomplete knockdown of Argonaute expression by specific dsRNA or siRNA is that certain level of Argonaute expression is required to maintain RNAi machinery in the cells. Upon the acquisition of Argonaute dsRNA, the Argonaute proteins that are already presence in the cells will be utilized to repress Argonaute expression. At certain time, once the Argonaute protein level is decreased due to the silencing of its expression, the RNAi will become less effective, and allows de-repression of Argonaute expression, thus produce more Argonaute mRNA once again. The more substantial level of Argonaute knockdown could be achieved by using longer dsRNA that would give higher possibility to produce more effective siRNA or by knocking down the gene that encodes the Argonaute protein (86).

The unrelated dsRNA, dsGFP, was used to demonstrate specificity of Pem-AGO dsRNA to knockdown Pem-AGO mRNA. However, a small reduction in Pem-AGO mRNA level (approximately 15% less than the control) was still observed in the cells transfected with dsGFP (Figure 41). It has been reported that double-stranded RNA targeting the unrelated control gene, GFP, showed the induction of partial protection of antiviral defense in *Litopenaeus vannamei* by non-specific knockdown (88). Therefore it is possible that the slight decrease in Pem-AGO mRNA level by the unrelated dsGFP may be the result of this non-specific knockdown mechanism of dsGFP to the Argonaute transcript. In mammalian cell, non-specific antiviral defense by dsRNA is activated through the dsRNA recognition receptor called Toll-like

receptor 3 (TLR3) (89, 90). TLR3 is the germline-encoded family which recognized pathogen molecule, host protein-associated pathogen and including dsRNA from viral infection (91). In the presence of dsRNA, TLR3 induces the synthesis of type I interferon which activates two proteins. First protein is the RNA-dependent protein kinase (PKR) which inhibites viral protein synthesis (92). The second protein is 2'-5'-oligo adenylate synthetase which activates RNase L to degrade RNA in a non-specific sequence (89). Therefore, similar to the mammalian cell, dsRNA in the shrimp cell may induce both sequence-specific-gene suppression by RNAi and non-specific sequence suppression of protein synthesis and enhancement of mRNA degradation by recognizing through TLR3 (89). The Toll-like receptor has been found in *P. monodon* (93) and the gene that controls the immune function homolog to the interferon response, STAT, was also found in shrimp (94). Therefore, this toll-like receptor may be involved in sequence-independent antiviral immunity in shrimp (93). It is possible that there is the evolutionary link between innate antiviral immunity triggering by dsRNA in both vertebrate and invertebrate (88). These evidences support that induction of dsRNA in shrimp may go through two pathways, sequence-independent immunity and sequence-specific gene silencing of RNAi (95).

To determine the ability of Argonaute-depleted cells to drive RNAi pathway, a dsRNA corresponding to the endogenously expressed 5-hydroxytryptamine (5-HT) receptor gene was co-transfected with Pem-AGO dsRNAs into the Oka cells. Preliminary study suggested that transfection of the Oka cells with 2 ug of dsRNA of 5-HT receptor (ds5-HTR) triggered the inhibition of 5-HT receptor mRNA level at 48 h after transfection (96). In this study the efficiency of RNAi to knockdown 5-HT receptor expression by ds5-HTR in the Pem-AGO depleted environment (induced by co-transfection of Pem-AGO dsRNA) was investigated. At 72 h after transfection, the cells that were transfected with the combination of two Pem-AGO dsRNA (ds1 and dsPIWI) showed no inhibitory effect on 5-HT receptor mRNA level comparing to the control cell into which no dsRNA was introduced. This demonstrated that dsRNA of Pem-AGO did not have any effect on 5-HT receptor expression and thus confirm specificity of using dsRNA to silence mRNA target. The expression of 5-HT receptor mRNA was dramatically decreased in the cells transfected with ds5-HTR alone to the level of 15% of that expressed in the control cells. On the contrary, the expression of

5-HT receptor mRNA could be restored to a substantial extent by co-transfection of ds1 or dsPIWI with ds5-HT (Figure 43). This demonstrates that depletion of Pem-AGO mRNA leads to the impairment of RNAi mechanism in the cells. Similar level of the impaired siRNA in the cells that were depleted for Argonaute was also reported in the rat cells in which the ablation of Argonaute, GERp95, caused a de-repression of neuropeptide Y (NPY) gene expression from dsRNA that targeted NPY (86). As a result, Pem-AGO could be therefore considered as an essential component in the RNAi in *P. monodon*.

In addition, RNAi in the cells that had acquired Pem-AGO dsRNA was also investigated with exogenous dsRNA corresponding to the protease gene of YHV (dsYHV). It has been reported that the Oka cell culture that was transfected with 1 μg of dsYHV followed by infection with 10^{-5} titer of YHV showed complete inhibition in the YHV mRNA level at 48 h post-infection (84). In contrast to the result of the effect on expression of endogenous gene 5-HT receptor, co-transfection of ds1, dsPIWI or dsPAZ with dsYHV into the Oka cells was unable to rescue the expression of YHV in the cells comparing with the cells that received dsYHV alone. Although slight recovery of the YHV mRNA level was observed when dsYHV was co-transfected with ds1, the effect is not significantly different from the inhibited level in the cells transfected with dsYHV alone (Figure 44). The different effect of Pem-AGO depletion on the efficiency of RNAi against 5-HT receptor and YHV protease genes could be explained by the difference in the time at which their siRNA products meet the targets. Since 5-HT receptor is normally expressed in the lymphoid organ, the RNAi can function to degrade 5-HT receptor mRNA once the cells were administrated with ds5-HTR. Therefore if Pem-AGO was depleted by co-transfection with Pem-AGO dsRNA, the effect on the efficiency of RNAi to silence the expression of 5-HT receptor could be simultaneously observed. On the other hand, in the experiment with dsYHV, the cells were infected with YHV virus at 40 h after double-stranded RNA transfection and the cells were harvested at a further 72 h after viral infection. Therefore, the total time in collecting cell in this experiment is 112 h after administrated with dsRNA. At this time, it is possible that Pem-AGO level was recovered and therefore relieved the RNAi activity against dsYHV. Since the siRNA is unstable as a result from its short half-life, it has been reported that the effective duration in the transfection by using the

siRNA to mediate gene silencing should not be longer than 96 h post transfection (97-99). In order to obtain a more promising result of Pem-AGO depletion on the RNAi against dsYHV, appropriate duration of dsRNA transfection and YHV infection must be determined.

In summary, the Pem-AGO could be considered as one of the factors that associate with RNAi pathway in the shrimp *P. monodon*. This is supported by several evidences from this study; 1) Pem-AGO are closely related to dAgo1 of *D. melanogaster* that has been shown for its role in RNAi pathway. 2) Pem-AGO contains the two signature, PAZ and PIWI domains of the Argonaute family with the conserved functional residues. 3) The depletion of Pem-AGO had an impact on the RNAi activity in shrimp cells.

CHAPTER VII
CONCLUSION

7.1 The virtual transcript of a cDNA encoding Argonaute protein of *P. monodon* (Pem-AGO) was revealed by combination of the sequences from four overlapping cDNA fragments obtained by RT-PCR and RACE.

7.2 The cDNA harbouring the entire coding sequence of Pem-AGO was successfully cloned by means of RT-PCR with gene specific primers designed from the 5'end (the first ATG codon that is in-frame with the translated product) and 3' end (the TAA codon) of the combined virtual transcript.

7.3 The entire coding sequence of Pem-AGO is 2,829 nucleotides in length. The deduced amino acid sequence of Pem-AGO revealed a significant degree of 85% identity to Argonaute protein 1 of *D. melanogaster*. The Pem-AGO contained two conserved domains in Argonaute family, PAZ (417 bp) and PIWI (987 bp).

7.4 In the 5'region of Pem-AGO coding sequence, two types of sequences that are distinguished by the presence or the absence of nine nucleotides at position 319-327 were found suggesting the presence of two variants of Pem-Ago cDNA in *P. monodon*.

7.5 Three different regions located in the coding sequence of Pem-AGO were selected to synthesize three double-stranded RNAs; ds1, dsPIWI and dsPAZ. These dsRNAs of Pem-AGO were used to transfect into the primary Oka cell culture to investigate the function of Pem-Ago in RNAi.

7.6 The ds1, dsPIWI and dsPAZ showed comparable level of activity that exhibited 30% inhibition of Pem-AGO mRNA transcript in the Oka cells at 24 and 48 h after transfection.

7.7 The depletion of Pem-AGO experiment in the Oka cells caused the impairment of RNAi activity on endogenous gene (5-HT receptor) by specific dsRNA (ds5-HTR) that could be detected at 72 h after transfection. On the other hand, no significant impact of Pem-AGO depletion on RNAi mechanism against exogenous gene (dsYHV) was observed.

7.8 The Pem-AGO could be considered as one of the factors that is associated with RNAi pathway in the shrimp *P. monodon* due to the presence of conserved domain, PAZ and PIWI, and the impact on the RNAi activity in shrimp cell culture.

REFERENCES

1. Solis NB. Biology and Ecology. In: Biology and culture of *Penaeus monodon*. Brackishwater Aquaculture Information System. Aquaculture Department Southeast Asian Fisheries Development Center. Tigbauan, Hoilo, Philipines. 1981:1-36.
2. D'Abramo LR, Brunson MW. Production of freshwater prawns in ponds. Southern Regional Aquaculture Center (SRAC). 1996;484.
3. Trade Environment Databases (TED) case studies Thailand shrimp farming. Available from http://www.american.edu/TED/THAISHRIMP.html. [Updated on 2003 Feb 27].
4. D'Abramo LR, Brunson MW. Biology and life history of freshwater prawns. SRAC. 1996;483.
5. Zimmerman TL, Martin JW. Decapods. In:Zimmerman TL,Martine JW, Eds. Marine Invertebrates of Guana Island, British Virgin Islands 2000. http://www.nhm.org/guana/bvi-invt/bvi-surv/deca-inf.htm [Updated on 2003 Aug]
6. Bailey-Brock JM, Moss SM. Penaeid taxonomy, biology and zoogeography In: Fast AW, Lester LJ. Eds. Marine Shrimp Culture: Principles and Practices. Elsevier Science Publishers 1992:9-23.
7. Whitaker JD. Shrimp in South Carolina. South Carolina Rules&regulations (SCDNR). 2005:24-28
8. Solid NB. Biology and ecology. In: Biology and culture of *Penaeus monodon*. Brackishwater Aquaculture Information System. Aquaculture Department Southeast Asia Fisheries Development Center. Tijbauan, Hoilo, Phillipines. 1988:3-15.
9. Primavera JH. External and internal anatomy of adult penaeid prawn/shrimps. SEAFDEC, Aquaculture Department, The Philippines, Poster. 1990.
10. Auchau AG. Crustaceans In: Ratcliffe N.A. and Rowley AF. Eds. Invertebrate blood cells 1981:385-420.

11. Johnson PT. History of the blue crab, *Callinectes sapidus*. A model for the Decapoda 1980:440.
12. Sandeman DC. Organization of the central nervous system, In:Atwood HL, Sandeman DC. Eds. The Biology of crustacean.vol 3. Academic press 1982;3:1-4.
13. Boonyaratpalin S, Supamattaya K, Kasornchandra J, Direkbusarakom S, Ekpanithanpong U, Chantanachooklin C. Non-occluded baculo-like virus the causative agent of yellow-head disease in black tiger shrimp *Penaeus monodon*. Fish pathol. 1993;28(3):103-109.
14. Chantanachooklin C, Boonyaratpalin S, Kasornchandra J, Direkbusarakom S, Ekpanithanpong U, Supamattaya K, Sriurairatana S, Flegel TW. Histology and ultrastructure reveal a new granulosis-like virus in *Penaeus monodon* affected by yellow-head disease. Dis Aquat Org. 1993;17:145-157.
15. Loh PC, Tapay LM, Lu Y, Nalada ECB Jr. Viral pathogens of the penaeid shrimp. Adv Virus Res. 1997;48:263-312.
16. Wongteerasupaya C, Sriurairatana S, Vickers JE, Akarajamorn A, Boonsaeng V, Panyim S, Tassanakajon A, Withyachumnarnkul B, Flegel TW. Yellow-head virus of *Penaeus monodon* is an RNA virus. Dis Aquat Org. 1995;22(1):45-50.
17. Tang KF, Lightner DV. A yellow head virus gene probe: nucleotide sequence and application for in situ hybridization. Dis Aquat Org. 1999;35(3):165-173.
18. Sittidilokratna N, Hodgson RAJ, Cowley JA, Jitrapakdee S, Boonsaeng V, Panyim S, Walker PJ. Complete ORF1b-gene sequence indicates yellow head virus is an invertebrate nidovirus. Dis Aquat Org. 2002;50(2):87-93.
19. Chou HY, Huang CY, Wang CH, Chiang HC, Lo CF. Pathogenicity of a baculovirus infection causing white spot syndrome in culture penaeid shrimp in Taiwan. Dis Aquat Org. 1995;23(3):165-173.

20. Nakano H, Koube H, Umezawa S, Momoyama K, Hiraoka M, Inouye K, Oseko N. Mass mortalities of cultured kuruma shrimp, *Penaeus japonicus*, in japan in 1993-epizootiological survey and infection trials. Fish Pathol. 1994;29:135-139.

21. Chen SN, Wang CS. Establishment of cell culture systems from penaeid shrimp and their susceptibility to white spot disease and yellow head viruses. Methods Cell Sci. 1999;21(4):199-206.

22. Chen SN, Kou GH. Infection of cultured cells from the lymphoid organ of *Penaeus monodon* Fabricius by monodon-type baculovirus (NBV). J Fish Dis. 1989;12;73-76.

23. Hsu Y-L, Yang Y-H, Chen Y-C, Tung M-C, Wu J-L, Engelking MH, Leong JC. Development of an in vitro subculture system for the oka organ (lymphoid tissue) from *Penaeus monodon.* 1995;136:43-55.

24. Kasornchandra J, Khongpradit R, Ekpanithanpong U, Boonyaratpalin S. Progress in the development of shrimp cell cultures in Thailand. Methods Cell Sci. 1999;21(4):231-235.

25. West L. Mahony T, McCarthy F, Watanabe J, Hewitt D, Hansford S. Primary cell cultures isolated from *Penaeus monodon* prawns. Method Cell Sci. 1999;21(4):219-223.

26. Lu Y, Tapay LM, Loh PC, Brock JA, Gose RB. Distribution of yellow-head virus selected tissues and organs of penaeid shrimp *Penaeus vannamei*. Dis Aquat Org. 1995;25:67-70.

27. Lu Y, Tapay LM, Loh PC, Brock JA, Gose RB. Development of a quantal assay in primary shrimp cell culture for yellow head baculovirus (YBV) of penaeid shrimp. J Virol Methods. 1995;52:231-236.

28. Oka M. Studies in *Penaeus orientalis* Kishinouye-VIII Structure of the newly found lymphoid organ. Bull Jpn Soc Sci Fish. 1969;35:245-250.

29. Hammond SM, Boettcher S, Caudy AA, Kobayashi R, Hannon GJ. Argonaute2, a link between genetic and biochemical analyses of RNAi. Science. 2001;293:1146-1150.

30. Fire A. RNA-triggered gene silencing. Trends Genet. 1999;15(9):358-363.

31. Fagard M, Boutet S, Morel JB, Bellini C, Vaucheret H. AGO1, QDE-2, and RDE-1 are related for post-transcriptional gene silencing in plants, quelling in fungi, and RNA interference in animals. PNAS. 2000;97(21):11650-11654.

32. Denli AM, Hannon GJ. RNAi an ever-growing puzzle. Trends Biochem.Sci. 2003;28:196-201.

33. Sontheimer EJ, Carthew RW. Argonaute journeys into the heart of RISC. Science. 2004;305:1409-1410.

34. Bernstein E, Caudy AA, Hammond SM, Hannon GJ. Role for a bidentate ribonuclease in the initiation step of RNA interference. Nature. 2001;409:363-366.

35. Elbashir SM, Lendeckel W, Tuschl T. RNA interference is mediated by 21and 23 nt RNAs. Genes Dev. 2001;15:188-200.

36. Elbashir SM, Martinez J, Patkaniowska A, Lendeckel W, Tuschl T. Functional anatomy of siRNAs for mediating efficient RNAi in *Drosophila melanogaster* embryo lysate. EMBO J. 2001;20:6877-6888.

37. Zamore PD, Tuschl T, Sharp PA, Bartel DP. RNAi;double-stranded RNA directs the ATP-dependent cleavage of mRNA at 21-23 nucleotide intervals. Cell. 2000;101:25-33.

38. Lingel A, Izaurralde E. RNAi: Finding the elusive endonuclease. RNA. 2004;10:1675-1679.

39. Carmell MA, Hannon GJ. RNase III enzymes and the initiation of gene silencing. Nat. Struct. Mol. Biol. 2004;11:214-218.

40. Ryter JM, Schultz SC. Molecular basis of double-stranded RNA-protein interactions: structure of a dsRNA binding domain complex with dsRNA. EMBO J. 1998;17:7505-7513.

41. Zhang H, Kolb FA, Jaskiewicz L, Westhof E, Filipowicz W. Single processing center models for human dicer and bacterial RNase III. Cell. 2004;118:57-68.

42. Liu Q, Rand TA, Kalidas S, Du F, Kim HE, Smith DP, Wang X. R2D2, a bridge between the initiation and effector steps of the *Drosophila* RNAi pathway. Science. 2003;301:1921-1925.

43. Hammond SM. Dicing and slicing: The core machinery of the RNA interference pathway. FEBS. 2005;579:5822-5829.

44. Carmell MA, Xuan Z, Zhang MQ, Hannon GJ. The Argonaut family: tentacles that reach into RNAi, development control, stem cell maintenance, and tumorigenesis. Genes Dev. 2002;16:2733-2742.

45. Sasaki T, Shiohama A, Minoshima S, Shimizu N. Identification of eight members of the Argonaute family in the human genome. Genomics.2003;82:323-330.

46. Yan HK, Yan S, Farooq A, Han A, Zeng L, Zhou MM. Structure and conserved RNA binding of the PAZ domain. Nature. 2003;02129:1-8.

47. Marqusee S, Goedken ER. Co-crystal of Escherichia coli RNase HI with Mn2+ ions reveals two divalent metals bound in the active site. J Biol Chem. 2001;276:7266-71.

48. Yang W, Steitz TA. Recombining the structures of HIV integrase RuvC and RNaseH. Structure 3. 1995:131-134.

49. Song JJ, Smith SK, Hannon GJ, Joshua-Tor L. Crystal structure of Argonaute and its implications for RISC slicer activity. Science. 2004;10.1126:1-4.

50. Liu J, Carmell MA, Rivas FV, Marsden CG, Thomson JM, Song JJ, Hammomd SM, Joshua-Tor L, Hannon GJ. Argonaute 2 is the catalytic engine of mammalian RNAi. Science. 2004;10.1126:1-5.

51. Caudy AA, Myers M, Hannon GJ, Hammond SM. Fragile X-related protein and VIG associate with the RNA interference machinery. Genes & Dev. 2002;16:2491-2496.

52. Ivanov KI, Tselykh TV, Heino TI, Makinen K. The RISC component VIG is a target for dsRNA-independent protein kinase activity in *Drosophila* S2 cells. J RNAi & Genes Sile. 2005;1:12-20.

53. Heaton JH, Dlakic WM, Dlakic M, Gelehrter TD. Identifiaction and cDNA cloning of a novel RNA-binding protein that interacts with the cyclic nucleotide-responsive sequence in the Type-1 plasminogen activator inhibitor mRNA. J Biol Chem. 2001;276:3341-3347.

54. Caudy AA, Ketting RF, Hammomd SM, Denli AM, Bathoorn AMP, Tops BBJ, Silva JM, Myers MM, Hannon GJ, Plasterk RHA. A micrococcal nuclease homologue in RNAi effector complexes. Nature. 2003;425:411-414.

55. Ishizuka A, Siomi MC, Siomi H. A Drosophila fragile X protein interacts with components of RNAi and ribosomal proteins. Genes & Dev. 2002;16:2497-2508.

56. Schwarz DS, Tomari Y, Zamore PD. The RNA-induced silencing complex is a Mg^{2+}-dependent endonuclease. Curr. Biol. 2004;14:787-791.

57. Volpe TA, Kidner C, Hall IM, Teng G, Grewal SI, Martienssen RA. Regulation of heterochromatin silencing and histone H3 lysine-9 methylation by RNAi. Science. 2002;297:1833-1837.

58. Reinhart BJ, Bartel DP. Small RNAs correspond to centromeric heterochromatin repeats. Science. 2002;297:1831.

59. Bannister AJ, Zegerman P, Partridge JF, Miska EA, Thomas JO, Allshire RC, Kouzarides T. Selective recognition of methylated lysine 9 on histone H3 by the HP1 chromo domain. Nature. 2001;410:120-124.

60. Vaucheret H, Beclin C, Fagard M. Post-transcriptional gene silencing in plants. J Cell Sci. 2001. ;114:3083-3091.

61. Sontheimer EJ, Carthew RW. Argonaute journeys into the heart of RISC. Science. 2004;305:1409-1410.

62. Soldan SS, Plassmeyer ML, Matukonis MK, Gonzalez-Scarano F. La crosse virus non-structural protein NSs counteracts the effects of short interfering RNA. J Virol. 2005;79:234-244.

63. Lecellier CH, Dunoyer P, Arar K, Lehmann-Che J, Eyquem S, Himber C, Saib A, Voinnet O. A cellular microRNA mediates antiviral defense in human cells. Science. 2005;308:557-560.

64. Vargason JM, Szittya G, Burgyan J, Tanaka Hall TM. Size selective recognition of siRNA by an RNA silencing suppressor. Cell. 2003;115:799-811.

65. Lakatos L, Szittya G, Silhavy D, Burgyan J. Molecular mechanism of RNA silencing suppression mediated by p19 protein of tombusviruses. EMBO J. 2004;23:876-884.

66. Silhavy D, Molnar A, Lucioli A, Szittya G, Hornyik C, Tavazza M, Burgyan J. A viral protein suppresses RNA silencing and binds silencing-generated, 21 to 25 nucleotide double-stranded RNAs. EMBO J. 2002;21:3070-3080.

67. Hutvagner G. Small RNA asymmetry in RNAi :function in RISC assembly and gene regulation. FEBS. 2005;579:5850-5857.

68. Landthaler M, Yalcin A, Tuschl T. The human DiGeorge syndrome critical region gene 8 and its *D. melanogaster* homolog are required for miRNA biogenensis. Curr. Biol. 2004;14(23):2162-2167.

69. Gregory RI, Yan KP, Amuthan G, Chendrimada T, Doratotaj B. The microprocessor complex mediates the genesis of microRNAs. Nature. 2004;432:235-240.

70. Cerutti H. RNA interference :traveling in the cell and gaining functions. Trends Genet. 2003;19(1):39-45.

71. Lee RC, Feinbaum RL, Ambros V. The *C. elegans* heterochronic gene lin-4 encodes small RNAs with antisense complementarity to lin-14. Cell. 1993;75:843-854.

72. Wightman B, Ha I, Ruvkun G. Posttranscriptional regulation of the heterochronic gene lin-14 by lin-4 mediates temporal pattern formation in *C. elegans*. Cell. 1993;75:855-862.

73. Ha I, Wightman B, Ruvkun G. A bulged lin-4/lin-14 RNA duplex is sufficient for *C. elegans* lin-14 temporal gradient formation. Genes Dev. 1996;10:3041-3050.

74. Reinhart BJ, Slack FJ, Basson M, Pasquinelli AE, Bettinger JC, Rougvie AE, Horvitz HR, Ruvkun G. The 21-nucleotide let-7 RNA regulates developmental timing in *C. elegans*. Nature. 2000;403:901-906.

75. Collins R, Cheng X. Structural domains in RNAi. FEBS. 2005;579:5841-5849.

76. Yi R, Qin Y, Macara IG, Cullen BR. Exportin-5 mediates the nuclear export of pre-microRNAs and short hairpin RNAs. Genes Dev;17:3011-3016.

77. Hutvagner G, Zamore PD. A microRNA in a multiple-turnover RNAi enzyme complex. Science. 2002;297:2056-2060.

78. Grishok A, Pasquinelli AE, Conte D, Li N, Parrish S, Ha I, Baillie DL, Fire A, Ruvkun G, Mello CC. Genes and mechanisms related to RNA interference and regulate expression of the small temporal RNAs that control *C. elegans* development timing. Cell. 2001;106:23-34.

79. Tabara H, Sarkissian M, Kelly WG, Fleenor J, Grishok A, Timmons L, Fire A, Mello CC. The rde-1 gene, RNA interference and transposon silencing in *C. elegans*. Cell. 1999;99:123-132.

80. Reinhart BJ, Weinstein EG, Rhoades MW, Bartel B, Bartel DP. MicroRNAs in plants. Genes Dev. 2002;16:1616-1626.

81. Doench JG, Petersen CP, Sharp PA. siRNAs can function as miRNAs. Genes Dev. 2003;17:438-442.

82. Olsen PH, Ambros V. The lin-4 regulatory RNA controls developmental timing in *C. elegans* by blocking LIN-14 protein synthesis after initiation of translation. Dev Biol. 1999;216:671-680.

83. Bartel DP. MicroRNAs: genomics, biogenesis, mechanism and function. Cell. 2004;116:281-297.

84. Tirasophon W, Roshorm Y, Panyim S. Silencing of yellow head replication in penaeid shrimp cells by dsRNA. Biochem Biophys Res Commun. 2005;334:102-107.

85. Shi H, Djikeng A, Tschudi C, Ullu E. Argonaute protein in the early divergent eukaryote *Trypanosoma brucei* :control of small interfering RNA accumulation and retroposon transcript abundance. Mol. Biol. Cell. 2004;24:420-427.

86. Thonberg H, Scheele CC, Dahlgren C, Wahlestedt C. Characterization of RNA interference in rat PC12 cells: requirement of GERp95. BBRC. 2004;318:927-934.

87. Khvorova A, Reynolds A, Jayasena SD. Functional siRNAs and miRNAs exhibit strand bias. Cell. 2003;115:209-216.

88. Robalino J, Browdy CL, Prior S, Metz A, Parnell P, Gross P, Warr G. Induction of antiviral immunity by double-stranded RNA in a marine invertebrate. J. Virol. 2004;78(19):10442-10448.

89. Kariko K, Bhuyan P, Capodici J, Ni H, Lubinski J, Friedman H, Weissma D. Exogenous siRNA mediates sequence-independent gene suppression by signaling through toll-like receptor 3. Cells Tissues Organs. 2004;177(3):132-138.

90. Kariko K, Bhuyan P, Capodici J, Weissma D. Small interfering RNAs mediate sequence-independent gene suppression and induce immune activation by signaling through toll-like receptor-3. J. Immunol. 2004;172:6545-6549.

91. Schroder M, Bowie AG. TLR3 in antiviral immunity: key player or bystanding. Trends Immunol. 2005;26:462-468.

92. Levy DE, Garcia-Sastre A. The virus battles: IFN induction of the antiviral state and mechanisms of viral evasion. Cytokine Growth Factor Rev. 2001;12:143-156.

93. Westenberg M, Heinhuis B, Zuidema D, Vlak JM. siRNA injection induces sequence-independent protection in *Penaeus monodon* against white spot syndrome virus. Virus Res. 2005;114:133-139.

94. Barillas-Mury C, Han YS, Seeley D, Kafatos FC. *Anopheles Gambiae* Ag-STAT, a new insect member of the STAT fanily, is activated in response to bacterial infection. EMBO J. 1999;18:959-967.

95. Yodmuang S, Tirasophon W, Roshorm Y, Chinnirunvong W, Panyim S. YHV-protease dsRNA inhibits YHV replication in *Penaeus monodon* and prevents mortality. Biochem. Biophys. Res. Commun. 2006;341:351-356.

96. Ongvarrasopone C. Molecular cloning of a putative Dicer from black tiger shrimp (*Penaeus monodon*). In the proceeding of RNAi meeting. Cold Spring Harbor, NY. [2005, Sept 28-Oct 2]

97. Irie N, Sakai N, Ueyama T, Kajimoto T, Shirai Y, Saito N. Subtype- and species-specific knockdown of PKC using short interfering RNA. Biochem. Biophys. Res. Commun. 2002;298:738-743.

98. McManus MT, Haines BB, Dillon CP, Whitehurst CE, Parijs LV, Chen J, Sharp PA. Small interfering RNA-mediated gene silencing in T lymphocytes. J. Immunol. 2002;169:5754-5760.

99. Vickers TA, Koo S, Bennett CF, Crooke ST, Dean NM, Baker BF. Efficient reduction of target RNAs by small interfering RNA and RNase H-dependent antisense agents. J. Biol. Chem. 2003;278:7108-7118.

APPENDICES

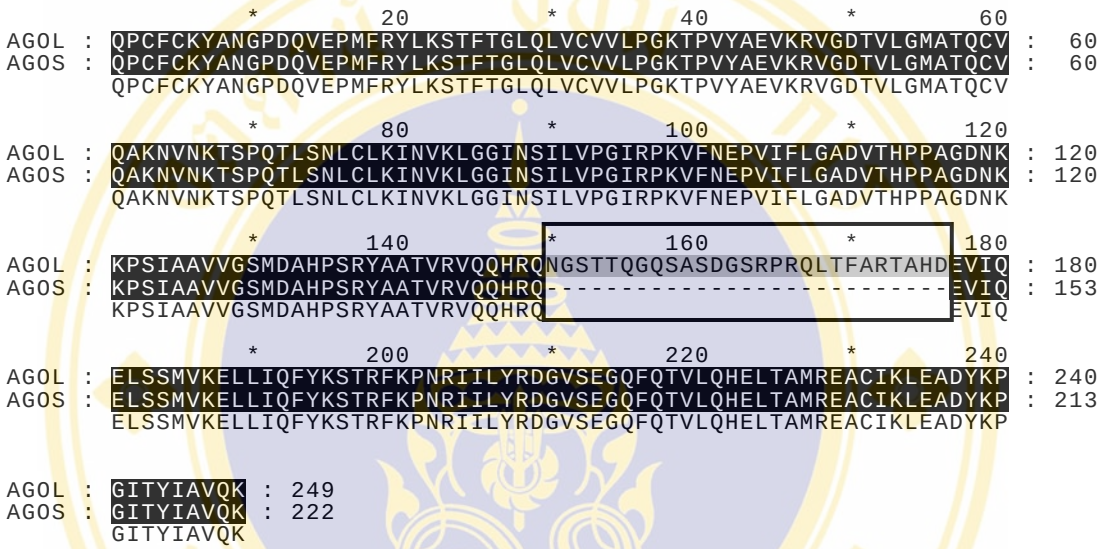

Appendix 1. The alignment of deduced amino acid sequence between short and long form of Pem-AGO

The alignment was conducted by Clustal X program. The amino acid sequences that are identical between two forms are highlighted in black. The deletion of eighty-one nucleotides sequence (27 amino acids) of the short form was shown in rectangular.

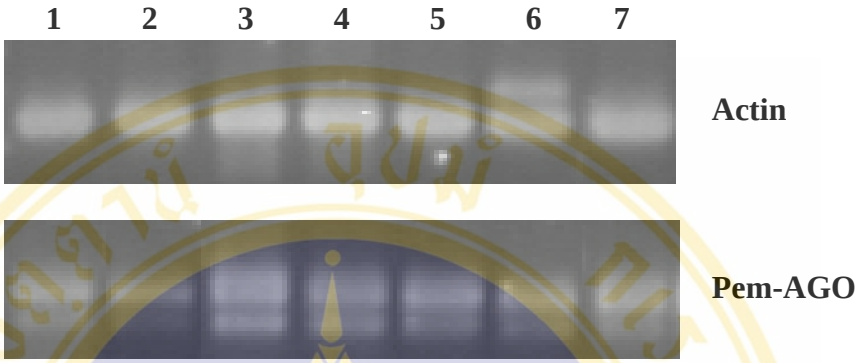

Appendix 2. Tissue distribution of Pem-AGO transcripts by RT-PCR

Tissue specific expression of Pem-AGO mRNA was performed using RT-PCR strategy with gene specific primers PIWI-F and PIWI-R. The cDNA template in this study were kindly provided by Dr. Chalermporn Ongvarrasopone. The expression of Pem-AGO mRNA was detected in all tissues at the expected size of 1 kb. The PCR products were observed on 1% agarose gel electrophoresis. The upper panel represents RT-PCR of actin transcripts from each tissue. The lower panel represents the RT-PCR analysis of Pem-AGO mRNA expression in various *P. monodon* tissues. Lanes 1, 2, 3, 4, 5, 6 and 7 represent the Pem-AGO transcript in nerve, hepatopancreas, ovary, gill, heart, abdominal muscle and lymphoid organ respectively.

gn||CDD30001, CD-Length = 144 residues, 100% aligned

Score = 128 bits (324), Expect = 3e-30

```
Query:  283  AQAVIEFMCEVLDIREIGEQRKPLTDSQRVKFTKEIKGLKIEITHCGAMRRKYRVCNVTR  342
Sbjct:  1    AQPVIEFLKEFLGFDTP----LGLSDNDRRKLKKALKGLKVEVTHRGNTNRKYKIKGLSA  56

Query:  343  RPAQMQSFPLQLENGQTVECTVAKYFLDKYKMKLRFPHLPCLQVGQEHKHTYLPLEVCNI  402
Sbjct:  57   EPASQQTFEL---KDGEKEISVADYFKEKYNIRLKYPNLPCLQVGRKGKPNYLPMELCNI  113

Query:  403  V  403
Sbjct:  114  V  114
```

Appendix 3. The identical consensus sequence of deduced amino acid sequence of PAZ domain from Pem-AGO

The deduced amino acid sequence of PAZ domain of Argonaute protein in *P. monodon* was submitted to blastp program. The result from NCBI conserved domain search showed that the conserved PAZ domain exhibited a significant identity to the gn||CDD30001 sequence of PAZ domain in the cdd.v2.o6 database.

gn||CDD23311, CD-Length = 300 residues, 99.7 % aligned

Score = 339 bits (870), Expect = 1e-93

```
Query:  5    QLVCVILPGKTP-VYAEVKRVGDTVLGMATQCVQAKNVNKTSPQ-TLSNLCLKINVKLGG  62
Sbjct:  1    LIVVVLPDENKPDVYYEIKKRELTDLGIPSQCIRLKTLKKRNKQFTLTNVLLKANMKLGG  60

Query:  63   INSILVPGIRPKVFNEPVIFLGADVTHPPAGDNKKPSIAAVVGSMDAHPSRYAATVRVQQ  122
Sbjct:  61   LNYKL--NIEPEPPLKPTLIIGFDVSHPNGGNGNNPSVAGVVANMDSHGTKFRGGVREQP  118

Query:  123  HRQNGSTTQGQSASDGSRPRQLTFARTAHDEVIQELSSMVKELLIQFYKSTRFKPNRIIL  182
Sbjct:  119  AGQ-------------------------ELLTDLKKIIKESLRSFYKSTRKLPKRIIV  151

Query:  183  YRDGVSEGQFQTVLQHELTAMREACIKLEADYKPGITYIAVQKRHHTRLFCSDKKEQSGK  242
Sbjct:  152  YRDGVSEGQFSQVLNYEVNQIKEACKTLSESYNPKLTVIVVQKRHHTRFFASDK---RDG  208

Query:  243  SGNIPAGTTVDVGITHPTEFDFYLCSHQGIQGTSRPSHYHVLWDDNHFDSDELQCLTYQL  302
Sbjct:  209  PQNPPPGTVVDDKITSPEYYDFYLCSQAGRQGTVKPTHYTVLYDEWGLSPDELQDLTYKL  268

Query:  303  CHTYVRCTRSVSIPAPAYYAHLVAFRARYHL  333
Sbjct:  269  CYMYQRSFRPVSLPAPVYYAHLLAKRGRNNL  299
```

Appendix 4. The identical consensus sequence of deduced amino acid sequence of PIWI domain from Pem-AGO

The deduced amino acid sequence of PIWI domain of Argonaute protein in *P. monodon* was submitted to blastp program. The result from NCBI conserved domain search showed that the conserved PIWI domain exhibited a significant identity to the gn||CDD23311 sequence of PAZ domain in the cdd.v2.o6 database.

BIOGRAPHY

NAME	Miss Manasave Dechklar
DATE OF BIRTH	November 24, 1981
PLACE OF BIRTH	Bangkok, Thailand
INSTITUTIONS ATTENDED	Mahidol University, 1999-2002 Bachelor of Science (Biology) Mahidol University, 2003-2006 Master of Science (Molecular Genetics and Genetic Engineering)
SCHOLARSHIP	Thailand Research Fund to Prof. Emeritus Sakol Panyim, Ph.D.
HOME ADDRESS	149/1 Jarunsanitwong Rd., Bangplud, Bangkok, Thailand e-mail: yuikamaiw@yahoo.com